EAST ENGINEERING LIBRARY

JUN 14 1948

TEXTILE RESEARCH JOURNAL

VOLUME XVIII | May, 1948 | NUMBER 5

PUBLICATION OF

TEXTILE RESEARCH INSTITUTE, INC.

AND

THE TEXTILE FOUNDATION

Editorial Office: 10 East 40th Street, New York 16, N. Y.

TEXTILE RESEARCH JOURNAL

VOL. XVIII, No. 5 May, 1948

In This Issue

An Experimental Study of the Creep of Rayon
M. T. O'Shaughnessy 263

Measurement of Friction Between Single Fibers
II. Frictional Properties of Wool Fibers Measured by the Fiber-Twist Method
Joel Lindberg and Nils Gralén 287

An Investigation of the Relationship Between Polymer Structure and Mechanical Properties
Part II. An Experimental Study of the Stress and Birefringence Properties of Several Relaxing Polymeric Systems
Richard S. Stein and Arthur V. Tobolsky 302

Book Reviews 315

Abstracts 317

Editor: Julian S. Jacobs *Managing Editor:* Julia M. Crisp

Associate Editors

H. J. Ball
Earl E. Berkley
Henry Eyring
Gustavus J. Esselen
Earl K. Fischer
Milton Harris
K. L. Hertel
H. Mark
E. R. Schwarz
Kyle Ward, Jr.

TEXTILE RESEARCH JOURNAL, published monthly at Prince and Lemon Streets, Lancaster, Pa., is devoted to the interest of research in textile and allied industries. It is the official publication of Textile Research Institute, Inc., and the Textile Foundation.

Manuscripts and communications should be sent to the editorial offices, 10 East 40th Street, New York 16, N. Y.

Subscription rates: General—$15.00 per annum; additional for postage, 50 cents to Canada, $1.00 to all other countries. Special—$10.00 per annum for United States and Canadian students, teachers, educational institutions, public libraries, governmental libraries and departments, plus 50 cents for postage to Canada. Single copies, $1.50 each.

Entered as second-class matter, April 27, 1945, at the postoffice at Lancaster, Pa., under the Act of August 24, 1912.

Contents copyrighted 1948 by Textile Research Institute, Inc.

Advertising rates supplied on request.

TEXTILE RESEARCH JOURNAL

VOL. XVIII, No. 5 May, 1948

An Experimental Study of the Creep of Rayon

M. T. O'Shaughnessy*

Contribution from the Rayon Department, E. I. du Pont de Nemours and Co., Buffalo, New York

Abstract

The mechanical properties of textile fibers are more complex than those of unoriented amorphous high polymers. The viscoelastic behavior of the latter, both cross-linked and uncross-linked, may be analyzed in terms of mechanical models of linear elements (Hookean springs and Newtonian dashpots); partially crystalline polymers, particularly textile fibers, are by contrast nonlinear in their behavior. From an experimental viewpoint such nonlinear behavior is best characterized by means of creep or relaxation experiments.

This paper deals with a thorough study of the creep behavior of du Pont textile rayon and textile Cordura yarns at 60% R.H. and 70°F, supplemented by a less detailed study of the creep of these materials when immersed in water. In addition to experiments in which creep of 24 hours' duration was followed by 24 hours' recovery, others were performed in which the duration of creep was varied systematically from 24 hours to 6 seconds. These experiments reveal that the creep curves of rayon, obtained on samples not "mechanically conditioned" in any way, follow a characteristic pattern which may be described as (1) an initial instantaneous and completely recoverable elongation, (2) a relatively rapid high elastic elongation exhibiting delayed but complete recovery, gradually giving place to (3) a slow process of elongation, proportional to log time in first approximation, which is not recoverable and which, as it goes on, results in changes in the capacity of the fiber to recover from the earlier elastic deformation components. Not all of the characteristic creep curve may be observed at an arbitrarily selected load, because of the strong nonlinearity; its character may be deduced from the totality of experiments. Wet rayons exhibit important differences, notably an increase in range and a great decrease in retardation of the high elastic deformation.

The experiments described were performed with constant dead loads. When these loads are corrected to tensions, taking account of the decrease of cross section of the yarn upon elongation, plots of initial and final creep deformations and of 24-hour recoveries against tension show very interesting regularities. So do plots of 24-hour recovery vs. total creep deformations for various loads and durations of creep. A composite plot of elongation divided by tension vs. log time for all loads provides a representation of the nonlinearity of the behavior of these fibers. Increasing load speeds up the deformation process in a manner which is suggestive of the effect of temperature upon the viscoelastic behavior of cross-linked amorphous polymers.

Introduction

The work of Leaderman [14] at the Massachusetts Institute of Technology on the creep of textile fibers, and his exhaustive discussion of the early history and theoretical background of creep studies, contributed greatly to establishing what is now a rather widespread interest in and appreciation of the time-dependent, viscoelastic aspect of the mechanical properties of fibers. There appears to be adequate justification for dating a critical approach to this problem, elsewhere, from the appearance of Leaderman's publication. Since then Mark [16] and

* Present address: Department of Chemistry, The Polytechnic Institute of Brooklyn, Brooklyn, N. Y.

Press [18], Eyring, Halsey, and coworkers [9], Dillon and Prettyman [8], and Burleigh and Wakeham [6] have investigated creep or stress relaxation in fibers or yarns experimentally, and Eyring and Halsey [9] and Dillon [7], and their coworkers at the Textile Research Institute Laboratories at Princeton, New Jersey, have proposed a theory of the tensile behavior of textiles and have elaborated it to take account of the widening scope of their own experimental results. Ray [19] has published, from this laboratory, a discussion of tensile and torsional moduli and of energy dissipation in small tensile extensions which represents a related approach to the problem of resilience.

The practical considerations underlying the current interest in time effects in fibers lie chiefly in the obvious close connection between fiber properties and such desirable fabric properties as resilience and crush-resistance and in the prospect that synthetic fibers can, perhaps, be tailored to mechanical specifications by chemical modification of their polymeric structure. Now that reproduction of the desirable mechanical properties of silk and particularly of wool has become a realistic goal in synthetic fiber research, the precise characterization of fiber properties is a very practical matter. Out of an adequate background of knowledge and of experimental techniques in this field will come surer and earlier evaluation of new candidate synthetic fibers, and valuable guidance in their development. Similar considerations apply to the case of new chemical treatments of the familiar fibers. Finally, widespread knowledge of detailed fiber properties should throw light on problems arising in textile processing and use.

Recent progress in the recognition and interpretation of viscoelastic behavior in fibers is one aspect of a similar development in the field of linear high polymers as a class, including elastomers and plastics as well as fibers. The key to the entire development is the quantitative formulation of the kinetic theory of high elasticity in rubber, first given by Guth and Mark, and by W. Kuhn independently, and since refined by many workers. A review [17] of this theory has appeared recently. This statistical-thermodynamic theory accounts for restoring forces accompanying large deformations which necessarily involve extensive molecular-scale rearrangement in the material in question.

A viscoelastic body may be defined as one in which the deformations which take place in response to applied stresses are in part retarded, or time-dependent. In this paper, we shall be concerned only with tensile deformations. The viscoelastic properties of amorphous, unoriented linear polymers may be represented qualitatively by a familiar mechanical analogy, reproduced in Figure 1 [2]. In this diagram, interpreted in terms of tensile behavior, the spring labeled by the (Young's) modulus E_1 represents instantaneous, short-range, crystal-like "ordinary" elasticity, involving no molecular-scale rearrangement but only deformation of the "lattice" of atoms. The spring E_2 in parallel with the dashpot η_2 (a "Voigt element") is interpreted as representing "high" elasticity, accompanied by extensive molecular rearrangement of portions of chain molecules beween points of relatively permanent attachment or entanglement. The restoring force is attributed to increase of free energy with deformation, a pure entropy effect in the ideal case; the viscosity, to resistance to internal rearrangement. The "open" dashpot η_3 represents viscous flow, the macroscopic aspect of internal rearrangements involving relative displacements of entire molecules. Quantitative representation of the behavior of actual materials usually requires a number of Voigt elements, of different values of E and E/η, in series. In materials cross-linked by covalent linkages, stable secondary valences, or extensive crystallization, flow is ordinarily not observed. For unoriented, amorphous polymers the data available indicate that the springs are Hookean

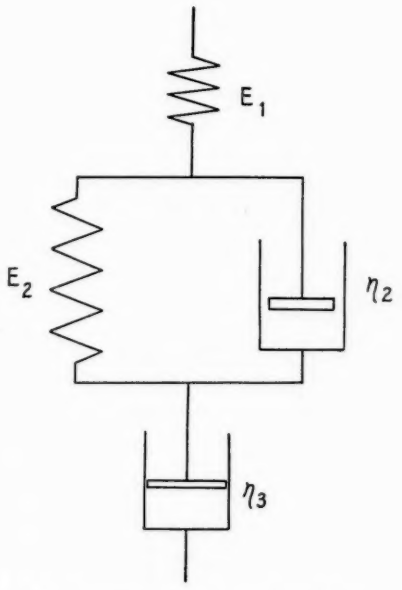

FIG. 1. *Mechanical model representing a linear viscoelastic material.*

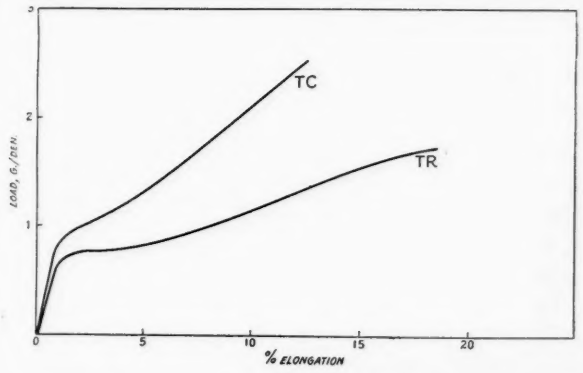

FIG. 2. *Stress-strain curves at 10% elongation per minute, 60% R. H., 70°F.*

and the dashpots Newtonian, to good approximation. Such materials are called "linear" because, so long as the time factor is held constant in comparisons, stress and strain are found to be directly proportional to one another. One of the particular characteristics of fibers, to be discussed later in this paper, is their marked nonlinearity of behavior, in the sense that they cannot be represented at all closely by models constructed entirely of linear elements. This departure from linearity is in fact characteristic of polymers in which x-rays reveal extensive regions of crystalline order, or degrees of order approaching crystallinity, whether the material be in fiber form or not.

Materials showing chiefly ordinary elasticity are easily characterized by stress-strain curves. Although these are obtained, usually, at constant rate of extension or at constant rate of application of load, the time factor is without significance in the case of pure "ordinary" elasticity. These techniques are also applied to viscoelastic materials, but the resulting curves are more difficult to interpret than are the results of simpler experiments in which one of the pair of variables—stress and strain—is held constant, and the variation of the other is observed as a function of time. In creep experiments the stress, or more generally the load, is held constant, whereas in relaxation experiments the strain is held constant and the variation of stress with time is observed. The interpretation of stress-strain curves requires, in general, that assumptions be made beforehand as to the mathematical relations existing among the variables stress, strain, and time. The very interesting papers of Eyring, Dillon, Halsey, and their coworkers at the Textile Research Institute Laboratories, cited above, illustrate the correlation and interpretation of a wealth of data with the aid of a basic assumption as to the form of this mathematical relation, drawn from the theory of absolute rates of chemical reactions as extended to flow processes. Their assumption accounts for nonlinearity in a natural way. As will be seen later, however, their theory is not free from objection.

The present investigation was based throughout on the conscious avoidance of such mathematical assumptions, in the hope that a sufficient number and variety of simple creep experiments would eventually indicate the nature of the processes operating in textile fibers and suggest starting assumptions for efforts at quantitative interpretation. This paper is concerned with one phase of a program of study of the creep of fibers which has been carried out in this laboratory; it reports the results of intensive investigation of the behavior in creep of du Pont bright textile viscose rayon, and of du Pont textile Condura. These yarns have been selected for discussion because the experimental data we have obtained with them are sufficient to fulfill, at least partially, our hope that creep experiments could be used for a searching experimental analysis of textile behavior.

Experimental Procedure

The creep experiments described in this paper were performed upon samples of (1) bright textile rayon yarn, 150 denier, 40 filament, and (2) bright textile Cordura yarn, 150 denier, 40 filament. Both samples were manufactured in the summer of 1945

TABLE I. PROPERTIES OF TEST YARNS

(Supplied by Dr. W. E. Roseveare, Viscose Research, September, 1945)

Yarn	Denier	Tenacity (g./den.) Dry	Wet	Loop	Elongation (%) Dry	Wet	Loop	Twist	Flex life
Textile rayon 150–40 bright	157*	1.72	0.81	1.67	22.5	29.8	18.3	2.2	1897
Textile "Cordura" 150–40 bright	148	2.78	1.76	1.73	15.1	16.9	8.8	2.2	1126

* Our more numerous measurements averaged approximately 152.

and subjected to a complete set of the standard physical tests shortly after manufacture. The results of these tests are listed in Table I. Samples were also tested on an experimental tensile testing machine in this laboratory, which records the tensile stress in a yarn sample, free of inertial and frictional errors, as the sample is elongated at constant rate. The results of tests on this machine, operated at 10-percent elongation per minute, appear in Figure 2.

In principle, the method used in creep experiments consists simply of hanging weights from the ends of yarn samples and observing their changes of length with time, both while the loads are in position and after their removal.

As the changes of length following changes of load are at first very rapid and later become extremely slow, we observed the extensions at logarithmically spaced times after load change. Thus, the standard times of observation during a 24-hour period of creep or recovery were 6, 12, and 30 seconds, 1, 1.9, 4.5, 8, 15, and 30 minutes, and 1, 2, 4, 6, and 24 hours after application or removal of load. Minor deviations from this standard schedule were frequent but unimportant for the results.

Three types of apparatus were used. In the simplest, 1-meter loops of yarn were suspended from yarn clamps mounted in a horizontal row on the wall of the air-conditioned (60% R.H., 70° F) physical testing laboratory. Light strips of $\frac{1}{32}$-in. aluminum (25 cm. long, 6 mm. wide, weight 2.5 ± 0.1 g.), with paper scales ruled in millimeters cemented to one side, were hung by hooks from the bottoms of these loops, and weights were suspended by cords from their lower ends. These aluminum and paper scales were suspended vertically through slots in plastic "scale guides," which prevented them from rotating, and between horizontal black index filaments which passed in front of them and thin black lines ruled on white background behind, which together with the index filaments defined planes with reference to which the displacements of the scales could be observed visually, without magnification, to ± 0.1 mm., or 0.01 percent of the initial length of the samples. The index threads and their backgrounds, together with the scale guides, were mounted individually on metal sliders of adjustable vertical position, running on vertical rods, one slider for each creep position. In this way it was possible to set the zeroes for creep and for recovery accurately at the zero points of the scales before applying or removing load, and thus to observe both elongation and recovery directly, without zero correction.

The second apparatus was a six-position creep balance similar in construction to that described by Leaderman [14], but simpler and somewhat less sensitive. The extension of the samples was observed in the same way as with the larger apparatus. The scales, ruled 50 to the inch, were made by photographic reduction of drawings; they were read to ± $\frac{1}{10}$ of a scale unit with the aid of a low-power magnifying glass. This apparatus was used for the measurements on yarns immersed in water.

The third apparatus consisted of a clamp for suspending a loop of yarn, mounted above a vertical rotating drum in such a way that the lower end of the loop was engaged by a hook attached to a light plastic slider running vertically along the drum on piano-wire guides. The working load was hung by a cord to a second hook on the slider, and a pen was connected to the slider by a flexible spring of shim stock in such a way that it wrote on the drum without appreciable friction and without vertical play. The drum rotated with a circumferential velocity of approximately 5 cm. per second. This apparatus was used only for experiments in which the creep was investigated during the period between a few tenths of a second and about ½ minute after loading. Because of the very rapid creep of the samples immediately after loading, this extension of the period of observation toward shorter times is desirable, although, as will be seen, further improvement of the means for doing so is needed.

In October and November, 1945, 24-hour creep, 24-hour recovery, and 24-hour second creep cycles were carried out on conditioned samples of each of the subject yarns over a range of loads from less than one-tenth the normal tenacity to approximately the maximum load the material would withstand for this period. Following the 24-hour experiments on each sample, experiments were performed in which the duration of creep was 0.1 minute, 0.5 minute, 10.0 minutes, or 120.0 minutes, and the duration of recovery was 24 hours. These we call "separation" experiments, because their purpose is to separate the elongation of the sample, as a function of time, into recoverable and nonrecoverable fractions. (It will be emphasized below that the recovery period determines the exact magnitude of the recovery; the "separation" here is a function of the recovery duration chosen.) These experiments were carried out at the same loads as the ordinary

creep experiments, with the exceptions that the lowest loads, at which creep is very small, were omitted and loads higher than the material would support for 24 hours were included. All of the creep and separation experiments were performed on duplicate samples.

Early in 1946, 24-hour creep, recovery, and second creep experiments were performed, on the creep balance, on samples of both yarns immersed in water at 70° F. Some additional separation experiments, at higher loads than the earlier ones, were performed on conditioned samples at about the same time.

Preliminary analysis of the creep data for conditioned samples, particularly of the bright textile yarn, revealed a number of indications that the yarn had changed with age in the direction of increased stiffness, particularly in reduced elongation under a given load during the earlier seconds and minutes of creep. Thus, for the bright textile yarn, the average elongations in 6 seconds from separation experiments were, for most loads, smaller than the average of duplicate values in the ordinary creep experiments, performed several days earlier. Ordinary creep experiments, and a few 0.1-minute separation experiments at high loads, were therefore repeated for this yarn, using samples from the original spool, in May, 1946, approximately 6 months after the first experiments. Also in the interval between completion of separation experiments at 0.3 to 1.2 g./den., for this yarn, in November, 1945, and the performance of separation experiments at 1.3 to 1.6 g./den. in January, 1946, a portion of the yarn had been skeined, and the latter experiments were performed on yarn which had remained in skein form for approximately 8 weeks. The discontinuity between the results of these last experiments and the earlier ones will be discussed. An incomplete set of experiments was performed on samples from this skein in May, 1946, for comparison with the May results on samples from the spool and with the earlier results. Both the skein and the spool were kept in the 60% R.H. Physical Testing Laboratory during this period of ageing.

Finally, in May, 1946, 10 samples of the bright textile yarn, taken from the skein, were subjected to first creep at 1.0 g./den. for 24 hours, allowed to recover 24 hours, and then 7 of these samples were subjected to second creep cycles and second recovery cycles of 24 hours' duration at 0.4, 0.5, 0.6, 0.7, 0.8, 0.9, and 1.0 g./den. An eighth sample was used in obtaining a stress-strain curve on the material stretched in creep (not reported), and the remaining two were allowed to recover for 43 days. The purpose of this experiment was to compare second creep curves at various loads for samples which were brought into the same physical state ("mechanically conditioned," in Leaderman's terminology) by first creep at the same high load.

In January, 1946, a number of short-time creep experiments were carried out on the bright textile and textile "Cordura" yarns with the recording apparatus. Inertial effects accompanying loading were shown to impair the accuracy of these experiments, so that no analysis of their results will be presented. The single figure (Figure 6) which deals with these measurements is included to substantiate certain statements to be made, later, relative to the course of creep at short times.

Discussion of Results

The data reproduced in this paper are given in the form of (1) reproductions of the experimental creep curves for ordinary creep experiments, (2) reproductions of a few plots of the data for separation experiments, sufficient to illustrate the nature of the results obtained by this method, (3) a number of plots of experimental and derived quantities which have been found quite revealing in the course of efforts to analyze the data, and (4) an Appendix of tabulated numerical results, included to facilitate efforts at quantitative interpretation, should others desire to undertake it.

The following abbreviations and symbols for certain experimental and derived quantities will be used for the sake of brevity:

TR—textile viscose rayon, bright, 150 denier, 40 filament

TC—textile "Cordura," bright, 150 denier, 40 filament

L = load (g./den.)

t = time (minutes) after loading, or, in case of recovery, unloading

E = elongation (percent of initial length = centimeters for 1-m. samples)

R = recovery (percent of *initial* length)

E_t = elongation reached during a time of creep t

$R_{t'/t}$ = recovery during a time t' from creep for a period of time t

Examples: $E_{0.1}$ = elongation during 0.1 minute under load

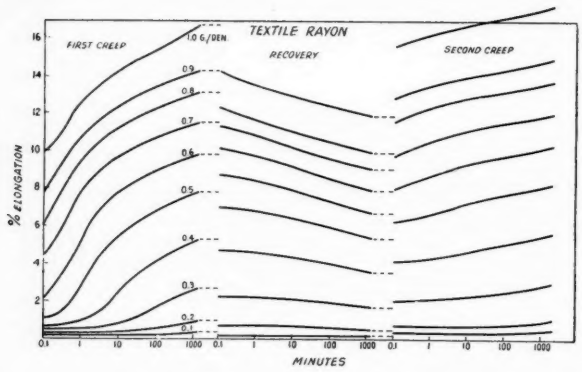

FIG. 3. *Textile rayon, 60% R. H.: 24-hour creep, recovery, and second creep; elongation vs. log time.*

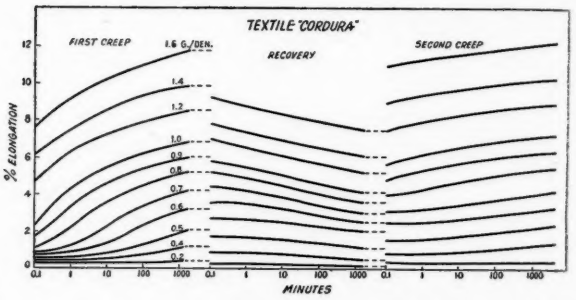

FIG. 4. *Textile Cordura, 60% R. H.: 24-hour creep, recovery, and second creep; elongation vs. log time.*

E_{1440} = elongation during 24 hours under load

$R_{1440/1440}$ = recovery in 24 hours from 24-hour creep

T = tension (g./den.), or load corrected for change of denier (and cross section) during elongation.

$T_{t(L)} = L \times \frac{100 + E_t}{100}$ tension, in sample creeping under a load L, at the time, t, at which time the sample has reached an elongation E_t

The calculated tensions, while actually final values just attained at the time in question, are quite good approximations to the time-average tensions.

I. Stress-Strain Curves

Figure 2 reproduces stress-strain curves for TR and TC obtained at a constant rate of elongation of 10 percent per minute. These define Young's moduli, for the initial linear portions, of 76 g./den. for TR and 105 g./den. for TC.

It should be mentioned that the tenacities and final elongations indicated in Figure 2 differ considerably from the standard tenacities and elongations given in Table I. The reason for the difference is to be found in the rate of testing, which is much lower here than for the Suter test or for the Scott inclined-plane test. The linearity of the stress-strain curve to the yield point and the rapid decrease in slope at the yield point are noteworthy in connection with the creep behavior. It will be observed that linearity is maintained on these curves to a higher load (0.6 g./den. for TR) than in the case of the $E_{0.1}$ values from the creep experiments ($\cong$0.4 g./den.; compare Figure 11). The reason therefor lies in the fact that, in the case of the creep experiments, the samples were exposed to the full load for 0.1 minute, whereas in the case of the stress-strain experiments approximately 0.075 minute was required to elongate the samples to the proportionality limit, and of this interval a major fraction was spent in the range of tensions in which both methods reveal proportionality.

II. Standard Creep Experiments, Conditioned Samples

The results of 24-hour creep, recovery, and second creep experiments are given for TR in Figure 3, from the experiments of October, 1945, and for TC in Figure 4. In these plots the elongations, with reference to the initial length as the base line, are plotted against separate logarithmic time scales for the first creep, recovery, and second creep cycles. While for these yarns the curves represent the data for duplicate samples quite closely in most cases, it is suggested that they be read for details in conjunction with the tabulated initial and final deformations (see Appendix) for each sample in each cycle.

It will be observed that first creep curves are roughly sigmoidal, the start of the S at the lower left being horizontal and the end at the upper right having a positive slope. The curves for the smallest loads exhibit only the start of the S in this time interval, those for certain intermediate loads reveal its entire course, and those for higher loads only the upper portion. This shift of that portion of the creep curve which is realized within the experimental interval, as load increases, is a demonstration of the "nonlinearity" of the viscoelastic behavior of this yarn, as will be discussed in more detail later.

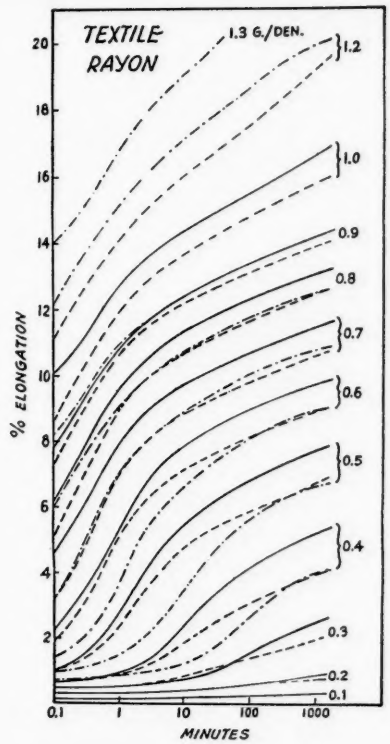

FIG. 5. *Textile rayon, 60% R. H.: Elongation vs. log time in 24-hour first creep.*
——————— *Experiments of October, 1945.*
— — — — *Experiments of May, 1946, samples from spool.*
— · — · — *Experiments of May, 1946, samples from skein.*

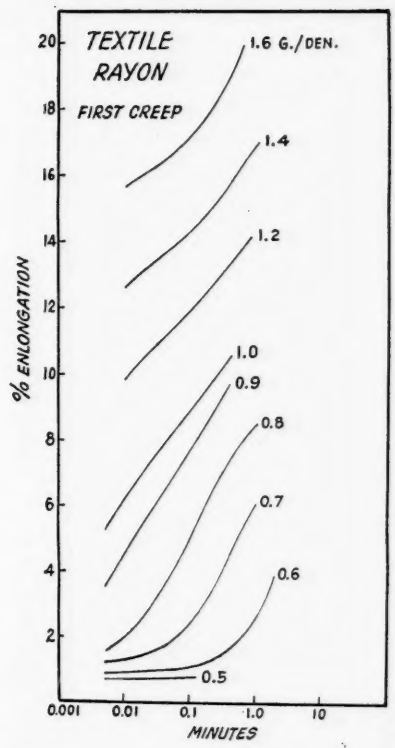

FIG. 6. *Textile rayon, 60% R. H.: Elongation vs. log time in first creep, data for short times.*

The recovery curves illustrate the relatively small recoverable fraction of the first creep elongations of viscose yarns, and the way in which this fraction is divided into rapid and delayed components. The second creep curves resemble the recovery curves much more closely than those for the first creep cycle; it may be said that, after first creep, additional creep elongations are chiefly elastic. However, at the higher loads, the initial deformations are larger in second creep than in recovery (a fairly general result first noted by Leaderman) and some additional elongation takes place in second creep.

The reason for the repetition of ordinary creep-cycle experiments on TR in May, 1946, has been stated. In Figure 5 the first creep cycles of these experiments, both on samples from the spool and on samples from the skein, are plotted in the usual manner, on the same graph with the first creep results of the original experiments. The curves at moderate load justify the generalizations (1) that the total elongations in creep of the samples stored 6 months in a conditioned atmosphere are generally smaller than those obtained for this yarn shortly after it was received, and (2) that the creep of the samples stored in skein form is delayed relative to that of the samples stored on the spool, although the total deformations in 24 hours are roughly the same.

Later, in connection with the analysis of first creep data, we shall use the assumption that a decrease in the time of the first observation after loading would have the effect of bringing creep curves for loads above 0.4 g./den. into initial proportionality with load, with the same proportionality factor that characterizes the relation between $E_{0.1}$ and T for the range to 0.4 g./den. The experimental evidence for this statement is contained in Figure 6, in which the creep of TR is plotted against log time in the interval from 0.01 to above 0.1 minute, from data obtained with the recording apparatus. Other data not reproduced establish this point somewhat more clearly. When these measurements were first made, in January, 1946, it was observed that they did not fit well with the earlier ordinary creep measurements. It is now apparent that a large

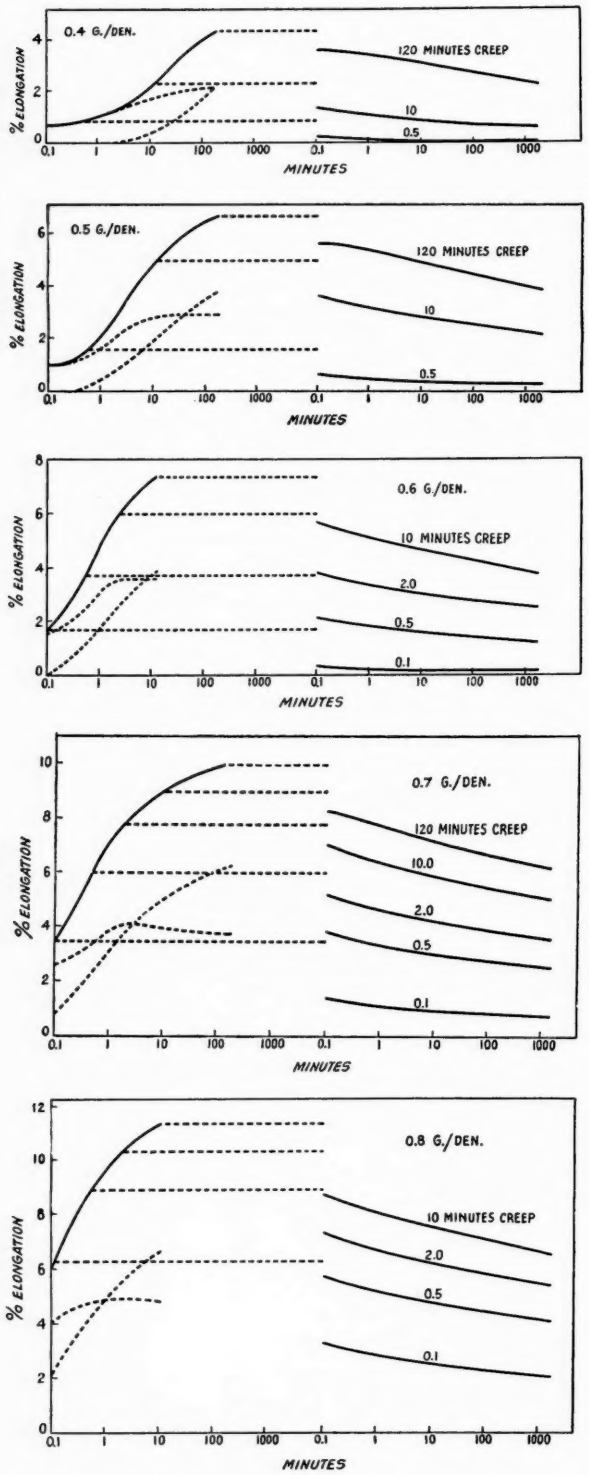

FIGS. 7A, B, C, D, E (*top to bottom*). *Textile rayon, 60% R. H.: Separation experiments at 0.4, 0.5, 0.6, 0.7, and 0.8 g./den., respectively. Dashed curve asymptotic to creep curve represents recovered elongation; dashed curve asymptotic to base line represents nonrecovered elongation.*

part of the discrepancy is to be accounted for by the ageing of the samples. A more serious fault of the recording experiments is evidence, not reproduced here, that the 0.01-minute deformation for large loads is extremely sensitive to the manner in which the weight is applied, so that it would be necessary to devise a method of loading which would eliminate inertial effects before the method would be quantitatively accurate. The large slopes of the creep curves for the higher loads in the interval between 0.01 and 0.1 minute are especially noteworthy; inertia-free loading would have increased these slopes.

III. Separation Experiments

The initial and final elongations of TR and TC in separation experiments are given in the tables in the Appendix. In Figure 7A–E, creep and recovery are plotted against log time, in the same manner as in the standard cycle experiments, for TR at 0.4, 0.5, 0.6, 0.7, and 0.8 g./den. In the construction of these plots, points representing observed elongations in the course of creep and recovery at a given load were entered upon a semilogarithmic chart with log time scales marked off from 0.1 to beyond 1,000 minutes for creep and for recovery. A sample which was kept under load for 0.1 minute was thus represented by a single point on the creep half of the chart, but by a succession of points on the recovery half of the chart. There were two such samples at each load. There were two more, represented by points for each standard time of observation within their intervals under load, for each additional duration of creep studied at the load in question. This group of points on the creep half of the chart defined a creep curve as far as the log time coordinate of the longest creep duration. The corresponding sets of recovery points defined a family of recovery curves which represented, as usual, the residual elongations at each time during the recovery. For purposes of tracing and reproduction, the best creep curve and the best curve to represent the course of the recovery from each duration of creep were then drawn. To provide reference points for estimating the absolute values of the recoveries, horizontal dotted lines were drawn, from the points on the creep curve representing each time of unloading to the 0.1-minute ordinate of the recovery half of the chart. The procedure described makes the general features of the creep and recovery behavior graphically obvious, but it hides approxi-

mations more serious than those introduced by similar procedure in the case of the ordinary creep experiments; the tabulated data should be consulted for accurate values of initial and final elongations and the curves should be used for interpolation.

The dotted curved lines appearing below the creep curves on the creep portions of the graphs represent (*a*) the course, in log time, of the recoverable fraction of the creep elongation and (*b*) the course of the nonrecoverable fraction. These curves were obtained from the solid curves by plotting (*a*) the difference between the elongation at the time of unloading and at the end of the 24-hour recovery, and (*b*) the residual elongation after 24-hour recovery against the logarithm of the time of unloading in the creep cycle.

These experiments reveal some very interesting regularities which will be discussed later. The curves themselves demonstrate the following facts:

1. The creep deformation is completely recoverable so long as it represents only the short-time flat portion of the generalized creep curve, with elongation proportional to load.

2. When the creep curve bends upward from this proportional relation the additional elongation is also completely recoverable for a short distance upward on the bend. Thus, for example, the recovery in 24 hours is almost complete, for TR, from creep at 0.5 g./den. for 0.5 minute and at 0.6 g./gen. for 0.1 minute.

3. At longer times (the time scale involved being understood with due reference to the load in question) the recoverable deformation continues to increase throughout a decade or more of time but eventually reaches a maximum and appears to decrease beyond it.

4. Quite early in the course of the delayed recoverable deformation a nonrecoverable fraction begins to make its appearance. It is asymptotic to the axis of abscissas at the start but increases rapidly in slope and crosses the line for the recoverable deformation somewhere in the neighborhood of the maximum of the latter. Beyond the maximum in the recoverable fraction the nonrecoverable fraction increases, necessarily, in a course approximately parallel with the increase of total deformation. Thus, at times beyond the maximum, all of the creep which is observed to take place in a sample within a given interval is nonrecoverable in the 24-hour period. The nonrecoverable fraction may, indeed, increase slightly faster than the total deformation because of the decay in recovery beyond its maximum.

5. It is quite likely that the appearance of a maximum in the curve representing the recoverable deformation vs. log time is a result of the use of an arbitrary recovery period of 24 hours. An examination of the recovery curves (Figures 7A–E) will reveal that they increase in slope as the duration of creep increases. There is also a decrease, with time under load, in the magnitude of the initial recovery deformation. If the recovery period were longer, say 1 year, it is likely that the total recoveries from longer durations of creep would overtake the total recoveries from the shorter creep periods and that the maximum mentioned above would be replaced by a gradual decrease to zero of the slope of the curve for the recoverable fraction.

6. There are no striking individual features revealed by the separation curves for the two yarns. Instead, an analysis of these data reveals closely comparable features, as will be seen later.

IV. Wet Creep Experiments

In Figures 8 and 9 are given the wet creep, recovery, and second creep curves for TR and TC. As compared with the curves for conditioned samples, the wet creep curves are remarkable for the very much greater deformations taking place at small loads, for the relatively greater instantaneous portions and smaller delayed portions of the total deformations, and for the very large fractions of the total deformations which are recoverable. The fact emphasized by Press [18]—that the nonrecovered fractions of the creep deformations of conditioned samples are largely recovered upon wetting out in water—would, of course, lead one to expect this behavior in wet creep.

V. Creep of "Mechanically Conditioned" Samples

Leaderman [14] reports that when viscose rayon, cellulose acetate, silk, or nylon filaments are subjected to 24-hour creep and recovery cycles at relatively small loads, the creep and recovery deformations in the experiments subsequent to the first are equal and follow the same course in time. He found, however, in the case of nylon at high loads, that the creep and recovery of mechanically conditioned samples, while equal in magnitude at 24 hours, did not follow the same course in time. The initial deforma-

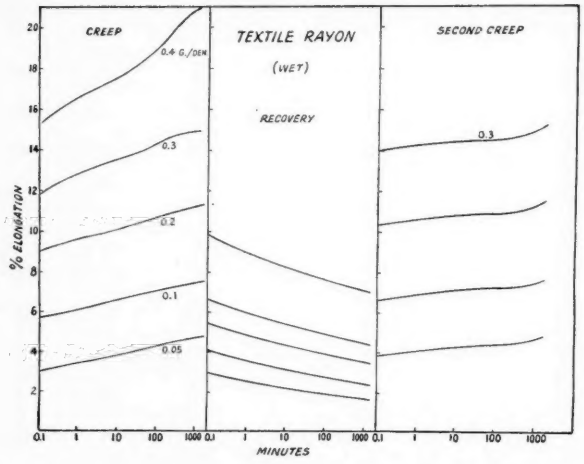

FIG. 8. *Textile rayon, wet: 24-hour creep, recovery, and second creep; elongation vs. log time.*

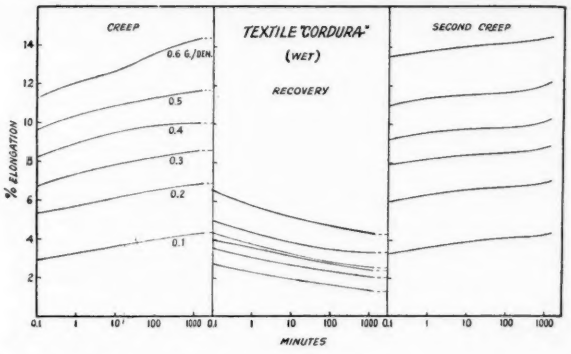

FIG. 9. *Textile Cordura, wet: 24-hour creep, recovery, and second creep; elongation vs. log time.*

tions were larger in the creep cycles and, correspondingly, the delayed deformations were larger in the recovery cycles. He considered this behavior to be a peculiarity of nylon; we have since observed it both in nylon and in other synthetic materials.

A comparison of the second creep and first recovery deformations for viscose at high loads reveals that second-creep initial and final elongations are larger than the corresponding values for recovery. It did not seem worth while to attempt an analysis of the second creep behavior in the ordinary experiments because the initial state for second creep is dependent upon the load in first creep. Figure 10 gives the results of a single set of experiments on TR, carried out in May, 1946, on samples from the skein, in which second creep and recovery cycles were carried out, at loads from 0.4 to 1.0 g./den., on samples which had previously undergone first creep and recovery at 1.0 g./den. The average residual elongation after 24-hour recovery from first creep was 11.5 percent. It is noteworthy that at loads above 0.6 g./den. the second recovery was not complete, and also that the initial deformations in second creep were larger than the initial deformations in recovery at loads above 0.4 g./den., as in nylon and other synthetic yarns.

VI. Analysis of Data

A. Plots of $E_{0.1}$, E_{1440}, and $R_{1440/1440}$ vs. T. The definition of the tension used in the analysis of these data has been given. Early attempts to find regularities in creep data by plotting observed quantities against load were not very successful. As will be seen below, use of the tension in place of the load leads to rather striking regularities. Figure 11 is a plot of $E_{0.1}$ and E_{1440} and $R_{1440/1440}$ vs. the tension, T, calculated in each case from the elongation and the time of observation in the case of creep, and from the final elongation in creep in the case of recovery, for the October, 1945, to January, 1946, experiments on TR. An examination of this figure reveals that the $E_{0.1}$ plot is at first linear, turns upward at about 0.4 g./den. into a region in which the slope at first increases and then slowly decreases, and eventually becomes linear again at about 1.3 g./den. There is a discontinuity between 1.35 and 1.47 g./den. (loads of 1.2 and 1.3 g./den.) which is to be accounted for by the fact that the lower portion of the curve is plotted from the average initial deformations in 24-hour experiments and separation experiments made on samples from the spool shortly after the yarn was received, whereas the points for the higher tensions are average initial deformations in separation experiments on samples studied after storage for 8 weeks in skein form. The slope and intercept of the linear part of the curve at high loads are determined by these last four sets of values. The E_{1440} curve is not linear in the neighborhood of 0.1 g./den.; a linear region at still smaller loads is not excluded but would be difficult to detect because of experimental errors. The curve increases rapidly in slope to about 0.3 g./den. and then decreases slowly and becomes linear, from about 0.65 g./den. onward. The $R_{1440/1440}$ line is initially concave upward but goes through an inflection point at about 0.4 g./den. and becomes linear above 0.65 g./den.

The initial portion of the $E_{0.1}$ line defines a modulus which agrees well with that defined by the ini-

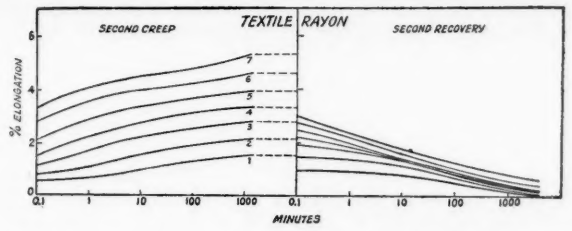

FIG. 10. *Textile rayon, 60% R. H.: Second creep and recovery of samples previously subjected to 24-hour first creep at 1.0 g./den., followed by 24-hour recovery (averaged nonrecovered extension 11.45 per cent).*

Curve No.	*Load based on original denier (g./den.)*	*Load based on denier at start of second creep (g./den.)*
1	*0.4*	*1.12*
2	*0.5*	*1.00*
3	*0.6*	*0.89*
4	*0.7*	*0.78*
5	*0.8*	*0.67*
6	*0.9*	*0.585*
7	*1.0*	*0.445*

tial straight portion of the stress-strain curve (Figure 2). It is interesting to define Young's moduli corresponding to the other linear ranges of the elongation curves. Thus the slope of the upper part of the $E_{0.1}$ curve is 9.03, corresponding to a modulus of 11 g./den., and the intercept is zero. The slope of the upper part of the E_{1440} curve is 13.6, corresponding to a modulus of 7.3 g./den., and the intercept is 0.83 percent elongation.

The features which have been discussed in some detail for the first experiments on TR are reproduced in Figure 12 for the May experiments on TR samples from the spool and in Figure 13 for TC. The $E_{0.1}$ curve for TC becomes linear so late in its course that it does not appear possible to define its final slope. Slopes, corresponding moduli, and the intercepts of the straight lines from which these are taken are compared in Table II, which includes the later experiments on TR. Curves for the May skein samples of TR have not been reproduced, in the interest of economy of space.

The initial moduli defined by the $E_{0.1}$ curves, 69 g./den. for TR and 107 g./den. for TC, are to be compared with 76 g./den. and 105 g./den., respectively, obtained from the stress-strain curves (Figure 2). It will be noted that the initial modulus of TR had increased to about 77 g./den. after 6 months' storage in spool form. It must be admitted that more accurate methods of obtaining the initial modulus

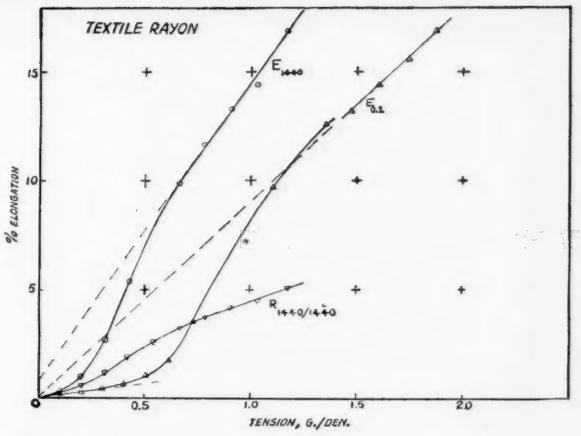

FIG. 11. *Textile rayon 60% R. H.: First creep and recovery; 0.1-minute creep, 24-hour creep, and 24-hour recovery vs. calculated tension in g./den. Experiments of October, 1945, and January, 1946 (last four points on $E_{0.1}$ curve).*

are available and that these figures should not be given too much weight. The final 0.1-minute modulus for TR was, as indicated in Table II, not defined by the experiments in October, 1945. The result from Figure 11 is for skein samples in January, 1946. Its value was little different for the spool samples tested in May, but appears to have been significantly lower for the May skein samples. Simultaneously with what changes of modulus occurred, the intercept of the final part of the $E_{0.1}$ curves took on increasing negative values. The final 24-hour modulus for TR was, roughly, unchanged by 7 months' storage in spool form. Lastly, it will be noted that while no final 0.1-minute modulus is sufficiently well-defined for TC to warrant inclusion in the table, the final 24-hour modulus for this yarn is well defined, relatively high, and associated with a zero intercept.

Figure 14 is a plot of $E_{0.1}$, E_{1440}, and $R_{1440/1440}$ vs. T for the wet creep data for both yarns. It is particularly noteworthy that the slopes of these curves are quite large at the origin and decrease as the tension increases. This is the opposite of the behavior observed for conditioned samples. The E_{1440} and $R_{1440/1440}$ curves appear to be linear over considerable ranges.

Figure 15 is a similar plot for the second creep and second recovery of samples of TR "mechanically conditioned" by first creep at 1 g./den. Here $R_{0.1/1440}$ is also plotted for comparison with $E_{0.1}$. The chief features brought out by this plot are:

1. The nonequivalence of $E_{0.1}$ and $R_{0.1/1440}$ for the higher loads.

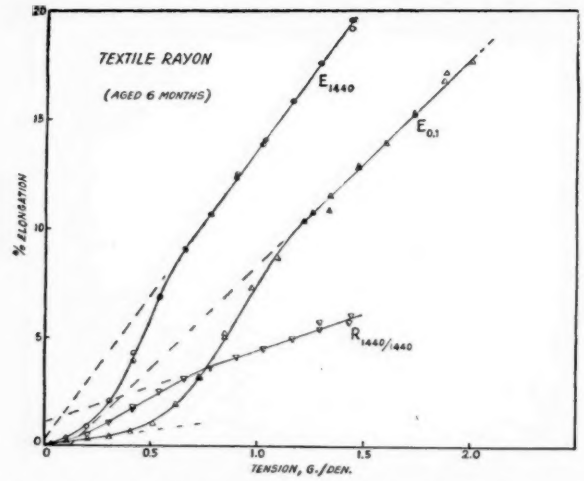

FIG. 12. *Textile rayon, 60% R. H.: First creep and recovery; 0.1-minute creep, 24-hour creep, and 24-hour recovery ($E_{0.1}$, E_{1440}, and $R_{1440\ 1440}$) vs. calculated tension; experiments of May, 1946, samples from spool.*

2. The nonequivalence of E_{1440} and $R_{1440/1440}$ for the higher loads.

3. The linearity of the higher load points for $R_{1440/1440}$, with zero intercept.

The fact that the initial creep deformations exceed the initial recoveries now appears to be general for textile fibers at large loads. If the difference between E_{1440} and $R_{1440/1440}$ is attributed to continuation of the nonrecoverable deformation process begun in first creep, and the recovery is considered to represent the elastc process, then the proportionality of $R_{1440/1440}$ to final tension may be considered an indication that the over-all elastic process obeys Hooke's law. The curvature of the $E_{0.1}$ and the $R_{0.1/1440}$ lines and their nonequivalence demonstrate that the elastic process involved is not a "linear" process throughout its course. In the discussion above it must, however, be noted that the separation of a given elongation into elastic and nonrecoverable fractions is somewhat arbitrary and depends on the duration of recovery.

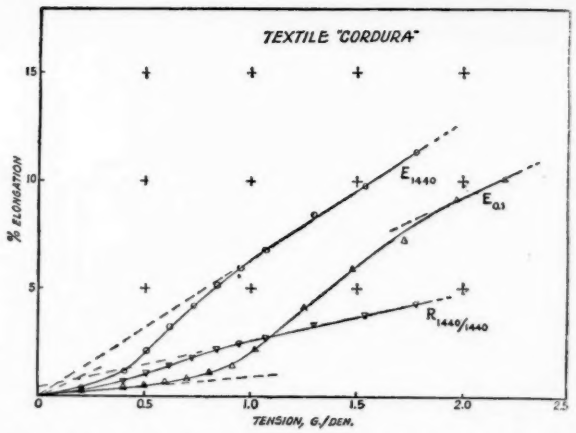

FIG. 13. *Textile Cordura, 60% R. H.: First creep and recovery; 0.1-minute creep, 24-hour creep, and 24-hour recovery vs. calculated tension.*

B. Plots of E/T vs. Log t. In the introduction to this paper, the statement is made that the viscoelastic behavior of textile fibers is nonlinear. Linear viscoelastic behavior manifests itself in creep experiments by direct proportionality between strain and applied stress, measured for a series of samples at the same time after loading, throughout the duration of the experiments. The situation can be represented by the equations:

$$\text{Strain} = \text{Stress} \times \text{function of time}$$
$$\text{Strain/Stress} = \text{Function of time}$$

It is possible in theory to construct a mechanical model of linear elements which will duplicate the observed viscoelastic behavior of a test material (Hookean springs, Newtonian dashopts) whenever a proportionality of stress to strain is maintained as time goes on in creep or relaxation experiments. The utility of the concept of linear viscoelastic behavior arises from the fact that many materials, particularly unoriented amorphous polymeric materials, exhibit behavior in small deformations which satisfies the re-

TABLE II. SLOPES, MODULI, AND INTERCEPTS FOR $E_{0.1}$, E_{1440}, AND $R_{1440/1440}$ VS. T PLOTS (FIGS. 11, 13, 21)

Figure	Yarn	Date	$E_{0.1}$, initial Slope	$E_{0.1}$, initial Modulus (g./den.)	$E_{0.1}$, final Slope	$E_{0.1}$, final Modulus (g./den.)	$E_{0.1}$, final Intercept (%)	E_{1440}, final Slope	E_{1440}, final Modulus (g./den.)	E_{1440}, final Intercept (%)
11	TR spool	Oct. 1945	1.44	69	*	*	*	13.60	7.3	0.83
11	TR skein†	Jan. 1945	*	*	9.03	11.0	0.0	—	—	—
12	TR spool	May 1946	1.30	77	9.50	10.6	−1.1	13.50	7.4	0.30
—	TR skein	May 1946	*	*	11.10	9.2	−2.0	*	*	*
13	TC spool	Nov. 1945	0.93	107	*	*	*	6.35	15.8	0.00

* Not defined; insufficient data.

† Note that last $E_{0.1}$ points for TR (Figure 11) are for skein-sample separation experiments in January, 1946 (1.3–1.6 g./den. load).

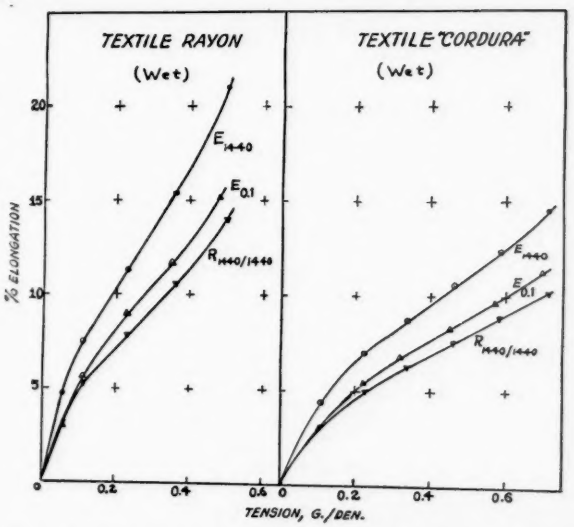

FIG. 14. *Textile rayon and textile Cordura, wet: First creep and recovery; 0.1-minute creep, 24-hour creep, and 24-hour recovery vs. calculated tension.*

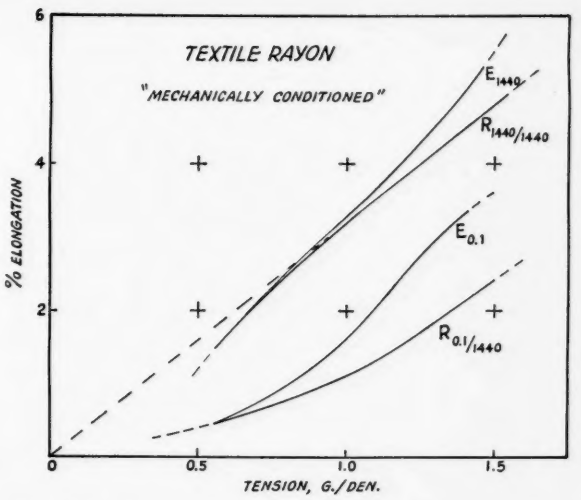

FIG. 15. *Textile rayon, 60% R. H.: Second creep and recovery following 24-hour first creep at 1.0 g./den. and recovery; 0.1-minute creep, 24-hour creep, 0.1-min-recovery, and 24-hour recovery vs. calculated tension.*

quirements of the definition quite closely. This correspondence between actual behavior and the behavior of a linear model can be proved by simple experiments—for example, creep—and the model (or an equivalent set of differential equations) may then be constructed from the results of such simple experiments as creep, and then used as a basis for deducing the behavior of the material under all manner of complex experimental conditions [3]. In the case of textile fibers, nonlinearity of mechanical behavior is so marked that no useful model can be constructed of linear elements, but the concept of linearity can be a convenient starting point in a detailed discussion of the actual behavior of fibers.

The condition for linearity states that if the deformations observed in a set of creep experiments at several tensions are divided by the corresponding tension in each case, the values of the compliance so obtained will fall on a single locus when plotted against time or a function of the time. In Figure 16 the elongation, divided by the tension calculated for the particular elongation in each case, has been plotted against the logarithm of the time, for the October, 1945, 24-hour creep experiments on TR. Figure 17 is a similar plot of TC. Lines have been drawn through the points representing the same static load. These lines are not equivalent to lines of constant tension, but they do not differ from the latter seriously.

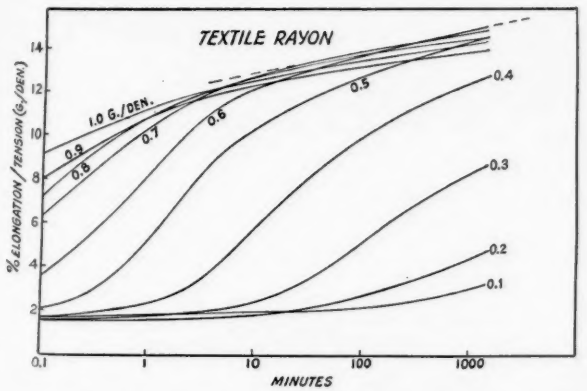

FIG. 16. *Textile rayon, 60% R. H.: First creep: elongation/tension vs. log time; data of October, 1945. Curves represent creep at constant load; tension varies moderately along curve.*

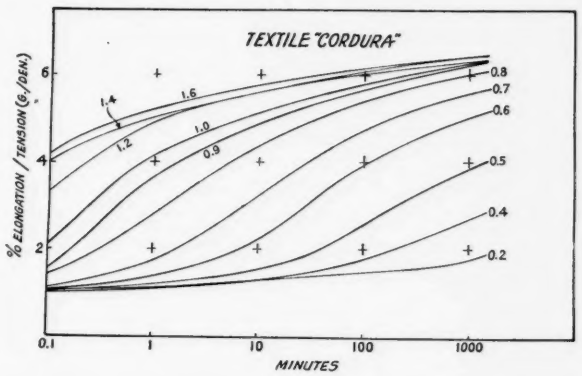

FIG. 17. *Textile Cordura, 60% R. H.: First creep, elongation/tension vs. log time. Curves are for constant load.*

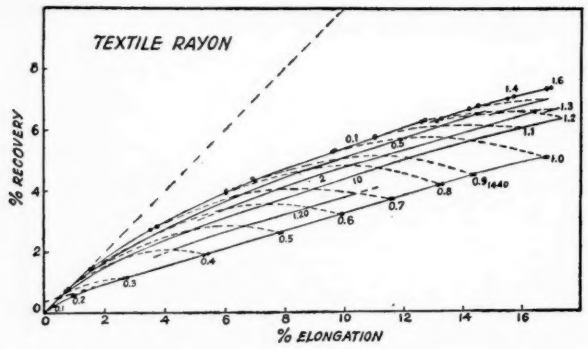

FIG. 18. *Textile rayon, 60% R. H.: Recovery in 24 hours vs. elongation in creep for various loads and times (R_{1440}/t vs. E_t). Solid lines are drawn through points for constant duration of creep and labeled 0.1, 0.5, 2, 10, 120, and 1440 (minutes). Dashed lines, convex upward, are drawn through points for constant load. Only a few experimental points have been reproduced because of the complexity of the figure. These, in pairs, indicate the agreement between duplicate experiments and the fit of the line to the experimental points. Loads are identified by figures placed at the longest duration of creep for which the load in question could be used.*

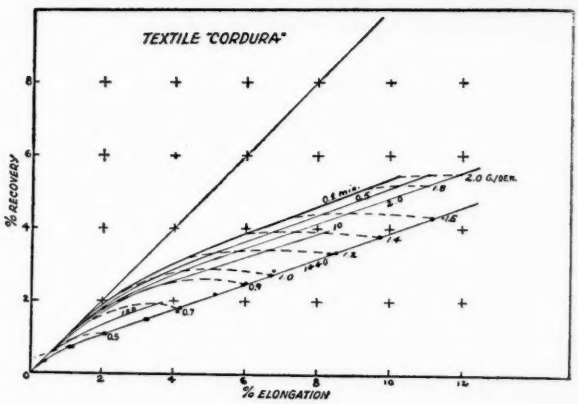

FIG. 19. *Textile Cordura, 60% R. H.: Recovery in 24 hours vs. elongation in creep for various loads and times. See explanation for Figure 18.*

It will be observed in Figure 16, for TR, that these lines of constant load behave as follows:

1. At short times the curves for 0.1 to 0.4 g./den. coincide approximately, at $E/T = 1.5$, and define a lower envelope which appears to be straight, with perhaps a very small positive slope. The individual curves of this group turn upward from this common locus in order of decreasing magnitude of load.

2. The curves for higher loads lie above this locus at 0.1 minute, but their shape indicates (and the recorded creep data for shorter times given in Figure 6 reinforce the indication) that they would join it, in order of increasing load, if the observations were extended from 0.1 minute in the direction of shorter times. After leaving the lower envelope the curves move upward, individually and with a wide separation between them, through a region in which their shape is sigmoidal.

3. Eventually, however, as they approach the top of the "*S*" they come together to form what may to first approximation be called an upper common locus, somewhat less well-defined than the lower. The upper envelope appears to be a straight line from about $t = 10$ minutes onward; its slope is about one unit of E/T (% elongation/g./den.) per cycle of logarithmic time. The curve for 0.4 g./den. just fails to reach this locus during the period of the experiments.

The systematic deviation of the experimental curves from the upper locus in Figure 16 arises in part from the positive intercept associated with the E_{1440} vs. T line in Figure 11. The curves represent only the ordinary creep experiments of 24 hours' duration conducted in October, 1945. If entered on this plot, the $E_{0.1/T}$ points from the separation experiments at large loads conducted in October and January would be grouped closely about $E/T = 9$ on the 0.1-minute ordinate line. Their grouping there is evidence that the upper envelope coincides approximately with the line for 1.0 g./den. static load in this region of log time.

In Figure 17 for TC, the general situation is quite similar, but there is a large increase in the number of decades of time required for the yarn to traverse the nonlinear part of the creep process, and a corresponding separation of the curves for the individual loads on the plot.

As has been stated, these plots of E/T vs. log t are direct representations of the nonlinearity of the viscoelastic behavior of the yarns in question. The striking features of these plots are, first, that the behavior is nonlinear in the course of an intermediate elongation process which appears to be included between an initial and a final linear process, and, second, that the shifting toward shorter times, with increasing load, of the nonlinear portions of the curves is strongly suggestive of the shifting of the creep curves (E/T vs. log t) for many polymers exhibiting linear behavior toward shorter times as the temperature is increased [1].

C. Recovery as a Function of Elongation in Creep. In Figure 18, the 24-hour recoveries ($R_{1440/t}$) observed in all the ordinary creep and separation experiments performed on TR in October and No-

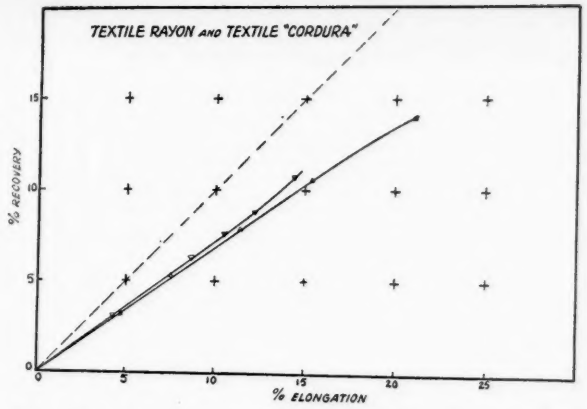

FIG. 20. *Textile rayon and textile Cordura, wet: Recovery in 24 hours vs. elongation in 24-hour first creep.*

vember, 1945, and in January, 1946, have been plotted as ordinates against the elongations at the time of unloading (E_t) as abscissas. Figure 19 is a similar plot for TC. The types of regularity observed in these plots will be discussed with reference to Figure 18:

1. It is, first of all, brought out clearly that the recoveries are incomplete except at small loads and short times (0.5-minute creep at 0.3 and 0.4 g./den.).

2. The points representing 24-hour creep may be represented quite exactly by a straight line in the range from 2 percent elongation (less than 0.3 g./den.) to 15 percent elongation (above 0.9 g./den.). A prolongation of this line to the recovery axis reveals a small positive intercept.

3. Lines may be drawn, in the same manner, through the points representing creep for shorter periods. In general, these lines have a slight upward convexity throughout their course. They lie above one another in order of decreasing duration of creep.

4. Dotted lines have been drawn through the sets of points representing creep at each of the various loads. These lines are convex upward and possess maxima; their maxima occur at durations of creep which decrease, as load increases, from the neighborhood of 24 hours for 0.3 g./den. to the neighborhood of 0.5 minute for 1.0 g./den. and above.

A special feature of Figure 18 is the discontinuity in the constant duration of creep lines for 0.1, 0.5, and 2 minutes, which occurs in each case between 1.2 and 1.3 g./den. load. The reason for this discontinuity has been discussed previously: it is the result of 8 weeks' ageing in skein form of the samples for the higher loads.

TABLE III

Yarn	Date	
TR	Oct. 1945	$R_{1440/1440} = 0.288\ E_{1440} + 0.37$
TR spool	May, 1946	$R_{1440/1440} = 0.280\ E_{1440} + 0.60$
TR skein	May, 1946	$R_{1440/1440} = 0.254\ E_{1440} + 0.60$
TC	Nov. 1945	$R_{1440/1440} = 0.350\ E_{1440} + 0.37$
TR wet	—	$R_{1440/1440} = 0.685\ E_{1440}$
TC wet	—	$R_{1440/1440} = 0.715\ E_{1440}$

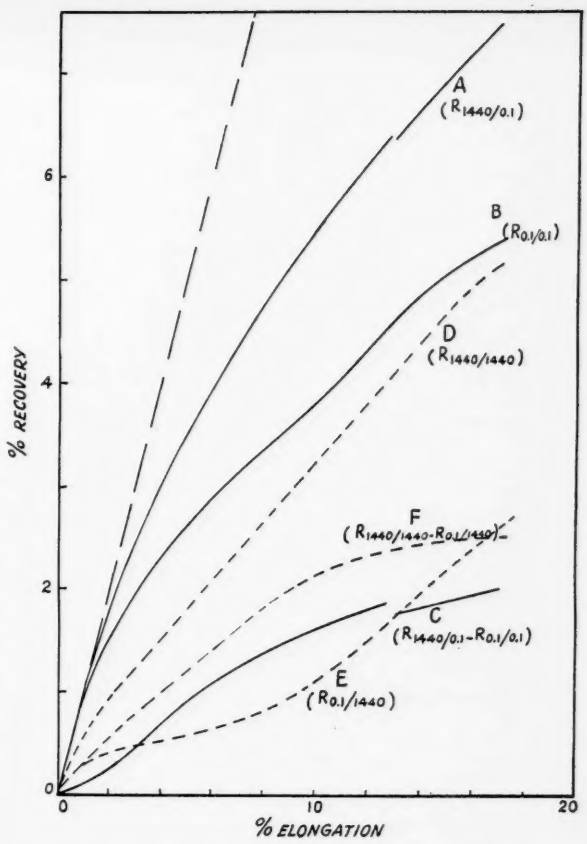

FIG. 21. *Textile rayon, 60% R. H.: Recovery vs. elongation in creep. Solid lines: A—Total 24-hour recovery from 0.1-minute creep; B—0.1-minute recovery from 0.1-minute creep; C—Delayed (0.1-minute to 24-hour) recovery from 0.1-minute creep. Broken lines: D—Total 24-hour recovery from 24-hour creep; E—0.1-minute recovery from 24-hour creep; F—Delayed (0.1-minute to 24-hour) recovery from 24-hour creep.*

Figure 19, for TC, is similar to Figure 18 in all its features, except for the absence of discontinuities.

Figure 20 is a similar plot for the 24-hour wet creep experiments. Here $R_{1440/1440}$ is directly proportional to E_{1440}; there is no intercept. The slopes portional to E_{1440}; there is no intercept. The slopes of the curves for both TR and TC are much higher than the corresponding slopes for the conditioned samples.

Table III compares the algebraic equations relating $R_{1440/1440}$ to E_{1440} in the extension linear regions of these plots, for the later experiments not otherwise reproduced here as well as for the cases just discussed.

The fractional recovery of textile "Cordura" is shown by this tabulation to be somewhat greater than that of the ordinary textile rayon, both wet and conditioned; the difference is considerable for the conditioned materials.

In the discussion of the separation experiments it has been stated that the initial recovery at a given load decreases with the duration of creep and that the delayed recovery increases. Figure 21 is a plot of the initial, final, and delayed recoveries from 0.1-minute and from 24-hour creep vs. the elongations in creep, for TR; it illustrates this change in the character of the recovery quite clearly.

Theoretical Considerations

The present incomplete state of knowledge of the molecular-scale structure of textile fibers and of the mechanisms involved in their deformations makes it impossible to give a definite explanation for the phenomena reported above in terms of accepted theory. Such relationships as are here reported should, in fact, be useful, in conjunction with experimental data from other sources, in the development of more refined conceptual models for the structures and processes involved. In the interest of brevity, there will be given below only an outline of the direction in which the author believes an explanation is to be sought, together with some remarks as to the relation of such an approach to other current theories. These ideas may be amplified and extended in a later publication.

1. The instantaneous short-range elongation, corresponding to the lower flat portion of the generalized creep curve, appears to be crystal-like, ordinary elasticity. As observed in rapid experiments, uncomplicated by creep, it is rapidly and completely recoverable. Its modulus is only slightly lower than the value obtained in velocity-of-sound measurements, at 10,000 cycles per second, by the method of Ballou and Silverman [5]. Any major configurational elastic component must therefore have a retardation time shorter than 10^{-6} minutes; such a component is unlikely. The mechanism of ordinary elasticity is the bending and stretching of chemical bonds of various types, without substantial molecular-scale rearrangement of the fiber substance. In wet samples it is unobservable in ordinary time scale because of the greatly reduced retardation of the second type of deformation, discussed below.

2. The entire time-dependent deformation process (the entire deformation minus the small ordinary elastic component) may be identified as configurational deformation—in the sense that the configurations of individual chain molecules change and that molecular-scale reorganization of the material is involved—of the crystallite-cross-linked polymeric network which constitutes the fiber. Its fundamental mechanism is stress-biased segmental diffusion in the amorphous material, and the restoring force is to be attributed, at least in part, to a decrease in entropy associated with the configurational changes which occur.

It is necessary to recognize clearly, and it will eventually be necessary to account for, certain peculiarities of the configurational-elastic process in this present case. As observed in linear polymers which are unoriented and essentially amorphous, such as plasticized films of vinylite [1] or, better, films of plasticized cross-linked polystyrene [4], this type of deformation is both linear and totally recoverable. Vinylite films appear to be cross-linked at ordinary temperatures in a manner not clearly understood; a minor fraction of quite small crystallites has been proposed as an explanation [20]. If cross-linking is absent, as in plasticized films of ordinary polystyrene, linear and recoverable high elasticity is superimposed upon a viscous-flow deformation which is a linear function of time. The flow is of course nonrecoverable. In the present case the deformation is incompletely recoverable, but the nonrecoverable fraction as isolated in the separation experiments is kinetically very different from viscous flow. Plotted against log time, it is slightly convex upward for most loads (a straight line in rough first approximation); its rate is therefore inversely proportional to the time. Furthermore, nearly all of this deformation is recovered upon wetting out [18]. The kinetic picture suggests slow approach to a limiting extension, and this is precisely what would be expected of a network in which the junction points (the crystallites) are stable under the given conditions of applied stress, degree of swelling, and temperature. Incomplete recovery of the network deformations is thus a major qualitative and quantitative effect, which must be accounted for in any rationalization of these deformation phenomena on the network model.

The second gross peculiarity is, of course, the nonlinearity. Here the original and powerful attack of Eyring and his coworkers [9] has had considerable success in fitting and even in predicting experimental data. It has been the nature of the approach of these authors to avoid preoccupation with conceptual models other than the model of an act of segmental diffusion across an energy barrier, the analysis of which forms the basis of their theory. This simplification appears to have been fully justi-

fied, as a temporary measure, by the rapid progress they have made on this basis. It appears to the writer that the molecular-scale conceptual model employed by these workers (as distinguished from their mechanical models analogous to Figure 1) is a model of a situation existing in the amorphous part of a fiber, and that the theory largely neglects the role of the crystallites. Furthermore, this theory, in its simplest formulation, does not account for incomplete recovery, and in a later formulation incomplete recovery was accounted for on the assumption of viscous flow, an assumption which is further indicative of neglect of the network concept and is untenable from the point of view of the present writer.

The author wishes to suggest that these two gross peculiarities of fiber deformations—nonlinearity and incomplete elasticity—may be intimately related, and that explicit consideration of the role of the crystallites may be necessary if a self-consistent explanation of both phenomena is to be attained. Even the most recent and most conservative estimates [10, 13] indicate that 20–25 percent of the rayon fiber structure is crystalline. The crystallites appear to be elongated platelets [11]; estimates of their length vary from 500 Å. (about 50 cellobiose units) upward. It is obvious that no deformation of the network can take place in which the crystallites do not take part [11], and their rotation into the stress direction (progressive orientation) has been observed as a function of the amount of nonrecovered stretch, most recently by P. H. Hermans on model filaments [12]. The individual crystallites, composed as they are of extended and parallel sections of chain molecules, cannot undergo deformations comparable in magnitude with those of the network, but must rather follow the general network deformation by changes of position and orientation. (Some disruption of crystallites may of course occur.) Now those chain sections in the amorphous material which enter crystallites at both ends (and thus can bear high elastic stress indefinitely) enter predominantly at the ends of these crystallites. In a stretched cellulose structure, rotation of the elongated crystallites into the stress direction would act, therefore, to decrease the components in the stress direction of the end-to-end lengths of these amorphous chain segments and thus, if the over-all strain is held constant, to decrease high elastic stress.

Now a certain amount of crystallite rotation will necessarily accompany any stretching of the network (Kratky's theory of "affined transformations," discussed by Hermans [11]), and if we are to connect progressive orientation with decay of stress we must posit an additional, time-dependent orientation process which involves motion of the crystallites in excess of that enforced by the geometry of the macroscopic strain. Hermans [12] has reported that orientation is a steeper function of stretch in cellulose gels than the theory of affined transformations would predict. In terms of the present postulate, this excess of orientation is related to creep and stress relaxation, and, by inference from experimental results, with the partially nonrecoverable character of the deformations. This last can be the case only if the resistance to such internal rearrangements and their reversal is of such character that the new, more highly oriented configuration is blocked from reverting. Finally, resistances of this type, providing for a sort of thixotropy, offer a basis for a qualitative explanation of nonlinear viscoelastic behavior.

The author will be the first to admit that what is here proposed is not a theory but rather a suggestion of the basis upon which a theory might be developed. The problem of the kinetics of fiber deformations is not simple, and progress is to be expected from a variety of approaches. In particular, it appears desirable to attempt kinetic deductions from the well-developed structural theory which has been built up by H. Mark [15], P. H. Hermans, and many others.

Summary

1. Du Pont textile rayon and textile Cordura have been subjected to creep experiments, at various loads, of durations from 6 seconds to 24 hours, followed by 24 hours' recovery and in some cases by a second creep cycle, both at 60% R.H. and 70° F, and immersed in water at 70° F.

2. The 60% R.H. creep behavior of the textile rayon has been investigated at times from 0.005 minute to 0.1 minute (6 seconds) in an exploratory way.

3. A group of samples of the textile rayon has been subjected, at 60% R.H., to 24-hour creep and recovery experiments at a series of loads, after preliminary "mechanical conditioning" 24 hours' creep at 1.0 g./den. (11.45% percent residual elongation after 24 hours' recovery).

4. The resulting data have been analyzed graphically. Regularities which may be of significance for the structure of the fiber and the detailed mechanism of the elongation process have been found in plots of: (1) the recoverable and nonrecoverable fractions of creep elongation vs. log time at various loads, (2) the elongation in certain times and the recovery vs. the tension, (3) the ratio of elongation

to tension vs. log time, (4) the total recovery vs. the total elongation in creep for constant duration and varying load.

Acknowledgment

The author wishes to express his appreciation for aid and encouragement in the prosecution and publication of this work to Dr. W. H. Charch, Director, and to many members of the Pioneering Research Section, Rayon Department Technical Division, E. I. du Pont de Nemours and Co. Particularly he wishes to thank Miss Violet Grenda, of the Physical Testing Laboratory, who carried out the experimental work with unfailing care and precision.

Literature Cited

1. Aiken, W., Alfrey, T., Janssen, A., and Mark, H., *J. Polymer Sci.* **2**, 178 (1947).
2. Alfrey, T., *The Mechanical Behavior of High Polymers* ("High Polymers," Vol. VI), New York, Interscience Publishers, Inc., 1948.
3. Alfrey, T., and Doty, P. J., *J. Applied Phys.* **16**, 700 (1945).
4. Alfrey, T., Stein, R., Tobolsky, A. V., and Wiederhorn, N. Paper in preparation for *J. Polymer Sci.*
5. Ballou, J. W., and Silverman, S., TEXTILE RESEARCH **14**, 282 (1944).
6. Burleigh, E. G., and Wakeham, H., TEXTILE RESEARCH JOURNAL **17**, 245 (1947).
7. Dillon, J. H., TEXTILE RESEARCH JOURNAL **17**, 207 (1947).
8. Dillon, J. H., and Prettyman, I. B., *J. Applied Phys.* **16**, 159 (1945).
9. Eyring, H., *et al.*, Mechanical Properties of Textiles, TEXTILE RESEARCH JOURNAL **15**, 295, 451 (1945); **16**, 13, 53, 124, 201, 329, 335, 378, 382, 635 (1946).
10. Hermans, P. H., "Contribution to the Physics of Cellulose Fibers," Amsterdam, Elsevier Publishing Co., 1946.
11. Hermans, P. H., *J. Polymer Sci.* **1**, 389 (1946).
12. Hermans, P. H., Hermans, J. J., Vermaas, D., and Weidinger, A., *J. Polymer Sci.* **1**, 393 (1946).
13. Ingersoll, H. G., *J. Applied Phys.* **17**, 924 (1946).
14. Leaderman, H., "Elasticity and Creep of High Polymers and Filamentous Materials," Washington, D. C., The Textile Foundation, 1943.
15. Mark, H., *Cellulose* ("High Polymers," Vol. V), New York, Interscience Publishers, Inc., 1943, Chap. IX, G.
16. Mark, H., and Press, J. J., *Rayon Text. Mo.* **24**, 57 (June 1943); 49 (July 1943); 45 (Aug. 1943).
17. Mark, H., and Whitney, G. S., editors, "Advances in Colloid Science," Vol. II, New York, Interscience Publishers, Inc., 1946.
18. Press, J. J., *J. Applied Phys.* **14**, 224 (1943).
19. Ray, L. G., Jr., TEXTILE RESEARCH JOURNAL **17**, 1 (1947).
20. Tobolsky, A., Wiederhorn, N., and Alfrey, T., *J. Polymer Sci.* In preparation.

APPENDIX

TABLE IV. TEXTILE RAYON, 24-HOUR CREEP, RECOVERY, AND SECOND CREEP, EXPERIMENTS OF OCTOBER 22–25, 1945

Pos.	Load	$E_{0.1}$	$T_{0.1}$	E_{1440}	T_{1440}	$R_{0.1}$	R_{1440}	$E_{1440}-R_{1440}$	$E(2)_{0.1}$*	$E(2)_{1440}$	$E(2)_{1440}-R_{1440}$
1	0.1	0.17	0.100	0.31	0.100	0.12	0.21	0.10	0.13	0.22	0.01
2	0.1	0.17	0.100	0.33	0.100	0.12	0.21	0.12	0.13	0.23	0.02
3	0.2	0.30	0.201	0.93	0.202	0.27	0.54	0.39	0.29	0.61	0.07
4	0.2	0.30	0.201	0.99	0.202	0.28	0.54	0.45	0.29	0.61	0.07
5	0.3	0.47	0.301	2.70	0.308	0.47	1.13	1.57	0.44	1.27	0.14
6	0.3	0.44	0.301	2.62	0.308	0.41	1.10	1.50	0.40	1.21	0.11
7	0.4	0.69	0.403	5.42	0.422	0.60	1.90	3.52	0.61	2.09	0.19
8	0.4	0.67	0.403	5.27	0.422	0.60	1.83	3.44	0.61	2.01	0.18
9	0.5	1.10	0.506	7.87	0.539	0.80	2.58	5.29	0.90	2.80	0.22
10	0.5	1.00	0.505	7.83	0.539	0.80	2.57	5.26	0.90	2.70	0.13
11	0.6	2.20	0.613	9.91	0.660	1.10	3.20	6.71	1.37	3.41	0.21
12	0.6	2.20	0.613	9.90	0.660	1.09	3.19	6.71	1.20	3.43	0.24
13	0.7	4.90	0.734	11.60	0.782	1.40	3.70	7.90	1.90	3.99	0.29
14	0.7	4.30	0.730	11.64	0.782	1.40	3.70	7.94	1.89	3.99	0.29
15	0.8	6.00	0.848	13.30	0.905	1.80	4.19	9.11	2.41	4.53	0.34
16	0.8	6.30	0.850	13.15	0.905	1.77	4.17	8.98	2.57	4.57	0.40
17	0.9	7.80	0.970	14.32	1.030	2.00	4.48	9.84	3.00	4.90	0.42
18	0.9	7.80	0.970	14.41	1.030	2.04	4.50	9.91	2.90	4.99	0.49
19	1.0	10.00	1.100	16.80	1.170	2.59	5.08	11.72	3.68	5.79	0.71
20	1.0	10.20	1.100	16.90	1.170	2.57	5.08	11.82	3.70	5.81	0.73

* $E(2)$ = Net elongation in second creep.

TABLE V. TEXTILE RAYON, 24-HOUR CREEP AND RECOVERY DATA, EXPERIMENTS OF MAY 2–5, 1946—SAMPLES FROM SPOOL

Pos.	Load	$E_{0.1}$	$T_{0.1}$	E_{1440}	T_{1440}	$R_{0.1}$	R_{1440}	$E_{1440}-R_{1440}$
5	0.10	0.12	0.100	0.33	0.100	0.11	0.23	0.10
6	0.20	0.28	0.200	0.81	0.202	0.27	0.46	0.35
7	0.30	0.40	0.301	2.02	0.306	0.38	1.01	1.01
8	0.40	0.64	0.403	4.28	0.417	0.60	1.78	2.50
9	0.40	0.60	0.402	3.89	0.416	0.52	1.60	2.29
10	0.50	1.00	0.505	6.80	0.534	0.78	2.50	4.30
11	0.50	1.00	0.505	6.87	0.534	0.80	2.50	4.37
12	0.60	1.90	0.612	9.07	0.654	0.99	3.10	5.97
13	0.60	1.90	0.612	9.00	0.654	0.99	3.08	5.92
14	0.70	3.15	0.722	10.70	0.775	1.27	3.60	7.10
15	0.70	3.20	0.722	10.67	0.775	1.28	3.60	7.07
16	0.80	5.00	0.840	12.40	0.899	1.58	4.09	8.31
17	0.80	5.20	0.842	12.59	0.901	1.62	4.11	8.48
18	0.90	7.30	0.966	13.90	1.020	2.00	4.49	9.41
19	0.90	7.30	0.966	14.10	1.030	2.00	4.52	9.58
20	1.00	8.70	1.087	15.90	1.160	2.40	4.99	10.91
21	1.13	10.80	1.252	18.61	1.340	2.96	5.51	13.10
22	1.10	10.40	1.214	17.70	1.290	2.70	5.40	12.30
23	1.10	10.40	1.214	17.70	1.290	2.80	5.70	12.00
24	1.20	10.90	1.331	19.27	1.430	3.13	5.72	13.55
25	1.20	11.60	1.339	19.71	1.440	3.20	6.09	13.62

TABLE VI. TEXTILE RAYON, 24-HOUR CREEP, RECOVERY, AND SECOND CREEP, EXPERIMENTS OF MAY 7–10, 1946—SAMPLES FROM SKEIN

Pos.	Load	$E_{0.1}$	$T_{0.1}$	E_{1440}	T_{1440}	$R_{0.1}$	R_{1440}	$E_{1440}-R_{1440}$	$E(2)_{0.1}$	$E(2)_{1440}$	$E(2)_{1440}-R_{1440}$
5	0.4	0.69	0.403	4.00	0.416	0.56	1.59	2.41	0.58	1.78	0.19
6	0.5	0.91	0.505	6.68	0.533	0.78	2.24	4.44	0.77	2.41	0.17
7	0.6	1.37	0.608	8.91	0.653	0.99	2.82	6.09	1.10	3.01	0.19
8	0.7	3.09	0.723	10.79	0.776	1.20	3.49	7.30	1.57	3.58	0.09
9	0.8	6.00	0.848	12.49	0.900	1.65	3.80	8.69	2.08	4.04	0.24
10	0.9	8.10	0.973	17.10*	1.050	1.98	4.42	12.68	2.67	4.40	−0.02*
11	1.1	11.10	1.220	17.90	1.300	2.69	5.01	12.89	3.70	5.80	0.79
12	1.1	10.90	1.220	17.79	1.300	2.62	5.00	12.79	3.68	5.72	0.72
13	1.2	12.20	1.350	19.99	1.440	3.10	5.41	14.58	4.20	6.56	1.15

* Omitted from plots—broken filaments.

TABLE VII. TEXTILE "CORDURA," 24-HOUR CREEP, RECOVERY, AND SECOND CREEP, EXPERIMENTS OF NOVEMBER 19–22, 1945

Pos.	Load	$E_{0.1}$	$T_{0.1}$	E_{1440}	T_{1440}	$R_{0.1}$	R_{1440}	$E_{1440}-R_{1440}$	$E(2)_{0.1}$	$E(2)_{1440}$	$E(2)_{1440}-R_{1440}$
1	0.2	0.22	0.200	0.38	0.200	0.19	0.29	0.09	0.20	0.32	0.03
2	0.2	0.22	0.200	0.38	0.200	0.20	0.30	0.08	0.20	0.32	0.02
3	0.4	0.40	0.402	1.19	0.405	0.31	0.70	0.49	0.38	0.94	0.24
4	0.4	0.41	0.402	1.11	0.404	0.34	0.70	0.41	0.36	0.92	0.22
5	0.5	0.51	0.503	2.05	0.510	0.42	1.08	0.97	0.49	1.32	0.24
6	0.5	0.50	0.503	2.09	0.510	0.42	1.08	1.01	0.48	1.33	0.25
7	0.6	0.69	0.604	3.22	0.619	0.56	1.48	1.74	0.60	1.72	0.24
8	0.6	0.69	0.604	3.19	0.619	0.54	1.46	1.73	0.60	1.72	0.26
9	0.7	0.80	0.706	4.10	0.729	0.64	1.71	2.39	0.71	2.02	0.31
10	0.7	0.81	0.706	4.18	0.729	0.63	1.80	4.77	0.71	2.10	0.30
11	0.8	1.11	0.809	5.13	0.841	0.87	2.18	2.95	0.90	2.44	0.26
12	0.8	1.19	0.810	5.13	0.841	0.80	2.19	2.94	0.99	2.47	0.28
13	0.9	1.70	0.915	5.90	0.953	0.92	2.43	3.47	1.18	2.72	0.29
14	0.9	1.80	0.916	6.01	0.954	0.92	2.48	3.53	1.21	2.77	0.29
15	1.0	2.30	1.020	6.71	1.070	1.10	2.70	4.00	1.49	3.02	0.32
16	1.0	2.40	1.020	6.77	1.070	1.15	2.79	3.98	1.41	3.03	0.24
17	1.2	4.80	1.260	8.50	1.300	1.58	3.34	5.16	2.23	3.71	0.37
18	1.2	4.70	1.260	8.30	1.300	1.50	3.30	5.00	2.21	3.69	0.39
19	1.4	6.10	1.490	9.72	1.540	2.00	3.78	5.94	2.80	4.20	0.42
20	1.4	6.10	1.490	9.72	1.540	2.05	3.79	5.93	2.84	4.20	0.41
21	1.6	7.50	1.720	11.50	1.780	2.50	4.30	7.20	3.40	4.68	0.38
22	1.6	7.60	1.720	11.16	1.780	2.60	4.28	7.33	3.50	4.81	0.53

TABLE VIII. TEXTILE RAYON, SEPARATION EXPERIMENTS

Sample	Load	t (min.)		$E_{0.1}$	E_t	$R_{0.1}$	R_{1440}	E_t-R_{1440}	Date
3–1	0.3	0.5		0.48	0.50	0.47	0.50	0.00	10/23/45
3–2	0.3	0.5		0.49	0.53	0.46	0.53	0.00	10/23/45
3–3	0.3	10.0		0.49	0.78	0.48	0.69	0.09	10/23/45
3–4	0.3	10.0		0.47	0.76	0.47	0.67	0.09	10/23/45
			Av.	0.48					
4–1	0.4	0.5		0.60	0.70	0.60	0.70	0.00	10/25/45
4–2	0.4	0.5		0.68	0.80	0.69	0.80	0.00	10/25/45
4–3	0.4	10.0		0.70	2.00	0.79	1.60	0.40	10/25/45
4–4	0.4	10.0		0.68	2.02	0.76	1.45	0.57	10/25/45
4–5	0.4	120.0		0.66	4.21	0.71	2.04	2.17	10/25/45
4–6	0.4	120.0		0.63	4.18	0.72	2.06	2.12	10/25/45
			Av.	0.66					
5–1	0.5	0.5		1.09	1.68	1.17	1.47	0.21	10/25/45
5–2	0.5	0.5		1.00	1.59	1.11	1.39	0.20	10/25/45
5–3	0.5	10.0		0.98	4.81	1.26	2.69	2.12	10/25/45
5–4	0.5	10.0		1.00	4.81	1.30	2.71	2.10	10/25/45
5–5	0.5	120.0		0.94	6.53	0.86	2.82	3.71	10/25/45
5–6	0.5	120.0		1.00	6.65	1.02	2.84	3.81	10/25/45
			Av.	1.00					
6–1	0.6	0.1		1.50	—	1.20	1.39	0.11	10/29/45
6–2	0.6	0.1		1.50	—	1.26	1.40	0.10	10/29/45
6–3	0.6	0.5		1.93	3.90	1.90	2.72	1.18	10/29/45
6–4	0.6	0.5		1.78	3.98	1.91	2.77	1.21	10/29/45
6–5	0.6	2.0		1.68	5.90	2.00	3.39	2.51	10/29/45
6–6	0.6	2.0		1.70	5.70	1.90	3.30	2.40	10/29/45
6–7	0.6	10.0		1.70	7.49	1.79	3.65	3.84	10/29/45
6–8	0.6	10.0		1.80	7.31	1.71	3.53	3.78	10/29/45
			Av.	1.70					
7–1	0.7	0.1		3.70	—	2.18	2.83	0.87	10/29/45
7–2	0.7	0.1		3.50	—	2.20	2.71	0.79	10/29/45
7–3	0.7	0.5		3.70	6.42	2.62	3.84	2.58	10/29/45
7–4	0.7	0.5		3.80	6.50	2.60	3.90	2.60	10/29/45
7–5	0.7	2.0		3.80	7.56	2.36	3.97	3.59	10/29/45
7–6	0.7	2.0		3.20	7.62	2.32	3.98	3.64	10/29/45
7–7	0.7	10.0		3.58	9.25	2.15	4.15	5.10	10/29/45
7–8	0.7	10.0		3.90	9.20	2.10	4.12	5.08	10/29/45
7–9	0.7	120.0		2.90	9.80	1.55	3.72	6.08	10/29/45
7–10	0.7	120.0		3.40	10.11	1.65	3.80	6.31	10/29/45
			Av.	3.54					
8–1	0.8	0.1		6.00	—	2.87	3.98	2.02	10/30/45
8–2	0.8	0.1		6.00	—	2.83	3.90	2.10	10/30/45
8–3	0.8	0.5		6.04	8.67	3.17	4.68	3.99	10/30/45
8–4	0.8	0.5		6.12	8.78	3.19	4.74	4.04	10/30/45
8–5	0.8	2.0		5.70	10.00	2.96	4.79	5.21	10/30/45
8–6	0.8	2.0		6.13	10.30	3.00	4.89	5.41	10/30/45
8–7	0.8	10.0		6.20	11.20	2.62	4.77	6.43	10/30/45
8–8	0.8	10.0		6.10	11.19	2.68	4.73	6.46	10/30/45
			Av.	6.05					
9–1	0.9	0.1		6.90	—	3.13	4.40	2.50	10/30/45
9–2	0.9	0.1		7.00	—	3.14	4.31	2.69	10/30/45
9–3	0.9	0.5		7.30	9.90	3.40	5.11	4.79	10/30/45
9–4	0.9	0.5		7.40	9.73	3.43	5.05	4.68	10/30/45
9–5	0.9	2.0		7.70	11.37	3.27	5.18	6.19	10/30/45
9–6	0.9	2.0		7.40	11.30	3.21	5.17	6.13	10/30/45
9–7	0.9	10.0		7.30	12.18	2.88	5.01	7.17	10/30/45
9–8	0.9	10.0		7.30	11.78	3.00	5.01	6.77	10/30/45
			Av.	7.21					

TABLE VIII—*Continued*

Sample	Load	t (min.)	$E_{0.1}$	E_t	$R_{0.1}$	R_{1440}	E_t–R_{1440}	Date
10–1	1.0	0.1	9.60	—	3.60	5.27	4.33	11/9/45
10–2	1.0	0.1	9.60	—	3.70	5.30	4.30	11/9/45
10–3	1.0	0.5	9.65	12.00	4.00	5.74	6.26	11/9/45
10–4	1.0	0.5	9.70	12.00	4.00	5.79	6.21	11/9/45
10–5	1.0	2.0	9.75	13.42	3.82	5.75	7.67	11/9/45
10–6	1.0	2.0	9.70	13.31	3.82	5.76	7.55	11/9/45
10–7	1.0	10.0	9.65	14.31	3.69	5.64	8.67	11/9/45
10–8	1.0	10.0	9.75	14.25	3.55	5.67	8.58	11/9/45
		Av.	9.67					
11–1	1.1	0.1	11.00	—	4.05	5.78	5.22	11/9/45
11–2	1.1	0.1	11.00	—	4.03	5.76	5.24	11/9/45
11–3	1.1	0.5	11.00	13.20	4.30	6.13	7.07	11/9/45
11–4	1.1	0.5	10.90	13.10	4.23	6.23	6.87	11/9/45
11–5	1.1	2.0	11.40	14.83	4.23	6.17	8.66	11/9/45
11–6	1.1	2.0	11.10	14.82	4.27	6.16	8.68	11/9/45
11–7	1.1	10.0	11.10	15.92	4.02	6.02	9.80	11/9/45
11–8	1.1	10.0	11.20	16.00	3.95	6.11	9.89	11/9/45
		Av.	11.09					
12–1	1.2	0.1	12.70	—	4.50	6.33	6.37	11/9/45
12–2	1.2	0.1	12.60	—	4.40	6.27	6.34	11/9/45
12–3	1.2	0.5	12.20	14.60	4.80	6.54	8.06	11/9/45
12–4	1.2	0.5	12.40	14.70	4.80	6.59	8.11	11/9/45
12–5	1.2	2.0	12.70	16.43	4.68	6.70	9.73	11/9/45
12–6	1.2	2.0	12.65	16.12	4.62	6.54	9.57	11/9/45
12–7	1.2	10.0	12.40	17.29	4.09	6.37	10.92	11/9/45
12–8	1.2	10.0	12.50	17.55	—	6.45	11.10	11/9/45
		Av.	12.52					
13–1	1.3	0.1	13.25	—	4.65	6.35	6.90	1/2/46
13–2	1.3	0.1	13.00	—	4.50	6.29	6.71	1/2/46
13–3	1.3	0.5	13.10	14.80	4.60	6.50	8.30	1/2/46
13–4	1.3	0.5	13.00	15.00	4.50	6.51	8.49	1/2/46
13–5	1.3	2.0	13.15	16.99	4.78	6.69	10.30	1/2/46
13–6	1.3	2.0	13.50	17.35	4.92	6.76	10.59	1/2/46
		Av.	13.20					
14–1	1.4	0.1	14.20	—	4.85	6.67	7.51	1/2/46
14–2	1.4	0.1	14.50	—	5.00	6.79	7.71	1/2/46
14–3	1.4	0.5	14.40	16.80	5.15	7.03	9.77	1/2/46
14–4	1.4	0.5	14.40	16.80	5.17	7.00	9.80	1/2/46
14–5	1.4	2.0	14.50	Broke	—	—	—	1/2/46
14–6	1.4	2.0	14.40	Br.	—	—	—	1/2/46
		Av.	14.40					
15–1	1.5	0.1	15.70	—	5.20	7.10	8.60	1/2/46
15–2	1.5	0.1	15.50	—	5.08	7.00	8.50	1/2/46
15–3	1.5	0.5	15.60	Br.	—	—	—	1/2/46
		Av.	15.60					
16–1	1.6	0.1	16.85	—	5.30	7.36	9.49	1/2/46
16–2	1.6	0.1	17.00	—	5.40	7.38	7.62	1/2/46

TABLE IX. TEXTILE "CORDURA," SEPARATION EXPERIMENTS

Sample	Load	t (min.)	$E_{0.1}$	E_t	$R_{0.1}$	R_{1440}	$E_t - R_{1440}$	Date
4–1	0.4	0.5	0.40	0.40	0.39	0.40	0.00	11/28/45
4–2	0.4	0.5	0.40	0.40	0.39	0.40	0.00	11/28/45
4–3	0.4	10.0	0.40	0.50	0.38	0.50	0.00	11/28/45
4–4	0.4	10.0	0.40	0.51	0.39	0.51	0.00	11/28/45
4–5	0.4	120.0	0.40	0.78	0.38	0.67	0.11	11/28/45
4–6	0.4	120.0	0.40	0.72	0.33	0.61	0.11	11/28/45
		Av.	0.40					
5–1	0.5	0.1	0.50	—	0.49	0.50	0.00	11/28/45
5–2	0.5	0.1	0.51	—	0.50	0.51	0.00	11/28/45
5–3	0.5	0.5	0.51	0.59	0.51	0.59	0.00	11/28/45
5–4	0.5	0.5	0.51	0.59	0.56	0.59	0.00	11/28/45
5–5	0.5	0.5	0.51	0.58	0.53	0.58	0.00	11/28/45
5–6	0.5	0.5	0.51	0.58	0.55	0.58	0.00	11/28/45
5–7	0.5	2.0	0.51	0.63	0.53	0.63	0.00	11/28/45
5–8	0.5	2.0	0.51	0.66	0.54	0.62	0.01	11/28/45
5–9	0.5	10.0	0.62	0.98	0.50	0.78	0.20	11/28/45
5–10	0.5	10.0	0.52	0.90	0.52	0.80	0.10	11/28/45
5–11	0.5	10.0	0.51	0.73	0.50	0.72	0.01	11/28/45
5–12	0.5	10.0	0.50	0.72	0.51	0.71	0.01	11/28/45
5–13	0.5	120.0	0.51	1.34	0.46	1.01	0.33	11/28/45
5–14	0.5	120.0	0.54	1.43	0.51	1.03	0.40	11/28/45
		Av.	0.52					
6–1	0.6	120.0	0.68	2.49	0.68	1.50	0.99	11/28/45
6–2	0.6	120.0	0.62	2.39	0.60	1.47	0.92	11/28/45
		Av.	0.65					
7–1	0.7	0.1	0.78	—	0.75	0.78	0.00	11/29/45
7–2	0.7	0.1	0.73	—	0.71	0.73	0.00	11/29/45
7–3	0.7	0.5	0.78	0.90	0.80	0.90	0.00	11/29/45
7–4	0.7	0.5	0.78	0.90	0.80	0.90	0.00	11/29/45
7–5	0.7	2.0	0.81	1.23	0.85	1.13	0.10	11/29/45
7–6	0.7	2.0	0.79	1.13	0.80	1.04	0.09	11/29/45
7–7	0.7	10.0	0.80	1.71	0.87	1.41	0.30	11/29/45
7–8	0.7	10.0	0.78	1.59	0.87	1.37	0.22	11/29/45
7–9	0.7	120.0	0.80	3.50	0.76	1.90	1.60	11/28/45
7–10	0.7	120.0	0.82	3.61	0.80	1.91	1.70	11/28/45
		Av.	0.79					
9–1	0.9	0.1	1.32	—	1.14	1.31	0.01	11/30/45
9–2	0.9	0.1	1.40	—	1.21	1.35	0.05	11/30/45
9–3	0.9	0.5	1.60	2.55	1.62	2.15	0.40	11/30/45
9–4	0.9	0.5	1.40	2.17	1.49	1.89	0.28	11/30/45
9–5	0.9	2.0	1.30	2.93	1.37	2.18	0.75	11/30/45
9–6	0.9	2.0	1.33	3.03	1.45	2.29	0.74	11/30/45
9–7	0.9	10.0	1.38	3.87	1.44	2.48	1.39	11/30/45
9–8	0.9	10.0	1.40	3.98	1.35	2.53	1.45	11/30/45
		Av.	1.40					
10–1	1.0	0.1	2.00	—	1.57	1.85	0.15	11/29/45
10–2	1.0	0.1	2.20	—	1.68	2.00	0.20	11/29/45
10–3	1.0	0.5	2.20	3.38	1.88	2.58	0.80	11/29/45
10–4	1.0	0.5	2.08	3.19	1.79	2.49	0.70	11/29/45
10–5	1.0	2.0	2.20	4.22	1.73	2.81	1.41	11/29/45
10–6	1.0	2.0	2.38	4.29	1.79	2.81	1.48	11/29/45
10–7	1.0	10.0	2.28	4.93	1.55	2.87	2.06	11/29/45
10–8	1.0	10.0	2.28	4.90	1.58	2.88	2.02	11/29/45
		Av.	2.20					
12–1	1.2	0.1	4.30	—	2.31	3.18	1.12	12/3/45
12–2	1.2	0.1	4.34	—	2.34	3.13	1.21	12/3/45
12–3	1.2	0.5	4.10	5.10	2.35	3.30	1.80	12/3/45
12–4	1.2	0.5	4.10	5.10	2.39	3.30	1.80	12/3/45
12–5	1.2	2.0	4.10	5.90	2.20	3.40	2.50	12/3/45
12–6	1.2	2.0	4.10	5.90	2.20	3.40	2.50	12/3/45
12–7	1.2	10.0	4.20	6.42	2.01	3.36	3.10	12/3/45
12–8	1.2	10.0	4.00	6.47	1.97	3.37	3.10	12/3/45
		Av.	4.15					

TABLE IX—*Continued*

Sample	Load	t (min.)	$E_{0.1}$	E_t	$R_{0.1}$	R_{1440}	E_t-R_{1440}	Date
14–1	1.4	0.1	6.10	—	2.87	3.88	2.22	12/3/45
14–2	1.4	0.1	5.90	—	2.78	3.79	2.11	12/3/45
14–3	1.4	0.5	5.70	6.61	2.89	3.91	2.70	12/3/45
14–4	1.4	0.5	6.00	6.80	2.80	3.95	2.85	12/3/45
14–5	1.4	2.0	5.90	7.38	2.68	3.89	3.49	12/3/45
14–6	1.4	2.0	5.90	7.32	2.58	3.87	3.45	12/3/45
14–7	1.4	10.0	6.10	8.01	2.42	3.86	4.15	12/3/45
14–8	1.4	10.0	5.90	8.00	2.50	3.90	4.10	12/3/45
		Av.	5.92					
16–1	1.6	0.1	7.25	—	3.05	4.25	3.00	12/3/45
16–2	1.6	0.1	7.20	—	3.20	4.31	2.89	12/3/45
16–3	1.6	0.5	7.13	8.04	3.16	4.36	3.68	12/3/45
16–4	1.6	0.5	7.40	8.28	3.28	4.48	3.80	12/3/45
16–5	1.6	2.0	7.20	8.71	3.11	4.48	4.33	12/3/45
16–6	1.6	2.0	7.22	8.71	3.01	4.44	4.37	12/3/45
16–7	1.6	10.0	7.40	9.46	3.00	4.36	5.12	12/3/45
16–8	1.6	10.0	7.10	Broke	—	—	—	12/3/45
		Av.	7.24					
18–1	1.8	0.1	9.10	—	3.80	5.00	4.00	1/3/46
18–2	1.8	0.1	9.30	—	3.88	5.13	4.17	1/3/46
18–3	1.8	0.5	9.20	10.45	4.00	5.28	5.17	1/3/46
18–4	1.8	0.5	9.00	10.10	3.85	5.15	4.95	1/3/46
18–5	1.8	2.0	9.00	10.61	3.81	5.19	5.42	1/3/46
18–6	1.8	2.0	9.30	11.40	4.00	5.29	6.11	1/3/46
		Av.	9.15					
20–1	2.0	0.1	10.10	—	4.10	5.42	4.68	1/3/46
20–2	2.0	0.1	10.20	—	4.12	5.42	4.78	1/3/46
20–3	2.0	0.5	9.90	10.98	4.08	5.38	5.60	1/3/46
20–4	2.0	0.5	10.00	10.90	3.92	5.38	5.52	1/3/46
20–5	2.0	2.0	10.22	12.00	4.00	5.45	5.55	1/3/46
20–6	2.0	2.0	10.20	12.46	4.00	5.57	6.89	1/3/46

TABLE X. WET CREEP DATA FOR TEXTILE RAYON

Load	E_w	$E_{0.1}$	$T_{0.1}$*	E_{1440}	T_{1440}*	$R_{0.1}$	R_{1440}	$E_{1440}-R_{1440}$	$E(2)_{0.1}$	$E(2)_{1440}$
0.05	4.82	2.99	0.0539	4.77	0.0548	1.81	3.13	1.64	2.20	3.10
0.10	4.90	5.65	0.111	7.53	0.112	3.54	5.28	2.25	4.25	5.22
0.20	4.73	8.95	0.228	11.29	0.232	5.82	7.84	3.45	6.93	8.04
0.30	4.85	11.68	0.349	15.41	0.361	8.29	10.57	4.84	9.69	10.86
0.40	4.28	15.15	0.478	21.09	0.500	11.12	14.00	7.09	—	—

* Corrected for elongation upon wetting out as well as for creep elongation. E_w = elongation upon wetting.

TABLE XI. WET CREEP DATA FOR TEXTILE "CORDURA"

Load	E_w*	$E_{0.1}$	$T_{0.1}$	E_{1440}	T_{1440}	$R_{0.1}$	R_{1440}	$E_{1440}-R_{1440}$	$E(2)_{0.1}$	$E(2)_{1440}$	$E(2)_{1440}-R_{1440}$
0.1	1.81	2.92	0.104	4.36	1.060	1.64	3.06	0.13	1.98	3.12	0.06
0.2	2.22	5.36	0.215	6.90	2.180	3.39	4.90	0.20	3.96	5.04	0.14
0.3	2.12	6.74	0.327	8.69	3.320	4.58	6.23	2.46	5.52	6.51	0.28
0.4	2.02	8.24	0.441	10.52	4.500	5.70	7.55	2.97	6.70	7.78	0.23
0.5	1.77	9.63	0.557	12.25	5.700	6.81	8.86	3.39	7.64	8.78	−0.08
0.6	1.76	11.22	0.678	14.42	0.697	7.80	10.17	4.25	9.22	10.17	0.00

* E_w = elongation upon wetting out.

TABLE XII. TEXTILE RAYON, SECOND CREEP AND RECOVERY OF SAMPLES MECHANICALLY CONDITIONED AT 1.0 G./DEN., EXPERIMENTS OF MAY 7–11, 1946—SAMPLES FROM SKEIN

	First creep cycle												
Pos.	$E_{0.1}$ (1 g./den.)	E_{1440}	$R_{0.1}$	R_{1440}	$E_{1440}-R_{1440}$	2nd load g./den.	T_0	$E(2)_{0.1}$	$T(2)_{0.1}$	$E(2)_{1440}$	$T(2)_{1440}$	$R(2)_{0.1}$	$R(2)_{1440}$
16	9.63	15.90	2.30	4.61	11.29	0.4	0.445	0.45	0.447	1.52	0.45	0.50	1.51
17	9.65	16.20	2.29	4.69	11.51	0.5	0.558	0.79	0.562	2.13	0.567	0.68	2.10
18	9.85	16.31	2.38	4.71	11.60	0.6	0.670	1.10	0.675	2.78	0.687	0.88	2.69
19	9.60	16.01	2.30	4.67	11.34	0.7	0.780	1.50	0.791	3.30	0.802	1.11	3.19
20	9.70	16.12	2.37	4.70	11.42	0.8	0.890	2.09	0.907	3.90	0.923	1.43	3.70
21	9.90	16.33	2.34	4.71	11.62	0.9	1.000	2.79	1.03	4.52	1.04	1.86	4.22
22	9.75	16.29	2.37	4.70	11.59	1.0	1.120	3.30	1.15	5.27	1.17	2.30	4.70
						$R_{49,000}$							
23	9.80	16.31	2.30	4.68	—	5.38	—	—	—	—	—	—	—
24	9.75	17.00	—	4.74	—	—	—	—	—	—	—	—	—
25	9.75	15.88	—	4.60	—	5.30	—	—	—	—	—	—	—
Av.	9.74	16.24											

Measurement of Friction Between Single Fibers*

II. Frictional Properties of Wool Fibers Measured by the Fiber-Twist Method

Joel Lindberg and Nils Gralén

Swedish Institute for Textile Research, Gothenburg, Sweden †

Introduction

The frictional properties of animal hairs are different from those of other fibers, and it is generally regarded that the felting properties of wool are due to its special frictional properties—namely, the difference in friction in the two directions (tip and root) of the fiber. The modification of the felting properties of wool has been the object of several investigations in order to produce nonshrinkable wool fabrics. Another practical interest in such studies is the possibility of increasing the velocity of felting in a milling machine, thus diminishing the time for producing a certain felt.

Therefore it is considered very important to obtain as accurate measurement of the frictional properties as possible and a sound interpretation of their relation to the felting of wool. Several attempts have been made during the last two decades to do this. Some of the principles involved in these measurements will be mentioned in this paper.

The first successful attempts were made by Speakman and collaborators [17], and the method is referred to as the "violin bow" method. A mat of several fibers oriented in the same direction is arranged between two edges, as over two violin bridges. This mat is placed at an inclined plane and the inclination is increased until slipping occurs. By the application of a wool material to the inclined plane, it is possible to determine the wool-wool frictional coefficient. Bohm [2] used the same principle for establishing a fiber mat, but placed it on a horizontal plate and applied the necessary pulling force by continually increasing a load attached to the fiber mat. Speakman and Chamberlain [16] have designed a special apparatus called a "lepidometer." The fiber is attached with its tip end to a torsional balance and rubbed between two plates, which move antiparallel to each other along the fiber. Lipson and Howard [9] and also Martin and Mittelmann [11] used the well-known principle of letting a string slip over a cylindrical surface. The frictional coefficient is given by $P_2/P_1 = e^{\mu\varphi}$, where P_1 and P_2 are the forces applied to the ends of the fiber when it slips, φ is the angle of contact, and μ is the frictional coefficient. Lipson and Howard used a keratin rod as a cylinder in order to get a surface of the same chemical composition as the wool fiber. They treated the keratin rod in the same way as the fiber in order to obtain changes in friction, and they claimed to get results that could be consistent for wool-wool friction. Mercer and Makinson [14] have pointed out that the interior keratin layer of horn is not likely to give the same effect as the surface layer of wool when treated according to a nonfelting process. Martin and Mittelmann [11] have used different materials for the cylinder surface and have also used a piece of cloth of the same wool as the single fiber attached to the rod. Mercer [13] has used the Bowden and Leben [3] stick-slip method for measuring the friction between a fiber and a piece of horn keratin.

However, it is of only minor interest to know the friction between a wool fiber and another material such as horn, glass, rubber, and so on. Hennings [8] measured the friction between single fibers by using the frictional force for damping the oscillation of a spiral spring. At this Institute some efforts have been devoted to the measurement of the friction between two single fibers. Gralén and Olofsson [6] have used a modification of the Bowden-Leben method. In their apparatus, the two fibers are fastened to holders, one of which is attached to a horizontal wheel moving with a constant low speed and the second one is attached to a balance which

* The first paper in this series appeared in the September, 1947, issue, page 488, of this JOURNAL, and in *Proceedings of the Swedish Institute for Textile Research*, No. 3 (1947). This one will be published also in the same *Proceedings*, No. 6 (May, 1948).

† Dr. Gralén is Director of the Institute.

is attached to a torsion wire. The balance axis is at right angles to the wire. The balance can be loaded with a convenient load which is acting as the normal force between the fibers. The maximum deviation of the piano wire gives the frictional force.

The measurements of wool fiber in this apparatus showed considerable dispersion, especially in the anti-scale direction. This is considered to be due to the small area of contact between the two fibers, which allows only a few scales to hook into each other. The nature and the shape of the scales are obviously very different in different parts of the fiber and consequently the values vary. In order to obtain a good average it is necessary to measure a large number of points along the fiber.

Therefore it was desired to have an apparatus for friction measurement with an increased area of contact. The principle used consists in twisting two fibers a certain number of turns and applying different loads at the fiber ends. By increasing the load at one of the four ends slippage can be produced, and the sizes of the loads give the frictional forces.

Theory for the Fiber Twist

Symbols used:

β = angle between the two fibers in the twist
R = curvature radius of the helix
r = fiber diameter
l = length of the twist
N = normal force per unit length or normal pressure
N_{tot} = total normal force between the two fibers
P = tension of the fiber
n = number of turns in the twist
μ = frictional coefficient
μ_{1s} = static with-scale frictional coefficient
μ_{1k} = kinetic with-scale frictional coefficient
μ_{2s} = static anti-scale frictional coefficient
μ_{2k} = kinetic anti-scale frictional coefficient
$d_s = \mu_{2s} - \mu_{1s}$
$d_k = \mu_{2k} - \mu_{1k}$
$\delta_s = \dfrac{\mu_{2s} - \mu_{1s}}{\mu_{2s} + \mu_{1s}}$
$\delta_k = \dfrac{\mu_{2k} - \mu_{1k}}{\mu_{2k} + \mu_{1k}}$
F = frictional force
Q = average scale resistance
A = total number of scales on a certain area of contact
c = fraction of active scales

Two cylindrical fibers with the same diameter are twisted around each other, as shown in Figure 1. The area of contact will be along the straight line A–A_1. The fiber tension is considered to be localized to the fiber axis and to have the value of P everywhere. The fiber axis forms a helix and the axis of the helix is the line A–A_1. The pitch angle of the helix is $\frac{\pi}{2} - \frac{\beta}{2}$. The curvature radius R of the helix is $\dfrac{r}{\sin^2 \frac{\beta}{2}}$. According to Figure 2, where dl is a small element of the helix,

$$dl = \frac{r d\alpha}{\sin \frac{\beta}{2}}. \tag{1a}$$

The angle at the center of curvature of the element dl is $d\varphi$.

$$\frac{r}{\sin^2 \frac{\beta}{2}} d\varphi = \frac{r d\alpha}{\sin \frac{\beta}{2}} \tag{1b}$$

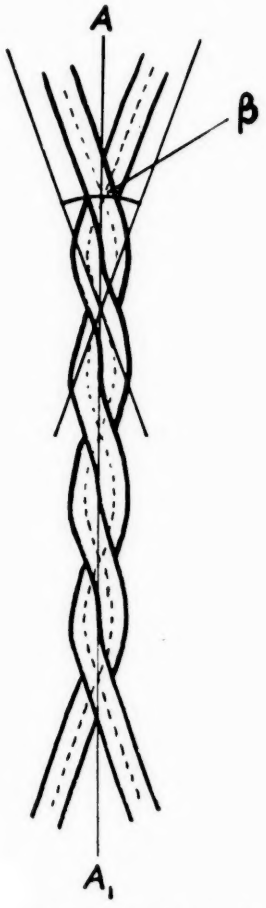

FIG. 1. *The fiber twist with 2 turns.*

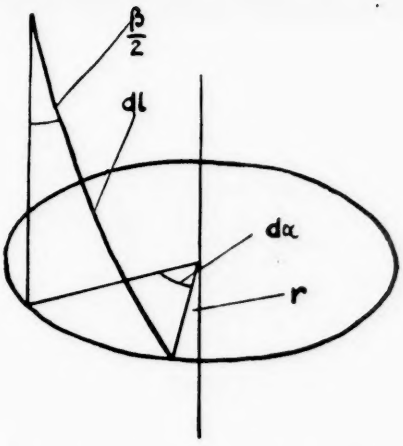

FIG. 2. *A small element* dl *of the helix.*

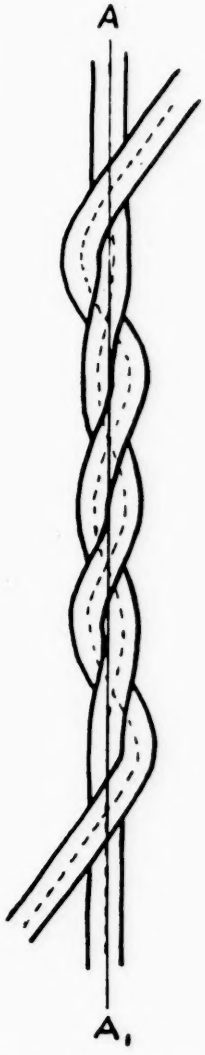

FIG. 4. *The distorted fiber twist.*

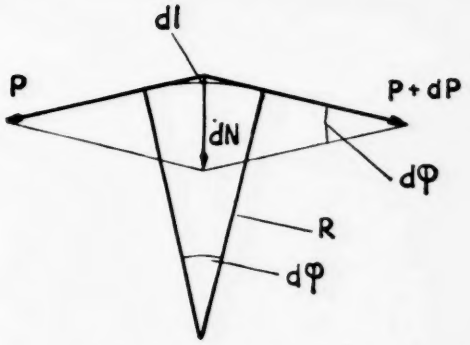

FIG. 3. *A small element* dl *of the helix with its radius of curvature,* R, *the angle at the center of curvature,* d, *and the forces acting on the element.*

and

$$d\varphi = \sin\frac{\beta}{2}\,d\alpha. \tag{1c}$$

The fiber tension is P (see Figure 3).

$$dN = Pd\varphi, \tag{2a}$$

$$dN = P\sin\frac{\beta}{2}\,d\alpha. \tag{2b}$$

This equation can be integrated between $\alpha = 0$ and $\alpha = 2\pi n$, where n is the number of turns.

$$\int_0^{N_{tot}} dN = P\sin\frac{\beta}{2}\int_0^{2\pi n} d\alpha. \tag{3}$$

$$N_{tot} = 2P\pi n\sin\frac{\beta}{2}. \tag{4}$$

Equation (4) expresses the total normal force acting between the two fibers.

If the tension in one end of two fibers is increased, the difference in tension between the two ends of the fiber will be accumulated by the friction between the fibers until the critical value is reached when the fibers will slip apart. During this operation the helix of the fiber axis will be distorted, as approximately shown in Figure 4.

If the complement of the pitch angle is smaller than 5° this means that the length of the twist is large in relation to the fiber diameter and the deformation of the original helix will be negligible, and therefore the curvature radius of the helix will be approximately the same at each point and the contact line will be approximately a straight line, as in the equilibrium state. The normal force over a small length dl of the twist is dN. Hence

$$\mu dN = dP. \tag{5}$$

From equations (5) and (2b):

$$\mu P \sin \frac{\beta}{2} d\alpha = dP. \tag{6}$$

As $\frac{\beta}{2}$ is a small angle, the angle can be substituted for the sine. Thus

$$\int_{P_1}^{P_2} \frac{dP}{P} = \mu \frac{\beta}{2} \int_0^{2\pi n} d\alpha. \tag{7a}$$

Integrating gives

$$\ln \frac{P_2}{P_1} = \mu \beta \pi n, \tag{7b}$$

$$\mu = \frac{\ln \frac{P_2}{P_1}}{\pi n \beta}. \tag{8}$$

The total normal force between the two fibers will be

$$N_{\text{tot}} = \frac{P_2 - P_1}{\mu}. \tag{9}$$

The normal force per unit length of the twist (the normal pressure) will be given by $\frac{N_{\text{tot}}}{l} = N$.

The Apparatus

Figure 5 is a full view of the apparatus. Figures 6A and 6B are drawings in two projections. The main parts of the apparatus are two torsional balances and two ordinary balances. To these four balances the four ends of the fiber twist are fixed (this is shown in Figure 7). The torsional balance consists of a lever, *A*, with a clip, *B*, at one end for fastening the fiber and a hook, *C*, at the other for an additional load. The lever, *A*, is fastened to a piano wire, *D*, acting as a supporter. This piano wire can be rotated by the screw *E*, thus adjusting the zero point of the balance, which is indicated by a metal tongue. The tension of the piano wire is regulated by the screw *F*. To the lever is fastened a torsional spiral, whose other end can be revolved by the handle *G* which is connected with the needle *H*, indicating the torsional moment on the scale. The balance is arrested by an eccentric cylinder, *I*. The levers of the lower balances *K* are bent so that

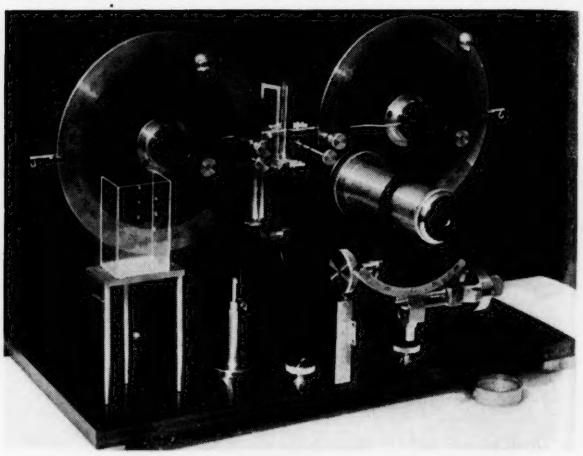

FIG. 5. *Full view of the apparatus.*

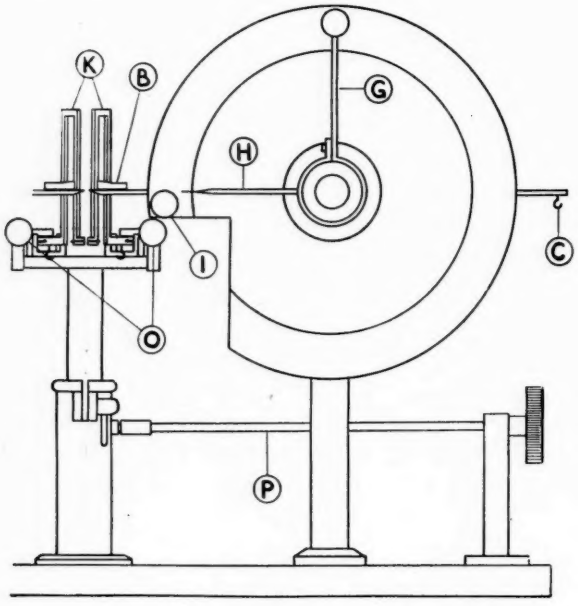

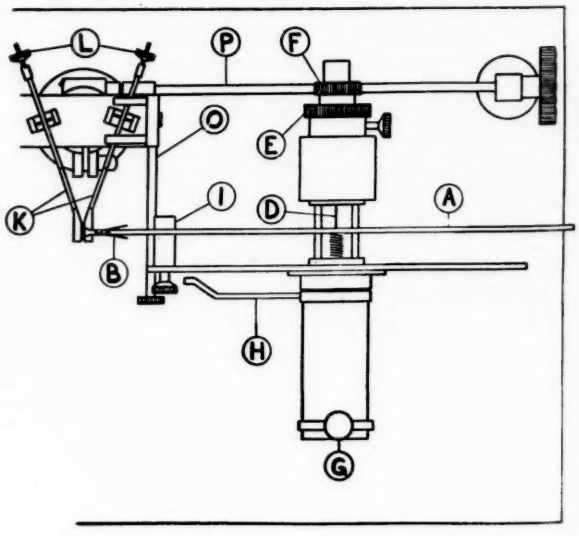

FIG. 6A (*left*) *and* FIG. 6B (*right*). *One-half of the apparatus shown in two projections.*

it is possible to immerse the twist in a fluid medium. On each balance is a screw, L, for adjusting the equilibrium, a hook, M, for the load, and a clip, N, for fastening the fiber. The balances are carried by steel needle bearings. In the edge just in front of each of the four clips is a slit through which the fiber is run, thus fixing it on a certain point of the balance. The lower balances are arrested by forks, O. The distance between the upper and lower balances is regulated by a rack-and-pinion, P.

Before any measurement is started the apparatus is calibrated. The torsional balances are calibrated by means of known loads. Then one fiber is stretched from the right of the upper balances to the left of the lower, and another fiber from the left of the upper to the right of the lower balances. The fibers are placed so that they cross each other at an angle of 5°, which is the same value as that used for β in the fiber twist. Then the different loads on the balances K are determined by weighing with the torsional balances, thus avoiding a correction term for the friction in the steel needle bearing. When the measurements are to be made in a liquid, the calibration is made with the balance levers immersed in the liquid, in order to correct for the buoyancy.

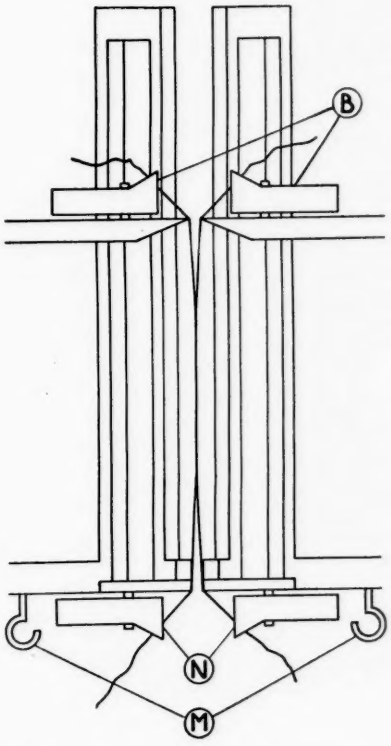

FIG. 7. *Details of the apparatus.*

The measurements are performed in the following way. A clip is attached to one end of each fiber. The fibers are then fixed to the upper balances by the clips B. The two free clips are parted by a plate which can be revolved in the holder. The fibers are twisted a certain number of turns by revolving this plate. When the distance between the upper and lower balances has been regulated to give a convenient angle β, the two fibers are fixed by the clips N. One fiber runs from the right-hand upper balance to the right-hand lower one, and the other from the left-hand upper to the left-hand lower. The force P_1 is applied to the fibers by means of the torsional balances, the lower balances being kept arrested. The same force is applied to the right-hand lower end by means of a load appended at the hook M. The size of this load should be known from the calibration. If the distance between the upper and the lower clips is changed by an eventual stretching of the fiber, it can be adjusted by moving the fiber in the clip B so that the metal tongue is kept at zero. For the measurement the right-hand lower balance is released, and the force of the right-hand torsional balance is continually increased, until slipping occurs. This value gives the force in the upper end of the fiber, P_{2s}. This value P_{2s} gives the static friction. In order to obtain the kinetic value, another procedure is necessary. The torsional balance is set at a certain value lower than P_{2s} and the balance A is given a small impulse by the arresting screw I. If the torsional force exceeds the frictional force owing to the kinetic friction, slipping will occur and the limit for slipping, P_{2k}, is determined by a few trials. The strength of the impulse within reasonable limits is found to have little influence. The value P_{2k} corresponds to the kinetic friction.

The measurements can be repeated on the left-hand fiber without changing the fibers in the twist. This is particularly of value in measurements of wool fibers. If one fiber is placed with its tip end upward, and the other with its tip end downward, the anti-scale friction can be measured at one side and the with-scale friction at the other.

The angle β between the fibers is measured by the microscope, which has a cross-haired eyepiece. The microscope can be revolved around its axis by means of a worm gear. The screw head is graduated for micrometer readings of the angle. A micrometer eyepiece is used for measuring and

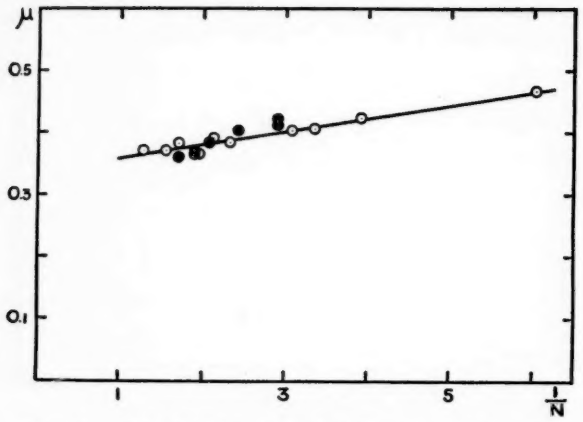

FIG. 8. *The frictional coefficient of nylon fiber at different loads.*

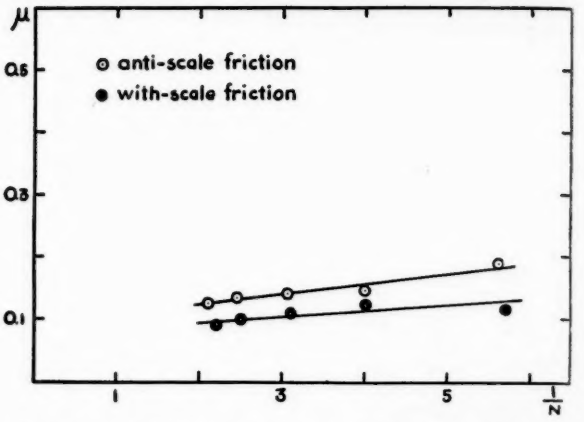

FIG. 9. *The frictional coefficient of air-dry wool at different normal pressures.*

controlling the length of the twist. The microscope can be moved in the vertical direction by a rack-and-pinion and its position read on a scale, which is provided with a vernier. The position of the lower balances is determined by using the microscope as a cathetometer. For focusing, the microscope can be moved in the horizontal direction by a rack-and-pinion.

Apparatus Tests

In order to test the apparatus and the reproducibility of the measurements, the friction of smooth nylon fibers was determined at different tensions and contact areas. The results are shown in Table I. Figure 8 gives the frictional coefficient versus the inverse value of the normal force per unit length of contact area. Only the static friction was measured.

The curve in Figure 8 seems to follow the equation

$$\mu = \mu_0 + k_1 \frac{S}{N}. \qquad (10)$$

The result is in agreement with that of Gralén and Olofsson [6]. Here S means the actual contact area, which might be considerably smaller than the apparent contact area. The value of S might be dependent on the normal pressure. The value of the frictional coefficient for different apparent contact areas (different n) has been investigated (nos. 16–21 in Table I; represented by the black dots in the diagram). Obviously, the variation of the contact area has practically no effect on the frictional coefficient.

If the tension of the fiber is too small it cannot overcome the rigidity of the fiber and the result will be a non-ideal twist. In this non-ideal twist the complement of the pitch angle will be smaller than the angle between the fibers, and since the pitch angle is determined by the radius of the fiber and the length of the twist, and the radius is constant, the complement of the pitch angle will be inversely

TABLE I. FRICTION BETWEEN AIR-DRY NYLON FIBERS
(σ = standard deviation of μ; ϵ = the probable statistical error of μ; m = number of measurements)

No.	N	$\frac{1}{N}$	μ	P_1	n	β	σ	ϵ	m
1	0.790	1.27	0.369	2.75	4.5	5.39	0.012	0.006	5
2	0.643	1.55	0.370	2.32	4.5	5.32	0.008	0.004	5
3	0.533	1.88	0.364	1.89	4.5	5.42	0.017	0.007	6
4	0.469	2.13	0.390	1.49	4.5	5.50			
5	0.300	3.35	0.405	1.06	4.5	5.53	0.018	0.009	5
6	0.224	4.46	0.447	0.66	4.5	5.60			
7	0.129	7.75	0.473	0.43	4.5	5.80			
8	0.593	1.69	0.382	3.06	4.5	4.39	0.014	0.007	5
9	0.517	1.94	0.365	2.75	4.5	4.43	0.006	0.003	5
10	0.430	2.32	0.382	2.32	4.5	4.45	0.012	0.006	5
11	0.324	3.08	0.402	1.87	4.5	4.15	0.020	0.009	5
12	0.256	3.90	0.422	1.49	4.5	4.17	0.014	0.007	5
13	0.166	6.02	0.467	1.06	4.5	4.26	0.017	0.008	5
14	0.118	8.45	0.467	0.66	4.5	4.27			
15	0.073	13.7	0.527	0.46	4.5	4.36			
16	0.346	2.89	0.422	2.32	1.5	4.24	0.017	0.009	5
17	0.347	2.89	0.412	2.32	2.5	4.37	0.014	0.007	5
18	0.413	2.42	0.402	2.32	3.5	4.40	0.014	0.007	5
19	0.483	2.07	0.384	2.32	4.5	4.67	0.013	0.007	5
20	0.529	1.89	0.367	2.32	5.5	4.77	0.011	0.006	5
21	0.588	1.70	0.359	2.32	6.5	4.91	0.008	0.004	5

TABLE II. FRICTION BETWEEN AIR-DRY WOOL FIBERS

No.	N	$\frac{1}{N}$	μ_{2s}	N	$\frac{1}{N}$	μ_{1s}	P_1	n	β
1	0.48	2.1	0.13	0.46	2.2	0.09	2.75	4.5	4.75
2	0.41	2.4	0.13	0.40	2.5	0.10	2.32	4.5	4.72
3	0.33	3.1	0.14	0.32	3.1	0.11	1.89	4.5	4.55
4	0.25	4.0	0.15	0.25	4.0	0.12	1.49	4.5	4.47
5	0.18	5.7	0.19	0.17	5.9	0.12	1.06	4.5	4.46

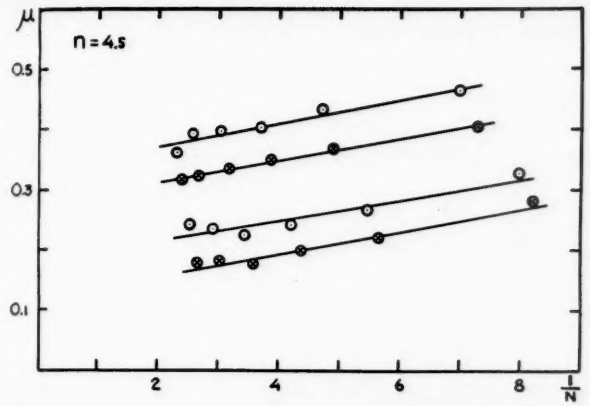

FIG. 10. *The frictional coefficient of wool in distilled water at different normal pressures.* n = 4.5.

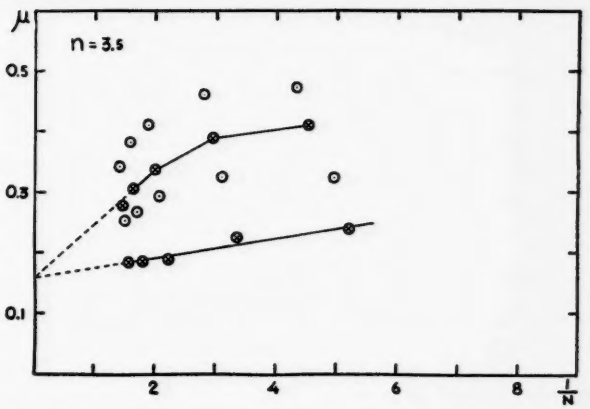

FIG. 11. *The frictional coefficient of wool in distilled water at different normal pressures.* n = 3.5.

proportional to the length of the twist. By measuring the length of the twist the minimum admitted value of the tension is determined. This was found to be about 1 g. for the nylon fibers, and also for wool fibers in water.

The difference between P_2 and P_1 should have the highest possible value with the object of diminishing the error, but P_2 is limited by the strength and the extensibility of the fiber. A value of 5° for β, 4.5 for the number of twists, and a value of 2 g. for P_1 have been found to give satisfactorily reproducible results for both nylon and wool.

In the tables, P_1 is given in g., N in g./mm., and β in degrees.

Measurements on Wool Fibers

In the following measurements, South American Full-Wool Chubut Merino 64s was used. It had been scoured in a factory.

Figure 9 and Table II show some measurements on air-dry wool fiber.

TABLE III. INFLUENCE OF REPEATED MEASUREMENTS ON THE ANTI-SCALE FRICTION
(EACH VALUE IS AN AVERAGE OF 5 READINGS)
(n = 4.5, P_1 = 2.18, β = 5.74°)

No.	μ_{2s}	No.	μ_{2s}
1	0.387	19	0.386
2	0.380	20	0.384
3	0.378	21	0.383
4	0.378	22	0.386
5	0.378	23	0.380
6	0.384	24	0.387
7	0.383	25	0.389
8	0.384	26	0.394
9	0.378	27	0.397
10	0.384	28	0.401
11	0.384	29	0.405
12	0.378	30	0.396
13	0.383	31	0.394
14	0.378	32	0.391
15	0.378	33	0.387
16	0.378	34	0.388
17	0.383	35	0.401
18	0.386	36	0.387

The coefficient of variation is 1.88%.

TABLE IV. FRICTION AT DIFFERENT NORMAL PRESSURES

	No.	N	$\frac{1}{N}$	μ_{2s}	N	$\frac{1}{N}$	μ_{2k}	N	$\frac{1}{N}$	μ_{1s}	N	$\frac{1}{N}$	μ_{1k}
n = 4.5	1	0.33	3.0	0.40	0.32	3.2	0.33	0.29	3.5	0.22	0.28	3.6	0.18
	2	0.27	3.7	0.40	0.26	3.9	0.35	0.24	4.2	0.24	0.23	4.4	0.20
	3	0.21	4.7	0.43	0.21	4.9	0.37	0.18	5.5	0.26	0.18	5.7	0.22
	4	0.14	7.0	0.46	0.14	7.3	0.40	0.13	8.0	0.33	0.12	8.2	0.28
	5	0.39	2.6	0.39	0.37	2.7	0.32	0.35	2.9	0.23	0.33	3.0	0.18
	6	0.44	2.3	0.36	0.42	2.4	0.31	0.40	2.5	0.24	0.38	2.7	0.18
n = 3.5	1	0.71	1.4	0.34	0.68	1.5	0.28	0.67	1.5	0.25	0.63	1.6	0.18
	2	0.64	1.6	0.38	0.61	1.6	0.31	0.59	1.7	0.27	0.55	1.8	0.19
	3	0.54	1.9	0.41	0.51	2.0	0.34	0.49	2.1	0.29	0.45	2.2	0.19
	4	0.36	2.8	0.46	0.34	3.0	0.39	0.32	3.1	0.33	0.30	3.4	0.23
	5	0.23	4.3	0.47	0.22	4.5	0.41	0.20	4.9	0.32	0.19	5.2	0.24

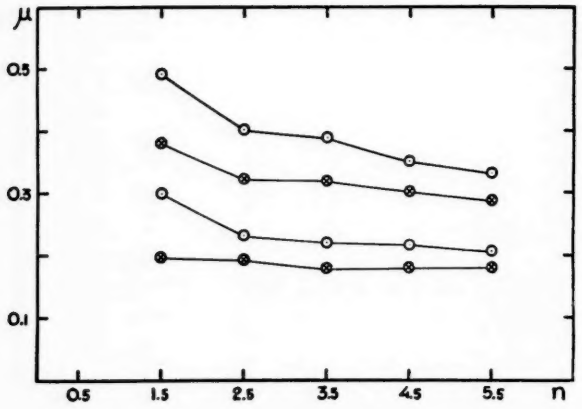

FIG. 12. *The frictional coefficient at different area of contact.*

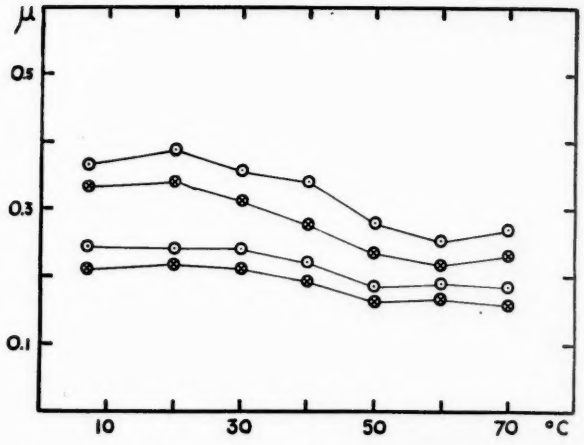

FIG. 13. *The variation of the frictional coefficient with temperature.*

Before the measurements the wool was cleaned according to the method of Mercer and Makinson [14], first by ether extraction, then by light soap-washing, and finally by a prolonged Soxhlet extraction with ether.

When the fibers were to be measured in a liquid medium they were immersed in that medium for at least 24 hours before the measurements.

A. Influence of Repeated Measurements on the Anti-Scale Friction

One hundred and eighty readings were taken and the averages of each 5 readings were determined. The measurements were performed in distilled water; the results are shown in Table III.

No noticeable variation in μ_{2s} due to abrasion of the fibers could be observed.

B. Variation of the Friction with Different Normal Pressures

The measurements were performed in distilled water; the results are shown in Table IV and Figures 10 and 11.

For $n = 4.5$ the curve μ *vs.* $\frac{1}{N}$ seems to follow the same equation as for the smooth nylon fiber, but for $n = 3.5$, and at considerably higher normal pressures, μ_{2s} and μ_{2k} decrease more rapidly.

C. Variation of Friction with Number of Turns

If β and P_1 are the same in each measurement, the normal pressure will also be the same. The apparent contact area will be proportional to the number of turns. The results are shown in Table V and Figure 12. The medium is distilled water.

At least the anti-scale friction seems to be dependent on the apparent area of contact and increases when this is diminished.

D. Variation of the Friction with the Temperature

The friction was measured in distilled water at different temperatures. The container was provided with a thermostat arrangement for these experiments. The results are shown in Table VI and Figures 13, 14, and 15.

From Table VI and Figure 13 it is evident that both the with-scale and the anti-scale frictions decrease with increasing temperature. The anti-scale friction seems to decrease more rapidly than the with-scale friction. There might be a minimum at 60°, or the curve might be horizontal at higher temperatures. The experiments made hitherto do not allow us to decide between these two possibilities. The investigation of this problem is to be continued.

E. Variation of the Friction at Various Points of the Fiber

The friction at different points along the fibers was measured in 7 cases and the results are shown in Table VII. The medium was distilled water.

TABLE V. FRICTION AT DIFFERENT NUMBER OF TURNS

$P_1 = 2.18$

n	μ_{2s}	μ_{2k}	μ_{1s}	μ_{1k}	β
1.5	0.49	0.38	0.30	0.20	5.33
2.5	0.40	0.32	0.23	0.19	5.37
3.5	0.39	0.32	0.22	0.18	5.37
4.5	0.35	0.30	0.22	0.18	5.44
5.5	0.33	0.29	0.21	0.18	5.26

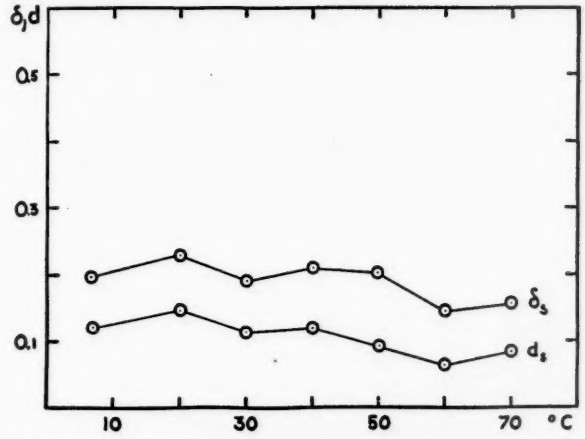

FIG. 14. *The variation of* δ_s *and* d_s *with temperature.*

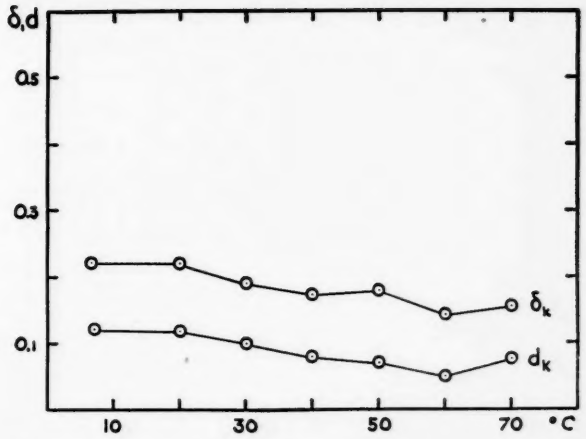

FIG. 15. *The variation of* δ_k *and* d_k *with temperature.*

These measurements were made to facilitate the estimation of the error due to the necessity of removing the fibers from the apparatus for special treatments. It is impossible to re-insert the fibers afterward in exactly reproducible position. It is seen that the variations are higher than in *A*.

F. Variation of the Friction with pH

McIlvaine's buffer solutions were used, from pH 2 to pH 9. These are made by mixing different amounts of 0.1*M* citric acid and 0.2*M* disodium phosphate. The fibers were immersed for 24 hours in the buffer solution of pH 2, then measured in this solution and afterward immersed in the solution of pH 3 for 24 hours, and so on. The results are given in Table VIII and Figures 16 and 17.

The friction was also measured in sulfuric acid at pH 1.2 and 2.4, in tap water at pH 7.5, and in sodium carbonate at pH 10.5 and 10.9. The results are shown in Table IX and Figure 18. The high value at pH 7 in Figure 16 is remarkable.

G. Friction After Different Treatments of the Fibers

The fibers were treated according to different processes for making wool unshrinkable. The measurements were performed in distilled water, and the same couple of fibers was used for the measurements before and after treatment. The result cannot be compared with milling tests, because milling is generally performed in other media than distilled water. Measurements at different milling conditions are being performed and will soon be published.

TABLE VI. FRICTION AT DIFFERENT TEMPERATURES

$P_1 = 2.8$ $n = 4.5$

Temp. (°C)	μ_{2s}	μ_{2k}	μ_{1s}	μ_{1k}	d_s	d_k	δ_s	δ_k
6–8	0.37	0.33	0.25	0.21	0.12	0.12	0.20	0.22
20	0.39	0.34	0.24	0.22	0.15	0.12	0.23	0.22
30	0.36	0.31	0.24	0.21	0.12	0.10	0.19	0.19
40	0.34	0.28	0.22	0.19	0.12	0.08	0.21	0.17
50	0.28	0.24	0.19	0.16	0.09	0.07	0.20	0.18
60	0.25	0.22	0.19	0.17	0.06	0.05	0.15	0.14
70	0.27	0.23	0.18	0.16	0.09	0.08	0.19	0.20

1. Alcoholic Potassium Hydroxide [13]. The fibers were immersed for 1½ minutes in 7-percent alcoholic solution of KOH. This was followed by neutralization in 7-percent alcoholic solution of sulfuric acid, and thorough washing in distilled water; 95-percent alcohol was used. The results are averages from measurements of 3 different couples of fibers.

2. Alcoholic Sodium Hydroxide [7]. The fibers were treated for 1 hour in a solution of 0.64 g. NaOH in 100 ml. *n*-butylalcohol, neutralized in alcoholic sulfuric acid, and washed thoroughly in distilled water.

3. Aqueous Chlorine [9]. The fibers were sealed with paraffin to small pieces of nickel-plated metal and treated together with 1 g. wool for 1 hour in a solution of 50 ml. 0.1*N* HCl and 1.5 ml. 4% sodium hypochlorite diluted to 200 ml. with water. After treatment with 0.1% solution of sodium bisulfite the fibers were thoroughly washed in distilled water.

4. Silica Dispersion [4]. The fibers were immersed for 2 minutes in a 20% colloidal dispersion of silica in water (Syton W-20) and dried for 10 minutes in air at room temperature.

5. Melamine Resin Impregnation [5]. The fibers were treated with a 25% solution of methylated methylol melamine, with diammonium phosphate as catalyst. After squeezing and drying, the resin-

impregnated fibers were baked at 140°C for 10 minutes. The results are averages from measurements of 2 different couples of fibers.

6. Benzoquinone [1]. The fibers were treated for 48 hours at 50°C in a 1% solution of benzoquinone in 5% alcohol buffered to pH 5. After the treatment they were washed in distilled water. The results are averages from measurements of 3 different couples of fibers.

TABLE VII. FRICTION AT VARIOUS POINTS AT THE FIBER

(v = coefficient of variation)

		μ_{2s}	μ_{2k}	μ_{1s}	μ_{1k}
(1)	P_1 = 2.17,		n = 4.5		
		0.286		0.178	
		0.292		0.172	
		0.283		0.194	
		0.313		0.211	
	v =	4.6%		v = 9.3%	
(2)	P_1 = 2.17,		n = 4.5		
		0.471		0.327	
		0.464		0.305	
		0.472		0.311	
		0.442		0.275	
	v =	3.0%		v = 7.1%	
(3)	P_1 = 2.17,		n = 4.5		
		0.489	0.372	0.354	0.253
		0.505	0.396	0.354	0.269
		0.456	0.377	0.324	0.254
		0.426	0.360	0.326	0.250
		0.432	0.374	0.306	0.258
		0.452	0.397	0.305	0.238
		0.493	0.423	0.370	0.279
		0.501	0.430	0.398	0.278
		0.473	0.392	0.343	0.271
		0.422	0.376	0.322	0.260
	v =	6.7%	v = 5.8%	v = 8.7%	v = 5.0%
(4)	P_1 = 2.84,		n = 4.5		
		0.214	0.214	0.142	0.142
		0.236	0.236	0.146	0.146
		0.248	0.248	0.153	0.153
		0.246	0.246	0.162	0.162
		0.226	0.226	0.146	0.146
	v =	6.1%	v = 6.1%	v = 5.2%	v = 5.2%
(5)	P_1 = 2.84,		n = 4.5		
		0.202	0.202	0.137	0.137
		0.250	0.250	0.167	0.167
		0.255	0.255	0.162	0.162
		0.236	0.236	0.149	0.149
		0.220	0.220	0.156	0.156
	v =	9.4%	v = 9.4%	v = 7.6%	v = 7.6%
(6)	P_1 = 2.17,		n = 4.5		
		0.411	0.348	0.230	0.206
		0.403	0.338	0.270	0.227
		0.387	0.341	0.238	0.208
(7)	P_1 = 2.17,		n = 4.5		
		0.416	0.368	0.279	0.234
		0.408	0.367	0.243	0.210
		0.411	0.366	0.285	0.246
		0.407	0.372	0.286	0.236
		0.415	0.339	0.310	0.245
	v =	1.0%	v = 3.7%	v = 8.6%	v = 6.2%

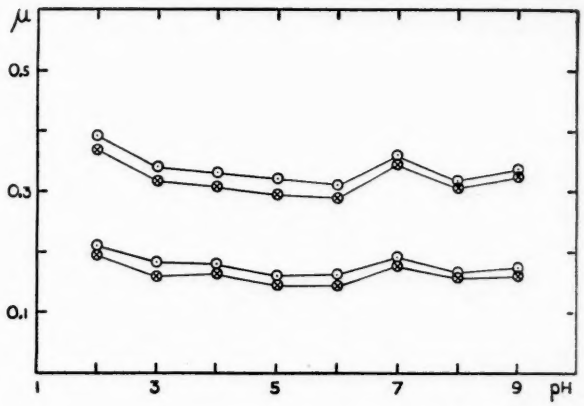

FIG. 16. *The frictional coefficient at different pH. (McIlvaine's buffer solutions.)*

Discussion

It is essential for the measurements to get a twist with a pitch angle which, first, will be the complementary angle of $\frac{\beta}{2}$ and, second, will not vary from time to time, when all other conditions are constant. Any deviation in the pitch angle will result in a change in the measured value of μ. This deviation will be different for different types of fiber and will, naturally, depend on the mechanical properties. Some of the results reported above give an idea of the reproducibility of the measurements for the case when the fibers have not been removed between two consecutive measurements. If the fibers are removed, treated, and measured again, it is not very likely that exactly the same parts of the fibers will come into contact. The surface of the wool fiber is not uniform, the scales are not of the same size and shape in different parts, and it is therefore unlikely that the friction will be the same in every part along the fiber. As shown above, the dispersion of the values is greater under these circumstances than when the measurements are repeated on the same part of the fiber. This fact must be taken into account when the results are interpreted. If the effect of a special treatment of the fiber is to be investigated, it is therefore not enough to make measurements on the same fiber or fibers, but an average must be taken for several different parts of the fiber or for several fibers. The latter method is easier and has in general been followed.

It is also of importance that the two fibers measured are of about the same diameter, since the formula is derived with this assumption. We have not made any microscopic measurements of the fiber

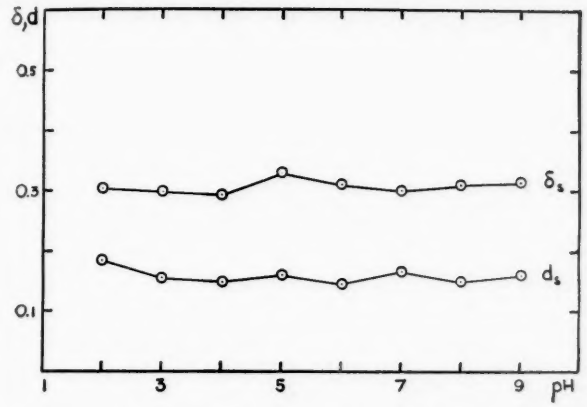

FIG. 17. *The variation of* δ_s *and* d_s *with pH.*

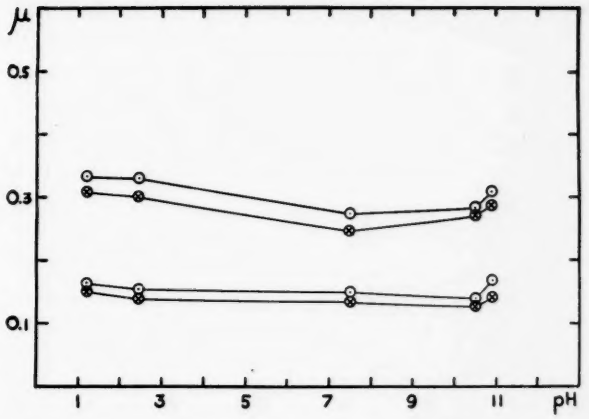

FIG. 18. *The frictional coefficients at different pH (sulfuric acid, water, and sodium bicarbonate).*

diameter, but have chosen those fibers that appeared to be of the same diameter to the naked eye. The difference between the diameters due to this imperfect measurement seems to have no noticeable influence.

A few measurements on dry wool have been made and the results are remarkable with respect to the low anti-scale friction that was obtained. However, since so few measurements were made we shall not discuss them here.

TABLE VIII. FRICTION AT DIFFERENT pH

	Fiber couple 1				Fiber couple 2			
pH	μ_{2s}	μ_{2k}	μ_{1s}	μ_{1k}	μ_{2s}	μ_{2k}	μ_{1s}	μ_{1k}
2.1	0.42	0.40	0.24	0.21	0.41	0.37	0.22	0.20
3.0	0.37	0.34	0.23	0.18	0.33	0.31	0.17	0.15
4.0	0.34	0.32	0.21	0.18	0.32	0.30	0.16	0.15
5.0	0.33	0.30	0.18	0.15	0.34	0.30	0.17	0.15
6.0	0.33	0.31	0.18	0.17	0.31	0.29	0.17	0.13
7.0	0.36	0.35	0.22	0.21	0.36	0.34	0.18	0.16
8.0	0.35	0.33	0.21	0.21	0.33	0.32	0.19	0.16
9.0	0.34	0.33	0.21	0.20	0.36	0.35	0.17	0.16
	Fiber couple 3				Fiber couple 4			
2.1	0.34	0.32	0.19	0.17	0.41	0.39	0.20	0.20
3.0	0.32	0.30	0.17	0.15	0.34	0.31	0.17	0.15
4.0	0.33	0.31	0.19	0.17	0.33	0.31	0.16	0.15
5.0	0.32	0.30	0.15	0.14	0.30	0.29	0.15	0.14
6.0	0.29	0.27	0.15	0.13	0.32	0.29	0.16	0.15
7.0	0.35	0.34	0.19	0.17	0.38	0.36	0.19	0.18
8.0	0.29	0.27	0.14	0.14	0.30	0.29	0.13	0.13
9.0	0.32	0.31	0.15	0.14	0.33	0.32	0.17	0.16
	Average of 1, 2, 3, and 4				d_s	d_k	δ_s	δ_k
2.1	0.39	0.37	0.21	0.20	0.18	0.17	0.30	0.31
3.0	0.34	0.32	0.18	0.16	0.16	0.16	0.30	0.33
4.0	0.33	0.31	0.18	0.17	0.15	0.14	0.29	0.30
5.0	0.32	0.30	0.16	0.15	0.16	0.15	0.33	0.34
6.0	0.31	0.29	0.16	0.15	0.15	0.15	0.31	0.33
7.0	0.36	0.35	0.19	0.18	0.17	0.17	0.30	0.32
8.0	0.32	0.31	0.17	0.16	0.15	0.15	0.31	0.32
9.0	0.34	0.33	0.18	0.16	0.16	0.16	0.32	0.34

Most of the measurements were made in water or water solution, since all felting and ordinary laundering processes are done in the presence of water.

Dependence of Frictional Properties on Normal Pressure and Area of Contact

The frictional properties of all measured fibers, including wool, depend on the normal pressure, as pointed out by several authors [6, 11, 14, 15]. Most measurements reported fit closely to the formula (equation (10))

$$\mu = \mu_0 + k_1 \frac{S}{N},$$

which has been mentioned previously. This formula seems to hold for the with-scale friction, but some authors have found certain anomalies in the case of anti-scale friction [11, 14]. It was expected that these anomalies might throw some light on the nature of the directed friction of animal hairs.

TABLE IX. FRICTION AT DIFFERENT pH

(Sulfuric acid, water, and sodium carbonate)

	Fiber couple 1				Fiber couple 2			
pH	μ_{2s}	μ_{2k}	μ_{1s}	μ_{1k}	μ_{2s}	μ_{2k}	μ_{1s}	μ_{1k}
1.2	0.28	0.27	0.15	0.13	0.38	0.35	0.18	0.17
2.4	0.30	0.28	0.15	0.14	0.36	0.32	0.15	0.14
7.5	0.28	0.25	0.16	0.14	0.27	0.24	0.14	0.12
10.5	0.28	0.27	0.15	0.13	0.29	0.26	0.13	0.12
10.9	0.32	0.30	0.19	0.18	0.30	0.27	0.15	0.13
	Average of 1 and 2				d_s	d_k	δ_s	δ_k
1.2	0.33	0.31	0.16	0.15	0.17	0.16	0.34	0.34
2.4	0.33	0.30	0.15	0.14	0.18	0.16	0.37	0.36
7.5	0.28	0.25	0.15	0.13	0.13	0.11	0.29	0.30
10.5	0.28	0.26	0.14	0.13	0.15	0.14	0.35	0.35
10.9	0.31	0.29	0.17	0.16	0.14	0.13	0.29	0.30

Two explanations of the nature of the directed friction have been offered—namely, the ratchet theory [12], which is most generally considered to be true, and Martin's theory [10] of the unidirectional arrangements of the molecular forces. If the ratchet theory is valid, we can assume that the anti-scale friction is composed of two fractions. One component is the same as the with-scale friction, and the second component is due to the scales.

$$F_2 = F_1 + F_s. \tag{11}$$

The with-scale friction obeys the formula

$$\frac{F_1}{N} = \mu_1 = \mu_0 + \frac{k_1 S}{N}. \tag{12}$$

The resistance offered by the scales, F_s, must also be in some way dependent on the normal pressure. At very low normal pressures, rather few scales will hook into each other because the scales are of various heights and will not always coincide with one another on the two fibers. At higher normal pressure, F_s will increase, but will reach a limit, when the maximum possible number of scales hook into each other. Thus we can assume the following equation to be valid:

$$\mu_2 = \frac{F_2}{N} = \frac{F_1}{N} + \frac{F_s}{N} = \mu_0 + \frac{k_1 S}{N} + \frac{F_s}{N}, \tag{13}$$

where $k_1 S$ is approximately constant, whereas F_s increases with increasing N to a maximum value $F_{s\,\max.}$. F_s can be assumed to consist of three independent factors:

$$F_s = cAQ, \tag{14}$$

where A is the total number of scales on a given area of contact, Q is the average scale resistance, and c is the fraction of active scales. Thus cA is the number of active scales, which is dependent on the normal pressure. The curves obtained can be explained by this theory. The difference $\mu_2 - \mu_1 = \frac{F_s}{N}$ is high for low N, but decreases when N increases, and for very high values of N, $\mu_2 - \mu_1$ is proportional to $\frac{1}{N}$. For $\frac{1}{N} = 0$, we reach the state where $\mu_2 = \mu_1$. This can be seen from Figure 11, where the possible extrapolations of μ_2 and μ_1 to $\frac{1}{N} = 0$ are indicated. The limitation of the strength of the fibers prevented us from studying the phenomenon at higher values of N.

According to this theory, it must be concluded that the value of F_s can increase with increasing contact area, if N is kept constant. It was found experimentally (Figure 12) that a decrease in the number of turns, n, at constant normal pressure caused an increase in the anti-scale frictional coefficient, but not in the with-scale frictional coefficient. This result further supports the theory sketched here, and, hence, the ratchet theory, whereas it does not favor Martin's theory of the unidirectional frictional forces.

Figure 11 also seems to indicate that the static and the kinetic frictional coefficients show a tendency to reach the same value for high values of N. We are not able to offer any explanation for this phenomenon.

Effect of Variation in pH

Since the directional frictional properties are generally regarded to be the primary cause of the felting of wool, the increased rate of felting in alkaline and acid media is sometimes supposed to be due to a change in the frictional properties. Bohm [2] claims to have obtained results which prove that this change in the felting properties is entirely due to the difference between the frictions in both directions. There has been some doubt about the significance of his results [12] and Mercer and Makinson [14] and Martin and Mittelmann [11] in their measurements have not obtained the same close relationship between the felting properties and the friction.

As in previous investigations [2, 11, 14], μ *vs.* pH is given in the diagrams, but it should be observed that also other ions than the hydrogen ions might affect the frictional properties, and it is therefore not quite correct to draw any immediate conclusions from these diagrams. When the anions are the same at different pH and only mixed in different proportions, as shown in Figures 14 and 15, the

TABLE X

	μ_{2s}	μ_{2k}	μ_{1s}	μ_{1k}	d_s	d_k	δ_s	δ_k
Untreated	0.38	0.34	0.21	0.18	0.17	0.16	0.29	0.31
Treated	0.66	0.50	0.48	0.33	0.19	0.17	0.16	0.20

TABLE XI

	μ_{2s}	μ_{2k}	μ_{1s}	μ_{1k}	d_s	d_k	δ_s	δ_k
Untreated	0.42	0.37	0.23	0.20	0.19	0.17	0.29	0.30
Treated	0.67	0.54	0.51	0.34	0.16	0.20	0.14	0.22

results at different pH might be compared, because there is a smooth variation in the concentration of the two anions. For the latter experiment the diagram (Figure 16) is given merely as an aid to a better survey.

Our results, as shown in Tables VIII and IX and in Figures 14 and 16, support the view of Mercer [14] and Martin [11]. If the general relation between the frictional properties and the felting is considered, it is obvious that the difference in friction is the most important factor. If Tables X–XII are compared with the well-known influences of these treatments on the felting, it is also obvious that μ_1, or the arithmetic mean of μ_1 and μ_2, is in some way related to the felting. Assuming d and the felting to be directly proportional, and the absolute friction and the felting to be inversely proportional (since no accurate figure for the relation is yet given, it is a matter of convenience to adopt the simplest relation) leads to the equation suggested by Speakman [17]:

$$\text{Scaliness} = \frac{\mu_2 - \mu_1}{\mu_1} 100,$$

or that suggested by Mercer [13]:

$$\delta = \frac{\mu_2 - \mu_1}{\mu_2 + \mu_1}.$$

Mercer called δ the "directional frictional effect" (D.F.E.). The only difference between these two expressions is the denominator. Figure 17 shows that both d and δ are fairly constant over the whole measured range of pH. The increased rate of felting cannot therefore be explained by a change in the frictional properties. Both μ_1 and μ_2 seem to have a maximum at pH 7 and minima on both sides of pH 7.

Effect of Variation in Temperature

The feltability of wool is known to be extremely dependent on the temperature, but little is known of the influence of the frictional properties on the felting rate at different temperatures. Martin and Mittelmann [11] report a decrease in both μ_1 and μ_2 with increasing temperatures up to 50°C. Mercer and Makinson [14] have also observed a decrease in μ_1 with increasing temperatures, but they have not given any figures. Our results confirm these observations and show a marked decrease in both μ_2 and μ_1; μ_2 falls more rapidly than μ_1, and both d and δ decrease slightly with increasing temperature.

The measurements were made in distilled water and we intend to repeat them at different pH. It is quite obvious from these experiments that the increased felting rate at higher temperatures cannot be ascribed to the change in the frictional properties, which would, rather, bring about a decreased felting rate. As pointed out in the preceding paragraph concerning the dependence of frictional properties on pH, other mechanical properties of the wool fiber must be taken into account for the explanation of the dependence of the felting on temperature.

Different Treatments of the Fibers

For making wool unshrinkable several treatments have been suggested. Their effects on the wool fibers with respect to the frictional properties have been measured by several authors with rather contradictory results, depending on the methods used. The measurement of the actual friction between two fibers ought to be the best way of obtaining results that can be applied to a discussion of milling properties, because, in milling, the fibers move under friction, primarily against each other. The investigation described here is not complete because the friction was measured only in distilled water, but some conclusions can still be drawn from the results.

If equation (13) is adopted for the anti-scale friction, this will consist of two independent factors, where $\frac{F_s}{N}$ is equal to d and μ_1 can be considered as a measure of the frictional resistance to fiber movement. If δ is a measure of the felting rate, it is obvious that there are two ways of changing the felting properties by changing the friction—namely, a change in d or a change in μ_1.

For a change in d, either Q or cA (equation (14)) must be changed. When the fibers are treated by caustic alkali in alcohol (Tables X and XI) only μ_1

TABLE XII

	μ_{2s}	μ_{2k}	μ_{1s}	μ_{1k}	d_s	d_k	δ_s	δ_k
Untreated	0.37	0.30	0.21	0.17	0.16	0.13	0.27	0.29
Treated	0.92	0.78	0.91	0.82	0.01	0.04	0.00	0.00

TABLE XIII

	μ_{2s}	μ_{2k}	μ_{1s}	μ_{1k}	d_s	d_k	δ_s	δ_k
Untreated	0.39	0.34	0.20	0.18	0.20	0.16	0.33	0.32
Treated	0.48	0.43	0.30	0.27	0.18	0.17	0.23	0.24

TABLE XIV

	μ_{2s}	μ_{2k}	μ_{1s}	μ_{1k}	d_s	d_k	δ_s	δ_k
Untreated	0.30	0.27	0.16	0.15	0.14	0.12	0.31	0.30
Treated	0.29	0.26	0.16	0.15	0.12	0.11	0.27	0.27

TABLE XV

	μ_{2s}	μ_{2k}	μ_{1s}	μ_{1k}	d_s	d_k	δ_s	δ_k
Untreated	0.40	0.35	0.24	0.19	0.16	0.16	0.26	0.29
Treated	0.35	0.27	0.21	0.18	0.13	0.09	0.23	0.20

is affected. The decrease in the felting rate is obviously caused only by the increase in the with-scale friction. Such an increase with the accompanying decrease in felting rate can probably be obtained in different ways without any risk of damaging the wool. If the Syton impregnation (Table XIII) could be made wash-resistant this would certainly also bring about a decrease in the felting rate.

The chlorination of the fibers gives very high frictional coefficients. The with-scale friction is increased about four times, and the difference in friction seems to disappear. Our measurements were made in distilled water, but it is quite possible that a change of pH is of little effect (*cf.* Figure 18).

Barr and Speakman [1] have found that wool fibers change their elastic properties and not their frictional properties on treatment with benzoquinone. The figures in Table XV confirm their results. The slight change in the anti-scale friction can be explained as a change in the elastic properties. If the fiber becomes more rigid, there is probably a decrease in cA in equation (14), which will overcome an eventual increase in the scale resistance Q.

As exactly the same result is obtained when the fibers are treated with melamine resin (Table XIV), this leads to the conclusion that the elastic properties and not the frictional properties are affected by this treatment. It is a widespread opinion that the effect of the melamine resin as an anti-shrink treatment is due to a masking of the scales on the fiber surface, but the results we have obtained do not support this view.

Summary

1. An apparatus for measuring the frictional forces between two single fibers has been constructed. The method for the measurements is based on the principle of twisting two fibers together a certain number of turns and then drawing them apart.

2. The theory for measuring both the static and the kinetic friction is developed.

3. The frictional properties of nylon fibers were measured at different loads and a linear relationship between the frictional coefficient and the inverse value of the normal pressure was found to be valid.

4. The friction of wool fibers at different loads and contact areas was measured, and the same linear relationship as for nylon fibers was found to be valid for the with-scale friction. For the anti-scale friction the relationship was found to be more complicated and the shape of the scales was indicated as being responsible for the difference in friction.

5. It is shown that the friction of wool fibers is dependent on the temperature, and both the with-scale and the anti-scale frictions decrease with increasing temperature, measurements having been performed at temperatures up to 70°C.

6. It is shown that the friction of wool is only slightly dependent on pH.

7. Wool fibers were treated according to different processes for making wool unshrinkable, and the friction before and after the treatment was measured. With treatments which attack the surface of the fiber (e.g., chlorination), both the with-scale and the anti-scale frictions were increased, and in some cases the difference was decreased. Sometimes the main cause was a change in the elastic properties, and there was no change in the friction (*e.g.*, on treatment with melamine resin or with benzoquinone).

Acknowledgment

Our thanks are due to Mr. B. Olofsson for valuable discussion, particularly concerning the theory of the measurements, and to Mr. L. Mattsson of the Laboratory Machine Shop for building the apparatus and for helpful suggestions in its design.

Literature Cited

1. Barr, T., and Speakman, J. B., *J. Soc. Dyers and Colourists* **60**, 335 (1944).
2. Bohm, L., *J. Soc. Dyers and Colourists* **61**, 278 (1945).
3. Bowden, F. P., and Leben, L., *Proc. Roy. Soc.* **169A**, 371 (1938–9).
4. Communication from Monsanto Chemical Co.
5. Dudley, J. R., and Lynn, J. E., in "Fibrous Proteins," Soc. Dyers and Colourists, May, 1946.

6. Gralén, N., and Olofsson, B., TEXTILE RESEARCH JOURNAL **17**, 488 (1947); *Proc. of Swed. Inst. for Text. Res.*, No. 3 (1947).
7. Hall, A. J., and Wood, F. C., U. S. Pat. 2,401,479.
8. Hennings, H. J., *Meiliand Textilber.* **18**, 945 (1937).
9. Lipson, M., and Howard, P., *J. Soc. Dyers and Colourists* **62**, 29 (1946).
10. Martin, A. J. P., *J. Soc. Dyers and Colourists* **60**, 325 (1944).
11. Martin, A. J. P., and Mittelmann, R., *J. Text. Inst.* **37**, T269 (1946).
12. Menkart, J., and Speakman, J. B., *Nature* **156**, 143 (1945).
13. Mercer, E. H., *J. Council Sci. Ind. Research* **18**, 188 (1945).
14. Mercer, E. H., and Makinson, K. R., *J. Text. Inst.* **38**, T227 (1947).
15. Morrow, J. A., *J. Text. Inst.* **22**, T425 (1931).
16. Speakman, J. B., Chamberlain, N. H., and Menkart, J., *J. Text. Inst.* **36**, T91 (1945).
17. Speakman, J. B., and Stott, E., *J. Text. Inst.* **22**, T339 (1931).

An Investigation of the Relationship Between Polymer Structure and Mechanical Properties*

Part II: An Experimental Study of the Stress and Birefringence Properties of Several Relaxing Polymeric Systems

Richard S. Stein† and Arthur V. Tobolsky‡

Contribution of the Textile Foundation and the Plastics Laboratory and Frick Chemical Laboratory, Princeton University, Princeton, New Jersey

Introduction

In Part I of this series, the nature of the relaxation processes for solid polymeric materials was considered in terms of the molecular processes involved. The effect of these processes on the stress (for samples relaxing at constant length) and on the birefringence (double refraction) was considered.

It was pointed out that the technique of simultaneous stress and birefringence measurements should prove useful in specifying the nature of the molecular configurational changes associated with the relaxation of stress. For rubberlike materials, theory indicates that the stress-birefringence ratio should be constant during the relaxation whereas for plastic or crystalline polymers the birefringence change is very much smaller than the corresponding change in stress. Thus, the method should prove useful in studying structural transitions such as the "softening point" of polymers.

In this paper relaxation experiments are reported on a series of polymers ranging in properties from rubbers to polycrystalline plastics, and an attempt is made to resolve the complex mechanical behavior of these systems into more fundamental contributions.

Experimental Procedure

The samples used in this investigation were in the form of transparent or semitransparent films ranging in thickness from 2–30 mils, approximately 1 cm. wide, and 2–10 cm. long. The stress and birefringence were measured simultaneously in the apparatus illustrated in Figures 12 and 13. The stress is measured by means of a relaxation balance contained in an air thermostat whose temperature may be maintained between 30°C and approximately 350°C with a precision of about ± 0.2°C.

The balance § consists of a vertical brass post, near the bottom of which is pivoted a small balance arm containing a clamp on one side and an adjustable counterweight on the other. A chromel wire is fastened to the arm directly in the line of action of the clamp. This wire is led through pulleys to a weight pan outside of the oven. The arm is also provided with electrical contacts which control a neon glow lamp indicating the position of balance. A second clamp is fastened to a rider which may slide up and down the vertical rod. The rider may be moved from outside the oven by a thin brass rod which extends through the top.

The clamps which hold the sample (Figure 14) are wedge-type so that they will tighten automatically as the sample softens on heating or as the stress is increased. The wedge is initially tightened by means of a set screw on a pivoted arm. The gripping surfaces are lightly grooved.

With this balance, loads of from 5 g. to 1,000 g. may be measured with a precision of about ± 2 g.

The oven is provided with double pyrex windows on front and back so that a beam of light may be

---

* Presented in part at the High Polymer Forum at the 111th Meeting of the American Chemical Society, Atlantic City, N. J., April 14, 1947.

Part I of this series appeared in the April, 1948, issue, page 201. The list of literature references for both parts was published with Part I. Equations 1–60 also appear in Part I.

AUTHORS' NOTE: In Part I, page 203, equation (1*b*) should read "$\left(\frac{\partial E}{\partial l}\right)_{V,T} = f - T\left(\frac{\partial f}{\partial T}\right)_{P,l} - MA\beta T$"; page 207, the right sides of equations 6, 7, 14, and 16 should be multiplied by -1; page 214, the line above equation (35) should read ". . . (assuming $\beta = \gamma = \alpha^{-\frac{1}{2}}$)."

† Fellow of the Textile Research Institute.

‡ Staff member, the Textile Foundation.

§ The balance was designed by Mr. Rodney D. Andrews and constructed by Mr. William Grove, both of Princeton University.

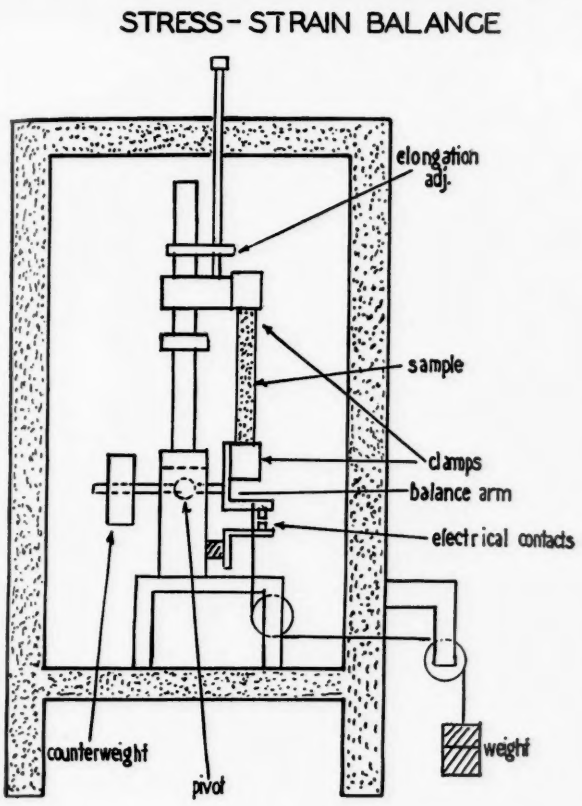

FIG. 12. *The stress-strain balance.*

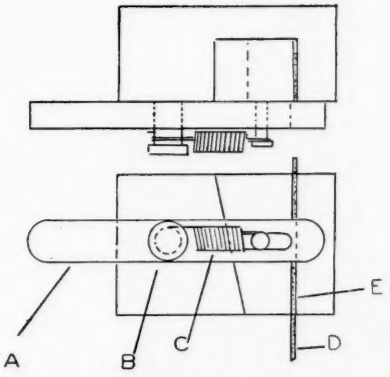

FIG. 14. *Clamp used for gripping the sample. The sample* (D) *is held between the grooved jaws* (E) *of a wedge-type clamp. The clamp is opened and closed by means of the lever* (A) *pivoted at* (B). *A set-screw (not shown) is provided to prevent loosening of the clamp on release of the tension. A spring* (C) *holds the movable jaw away from the fixed jaw when the clamp is open.*

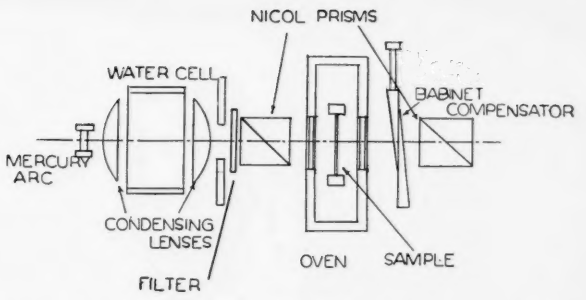

FIG. 13. *Optical system for the measurement of birefringence. The light beam from the mercury arc is cooled, collimated, filtered, and polarized at 45° to the direction of stretch of the sample. It is then passed through the sample, through a Babinet Compensator, and through a Nicol prism having its plane of polarization at 90° to that of the first Nicol prism.*

passed through the sample for the birefringence measurement.

Birefringence is measured by the retardation method. A beam of light from a D.C. mercury arc is collimated, rendered monochromatic (5,461Å.) by passing through a Wratten gelatin filter and plane polarized at 45° to the direction of stretching the sample by a Nicol prism. The light, after passing through the sample, goes through a Babinet Compensator and then through another Nicol prism which is oriented so that its polarization axis is at 90° to that of the first.

The Babinet Compensator [76] has as its principal component a quartz wedge which may be moved parallel to the direction of stretching the sample by means of a micrometer screw. The interference fringes resulting from the retardation of the wedge are shifted by an amount proportional to the birefringence of the sample. The birefringence is computed from the motion of the wedge required to compensate for this shift. The retardation due to the sample may be measured with a precision of about ± 1 percent of a wave length. It is essential that frequent blank readings be taken so as to correct for temperature fluctuations in the neighborhood of the compensator.

The entire optical assembly is mounted on an optical bench which passes under the oven. A rack and pinion mechanism is provided so that the optical bench may be moved in a direction perpendicular to that of the light path. In this manner, the light beam may be brought to pass alternately through the sample and alongside it for purposes of taking blank readings. The optical bench is also equipped with a

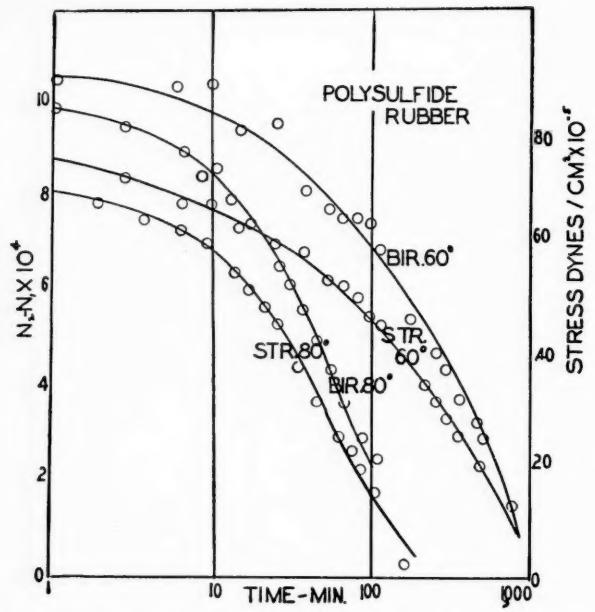

FIG. 15. *Relaxation of the stress and birefringence of a sample of polysulfide rubber stretched and held at 47% elongation at several temperatures.*

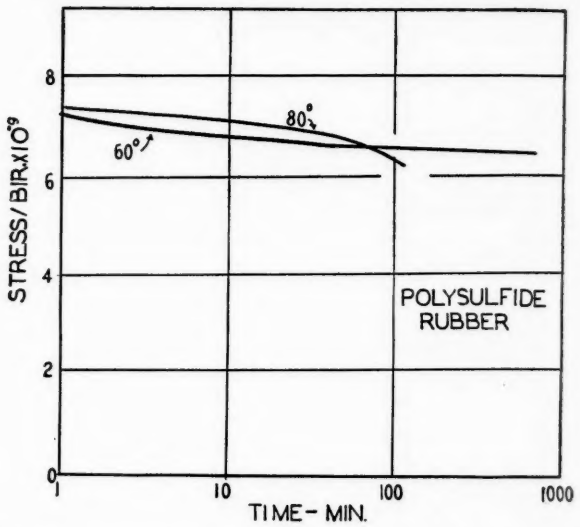

FIG. 16. *Variation of the ratio of stress to birefringence during the polysulfide rubber relaxation.*

screw feed to permit traveling in the vertical direction, so that any variation in birefringence along the length of the sample may be detected.

The samples, which were cut from uniform sheets, had been tested for any initial anisotropy. The thickness was measured by means of a dial gage with a precision of about $\pm$ 0.0001 in. and both the length and thickness were measured with a precision of about $\pm$ 0.02 cm. The samples were mounted in the clamps while they were cold and the position of the edge of the clamp jaws was used as a reference of length. The sharpness of the impression of the clamp grooves on the surfaces of the sample served as an indication of lack of slippage through the clamps.

After mounting the sample, the oven was heated to the desired starting temperature and allowed to reach a steady state. The samples were then rapidly stretched to a predetermined length and the subsequent changes in stress and birefringence were followed. With present instrumentation, it is not possible to obtain reliable readings in times shorter than 1 minute after the initial stretching.

Temperature changes were made slowly enough to avoid temperature gradients. Before making temper-

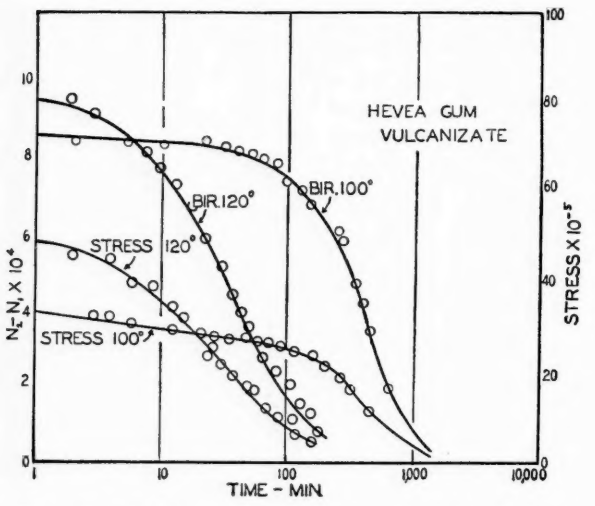

FIG. 17. *Relaxation of the stress and birefringence of a sample of Hevea gum vulcanizate stretched and held at 48% elongation at several temperatures.*

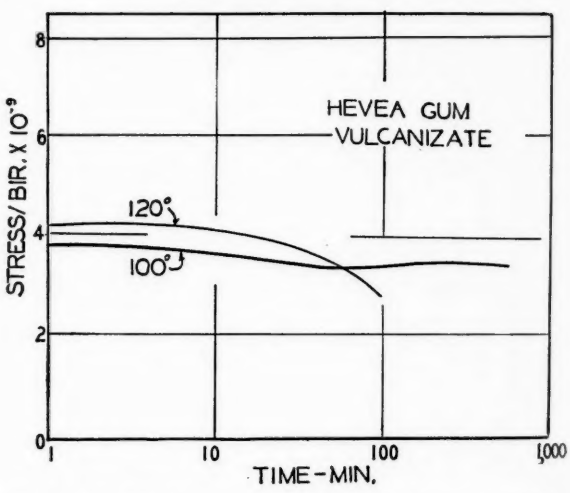

FIG. 18. *Variation of the ratio of stress to birefringence during the Hevea gum vulcanizate relaxation.*

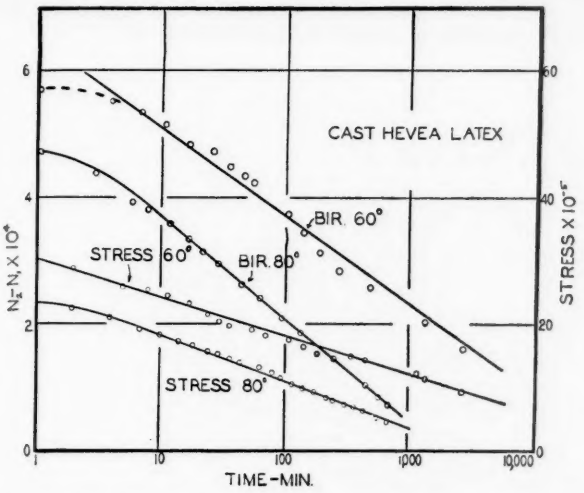

FIG. 19. *Relaxation of the stress and birefringence of a sample of cast Hevea latex stretched and held at 48% elongation at several temperatures.*

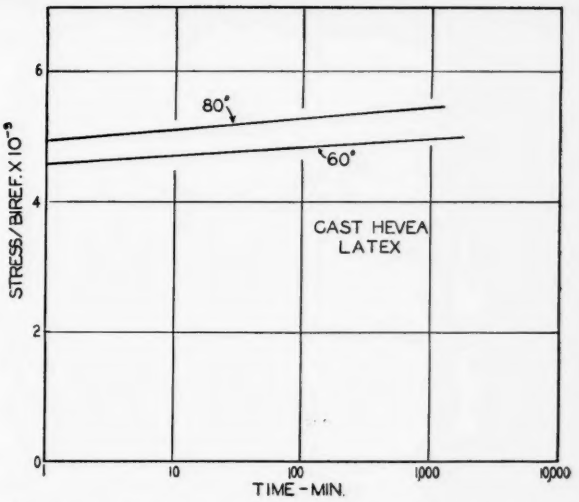

FIG. 20. *Variation of the ratio of stress to birefringence during the cast Hevea latex relaxation.*

ature changes a pseudo-equilibrium condition was assured by establishing the fact that properties were changing slowly enough that no appreciable change would take place in the time required for subsequent measurements.

Stresses are presented in units of dynes/cm² of the area finally attained (calculated from initial area on the assumption of Poisson's ratio of ½). Birefringence values are presented in units of refractive index difference (calculated from retardation by the finally attained thickness).

Successive runs on samples of the same type under the same conditions have indicated that the data obtained by these techniques are reproducible.

Results and Conclusions

The experimental approach was to study the relaxation processes of substances in the order of increasing energy interaction. The first set of experiments was made on materials whose mechanical properties indicate that they are in the rubberlike state and make a negligible internal energy contribution to stress. Later, experiments were made on materials in which the complications of energy interaction, crystallization, and plasticization were introduced. The experimental data presented here are not meant to represent a complete study but rather a survey of the scope of the field and of the problems which present themselves. It is hoped that much of the work presented here may be discussed in greater detail in future papers.

Rubberlike Substances

The first set of runs was made with polysulfide rubber,* which, as has been demonstrated [61], will relax by a chemical interchange-type mechanism. The stress and birefringence are plotted against log time for two temperatures in Figure 15. It can be seen that the two curves parallel each other and the ratio of stress to birefringence (Figure 16) is sensibly constant throughout the relaxation process.† The ratio is somewhat higher at the higher temperature in a manner indicative of proportionality with temperature as predicted by equation (45). In view of the foregoing discussion, we would therefore conclude that this substance behaves as an ideal rubber would behave. This is consistent with the fact that the stress is observed to behave in a manner predicted by the kinetic theory of elasticity.

In Figure 17 the decay curves of a Hevea gum vulcanizate are presented. The relaxation of this substance, which has been demonstrated to decay chiefly by oxidative scission, is similar to that of the polysulfide rubber. The ratio curves of Figure 18 also indicate ideality here. The fact that the initial stress of these samples is not always proportional to the absolute temperature (as would be expected for equation (17)) is probably due to slight variation in

* The polysulfide rubber used consists of a formal disulfide polymer cross-linked with 0.5 percent trifunctional groups.

† The deviation near the end of the relaxation is believed to be due to experimental error. In this region, the ratio of two small values is taken so that the ratio is very sensitive to the systematic error in both.

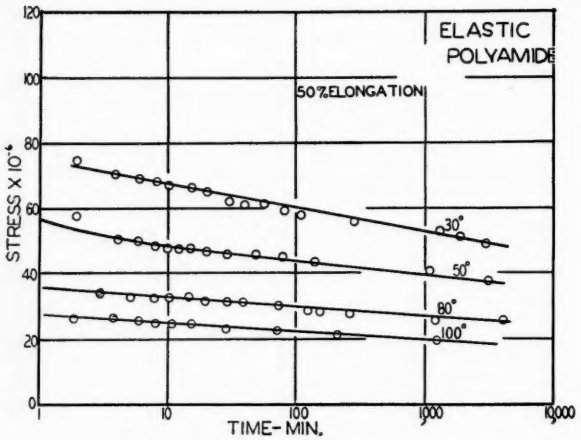

FIG. 21. *Relaxation of stress of a sample of elastic polyamide A stretched and held at 50% elongation at several temperatures.*

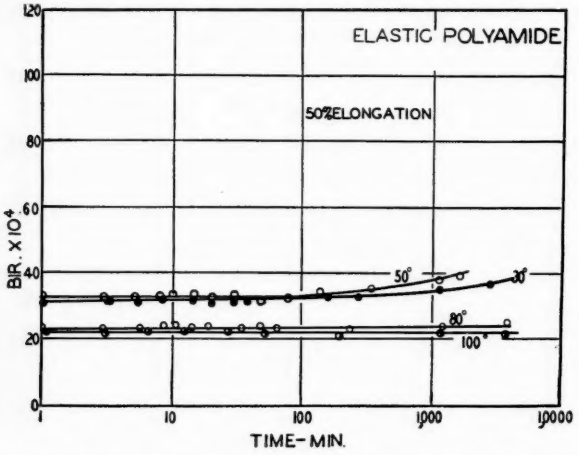

FIG. 22. *Relaxation of birefringence of a sample of elastic polyamide A stretched and held at 50% elongation at several temperatures.*

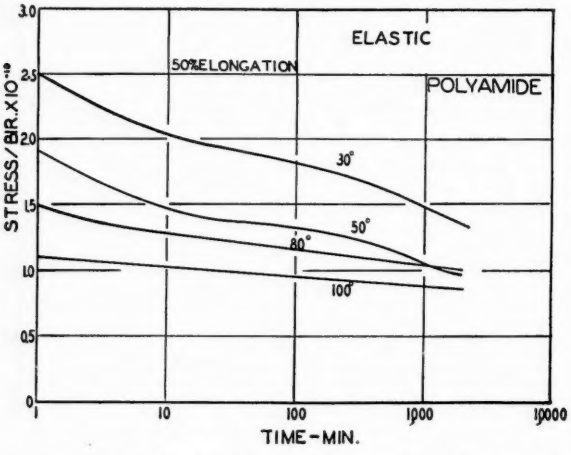

FIG. 23. *Variation of the ratio of stress to birefringence during the relaxation of elastic polyamide A.*

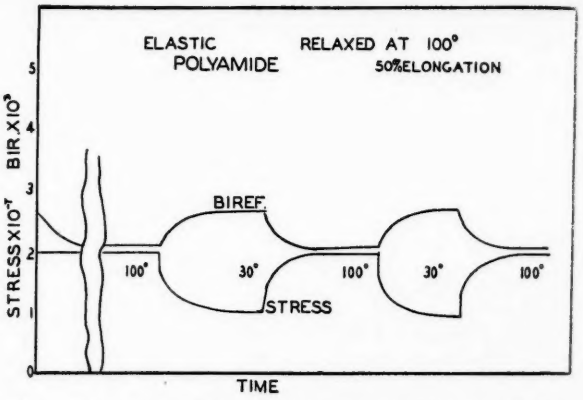

FIG. 24. *Reversible variation of stress and birefringence with temperature. The sample of elastic polyamide A was originally stretched and held at 50% elongation and relaxed at 100°C.*

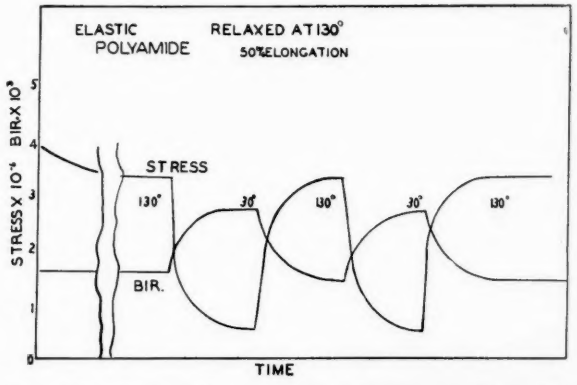

FIG. 25. *Reversible variation of stress and birefringence with temperature. The sample of Figure 24 was heated to 130°C, allowed to relax, and then the temperature was varied between 30° and 130°C.*

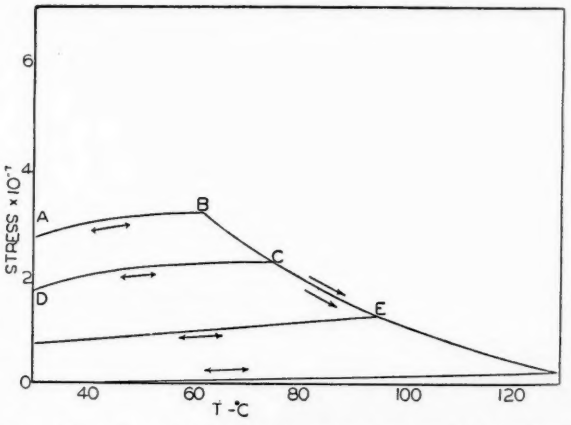

FIG. 26. *Complete stress-temperature cycle for elastic polyamide A. The sample was stretched and held at 100% elongation at 60°C and allowed to relax before these curves were determined. The double-headed arrows indicate reversible portions of the curve and the single arrows indicate irreversible portions.*

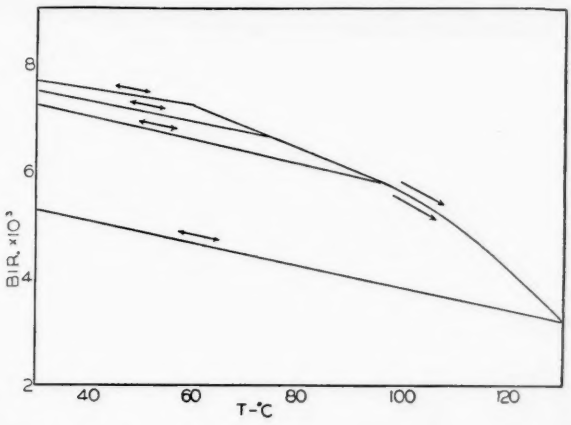

FIG. 27. *Complete birefringence-temperature cycle measured simultaneously with the stress curves of Figure 26.*

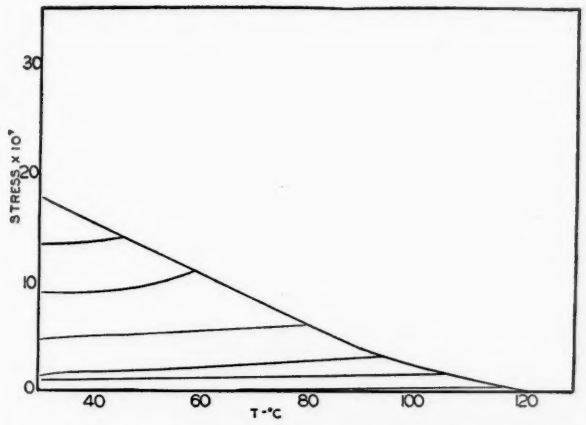

FIG. 28. *Stress-temperature cycle for a sample of elastic polyamide B stretched and held at 500% elongation at 30°C and allowed to relax.*

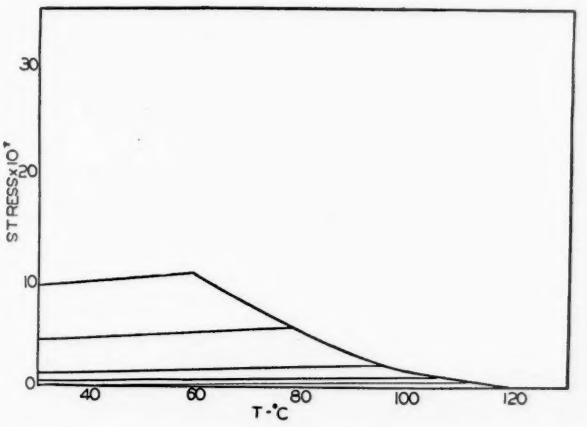

FIG. 29. *Stress-temperature cycle for a sample of elastic polyamide B stretched and held at 500% elongation at 60°C and allowed to relax.*

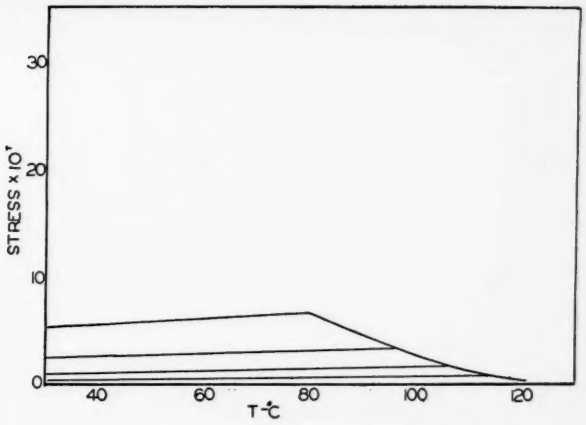

FIG. 30. *Stress-temperature cycle for a sample of elastic polyamide B stretched and held at 500% elongation at 80°C and allowed to relax.*

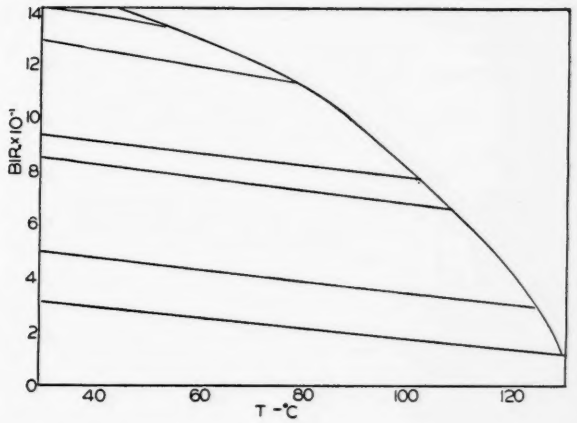

FIG. 31. *Birefringence-temperature cycle measured simultaneously with the stress curves of Figure 28.*

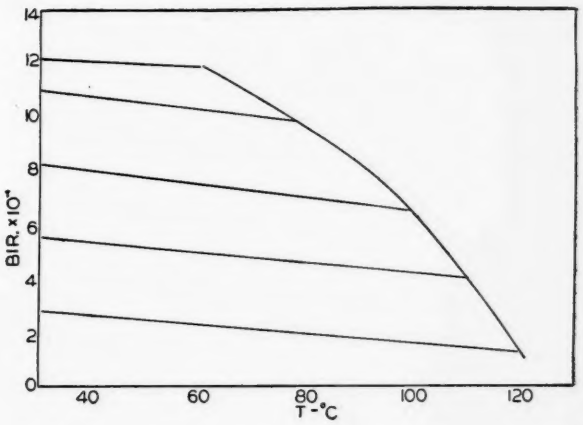

FIG. 32. *Birefringence-temperature cycle measured simultaneously with the stress curves of Figure 29.*

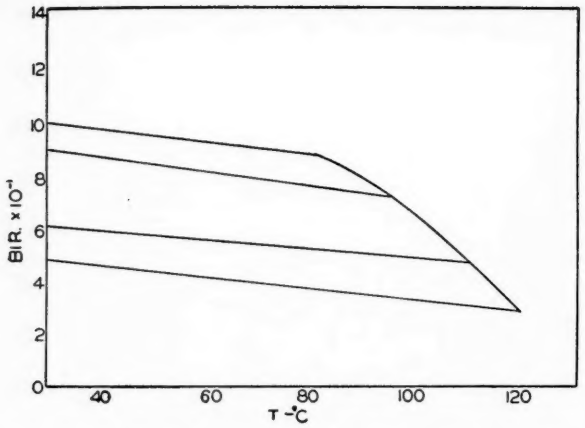

FIG. 33. *Birefringence-temperature cycle measured simultaneously with the stress curves of Figure 30.*

the degree of cure among the samples. Experiments in which the samples are more carefully characterized indicate that the proportionality rule is obeyed. The ratio curves which should be independent of the number of cross links (equation (45)) do appear to vary proportionately with temperature.

An illustration of a diffusion-type relaxation process is that of the relaxation of unvulcanized cast latex. As seen from Figure 19, the stress and birefringence curves decay almost linearly with logarithmic time. The creep and recovery of this material has been studied by Treloar [68]. He finds that only a very small fraction of the deformation represents true viscous flow and concludes that the relaxation process probably involves internal diffusion of the chains. He believes that there is a structure of steric cross links or entanglements which remain unbroken during the stretching process.

The observation that the initial stress (and birefringence) is lower at higher temperatures in apparent contradiction to the kinetic theory of elasticity is probably due to relaxation which occurred before the first reading was taken. That is, the curves probably crossed in earlier regions of log time. This is substantiated by the ratio curves (Figure 20) which are sensibly flat, indicating ideality, and which show the kinetic-theory type of temperature dependency.

Thus, the trend appears to be that for substances which are rubbery and which obey the kinetic theory of elasticity birefringence behavior is also ideal, irrespective of the detailed mechanism of the relaxation process. For substances not obeying the kinetic theory, deviations from a horizontal stress-birefringence ratio curve are observed, as described in the next section.

Elastic Polyamides

A polymer in which intermediate properties are demonstrable is an elastic polyamide. These materials are condensation polymers of dibasic acids with alkyl diamines which are substituted on the amino nitrogens to different degrees with alkyl groups [54]. The degree of energy interaction may be varied by (1) varying the heterogeneity of the size of the monomeric units, (2) varying the nature of the *N* substituent, and (3) varying the amount of substituent.

The first set of data on the material is for a polyamide (sample A) prepared by polymerizing a mixture of 40 mol parts of *N, N'*-diisobutyl hexamethylene diamine, 20 parts of mono-*N*-isobutyl hexamethylene diamine, and 40 parts of hexamethylene diamine with sebacic acid.

The stress, birefringence, and ratio curves (Figures 21–23) show large deviations from ideality. Here, the stress-decay curve plotted against log time is concave upward, the slope decreasing with log time and seemingly flattening off at a finite stress. The "initial" stresses are lower at higher temperature, as is true in the case of cast Hevea latex, and one is tempted to apply the same explanation—that is, a horizontal shift of the curve with temperature resulting from the changing time scale of the processes involved. It will be shown, however, that there are also vertical shifts of the curves with temperature changes, corresponding to structural changes.

Examination of the birefringence-relaxation curves reveals that in the early regions of relaxation (where the stress is decaying more rapidly) the birefringence is essentially constant, but later (where the stress is decaying more slowly) the birefringence is increasing. The rise is greater at lower temperatures.* The ratio of stress to birefringence (Figure 23) is, of course, not constant but decreases with log time, in what appears to be a two-stage process, and seems to approach a constant value.

In terms of the preceding discussion these phenomena may be interpreted as follows: The unstretched structure is characterized by energy interaction largely in the form of hydrogen bonds between C=O and N—H groups. These bonds (or crystal-

* The fact that the 50°C curve crosses the 30°C curve has been shown to result from a kinetic effect.

lites) act as temporary cross links and are in a state of equilibrium, the effective number being dependent upon temperature. At low temperatures, the structure, as is the case with a highly vulcanized rubber, loses its rubbery properties as the internal Brownian motion is greatly reduced. The entropy elastic modulus becomes comparable or greater than the modulus corresponding to distortion of structure. Therefore at the lower temperatures the energy of stretching is largely distortional with a modulus which decreases with increasing temperature. However, the initial distortion process does not represent the most economical distribution of energy corresponding to the strain. Therefore, a redistribution subsequently occurs in which the energy contribution due to the local bond stretching and bending is transferred to smaller motions of larger portions of the structure, resulting in an entropy decrease. For example, if a hydrogen bond breaks and re-forms, the distortion of the particular portion of the structure which it was constraining is relieved and a slight rearrangement of the structure as a whole takes place. The relaxation of this distortion is not (at first) accompanied by any significant change in birefringence.

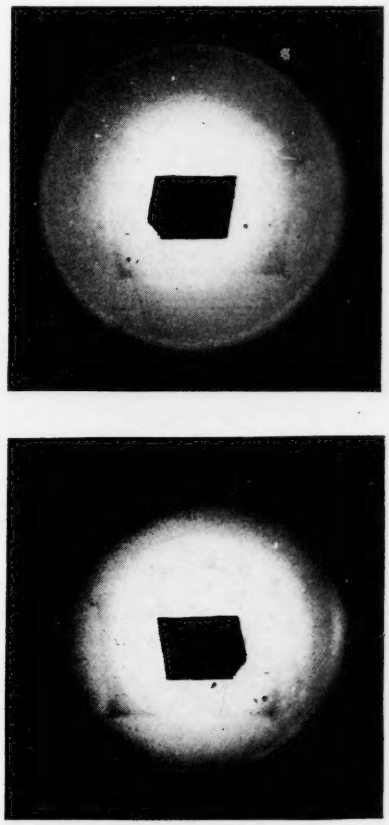

FIG. 34. *X-ray diffraction pattern* ($CuK\alpha$) *for elastic polyamide A. A (top)—Unstretched. B (bottom)—Stretched.*

This analysis does not completely eliminate the possibility of relaxation by a diffusion-type process. Experiments on rubberlike linear polymers have indicated that for these substances the birefringence decays in the same manner as does the stress. However, when energy interaction is appreciable, the relaxation in stress is not accompanied by the decreasing orientation which occurs with the simpler materials. If this does occur, the birefringence need not necessarily decay as the stress decreases.

As some of the restraints are relieved, orientation becomes possible, so that the material approaches an oriented structure in "equilibrium" with the number of cross links prevalent at the temperature of the relaxation. This oriented configuration is energetically favorable since the more regular arrangements of chains facilitate interaction between the attracting groups of a form which, in the limiting case, represents crystallization. The crystallization process is associated with a decrease in force and an increase in birefringence.

Representing the stress in this nonequilibrium case by the crude approximation of the thermodynamic equation, we have

$$f = \left(\frac{\partial E_D}{\partial l}\right)_T + \left(\frac{\partial E_A}{\partial l}\right)_T - T\left(\frac{\partial S}{\partial l}\right)_T, \quad (61)$$

where E_D is the distortional energy term which increases with elongation and is a function of the instantaneous structure at the temperature at which the initial elongation is carried out. E_A is the intermolecular attraction energy which decreases with elongation and represents the crystal-like interaction. It may be varied practically reversibly with temperature provided the contributions of the other terms remain constant.

The entropy term is a manifestation of the internal Brownian motion of the molecular segments and contributes little at low temperature but becomes more important as the energy constraints are "melted out."

Thus the early portion of the relaxation curve is associated with decreasing strain associated with the distortional energy E_D, which causes a large drop in stress but little change in birefringence. The rate of this relaxation is greater at higher temperatures.

At the lower temperatures, subsequent relaxation is associated with crystallization and decreasing $(\partial E_A/\partial l)$, as substantiated by the decreasing stress

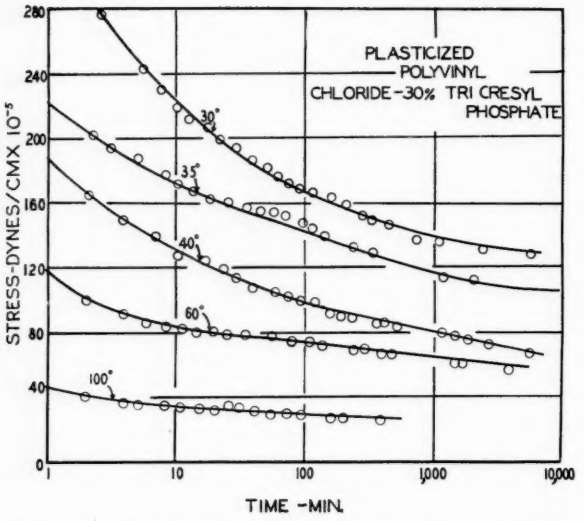

FIG. 35. *Relaxation of the stress of a sample of plasticized polyvinyl chloride containing 30% tricresyl phosphate (TCP) stretched and held at 50% elongation at several temperatures.*

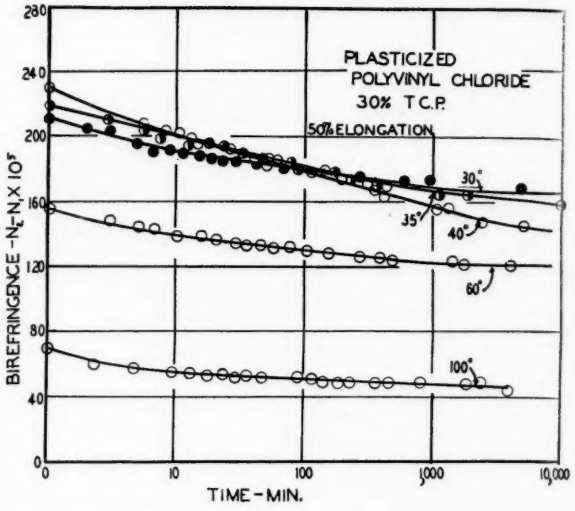

FIG. 36. *Birefringence relaxation corresponding to Figure 34.*

and increasing birefringence. More crystallization occurs at lower temperatures but at a slower rate. The additional structure imposed by this crystallization should result in increased modulus for further extension.

The residual stress is partly entropy elasticity of the chains which have been forced into low-probability configurations in the initial deformation, from which they have been prevented from returning by chain entanglements and crystal-like structure. The amount of this residual stress (and the modulus of the structure) is dependent upon the temperature because (*a*) the entropy elasticity is proportional to temperature, and (*b*) the number of constraining energy interaction "cross links" decreases with increasing temperature.

If the tension on the sample is removed, some of the birefringence will remain and the sample will not return to its original length, for, whereas the force goes to zero, $(\partial E/\partial l)_T$ and $T(\partial S/\partial l)_T$ will not each go to zero, but become equal and opposite in sign. Subsequently, the structure will rearrange very slowly until it again becomes isotropic and the chains will

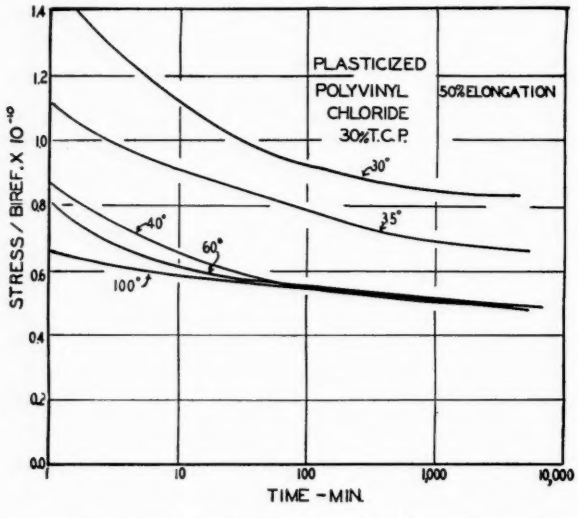

FIG. 37. *Variation of the ratio of stress to birefringence during the relaxation of plasticized polyvinyl chloride containing 30% TCP.*

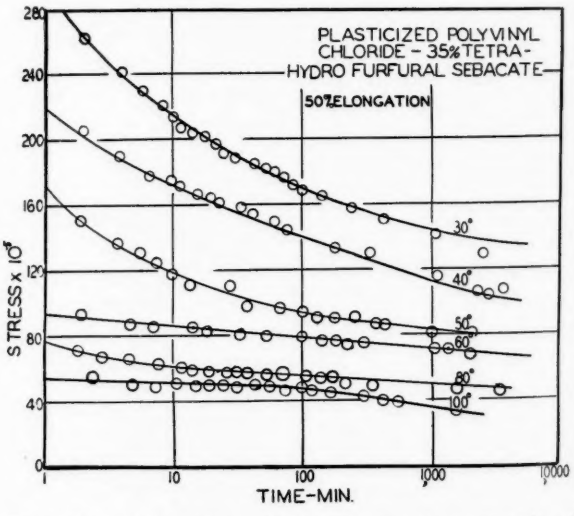

FIG. 38. *Relaxation of the stress of a sample of plasticized polyvinyl chloride containing 35% ditetrahydrofurfural sebacate (DTHFS) stretched and held at 50% elongation at several temperatures.*

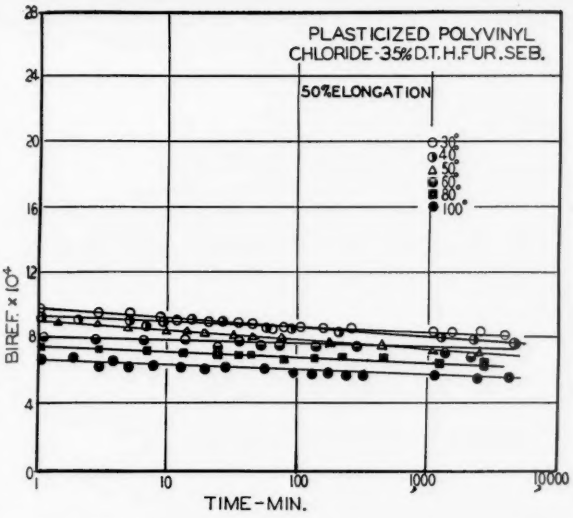

FIG. 39. *Birefringence relaxation curve measured simultaneously with the stress curves of Figure 38.*

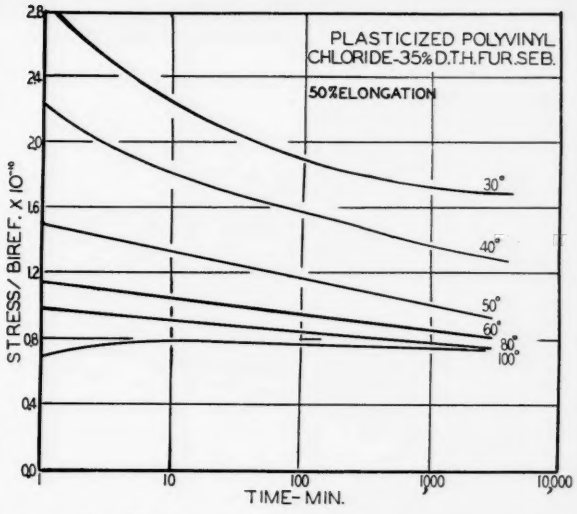

FIG. 40. *Variation of the ratio of stress to birefringence during the relaxation of a sample of plasticized polyvinyl chloride containing 35% DTHFS.*

have diffused to their most probable positions consistent with the equilibrium amount of energy interaction.

Some of these phenomena are nicely demonstrated if one varies the temperature of a sample held at constant length after the initial relaxation has (for all practical purposes) ceased. In Figure 24 the variations in stress and birefringence are plotted for a sample of this polyamide which has been preliminarily relaxed at 100°C, after which the temperature is varied between 100° and 30°C. The state of the sample is such that all E_D and entropy constraints which will relax out (in a sensible time) at temperatures up to 100°C have been removed. In cooling, it is observed that the stress decreases and the birefringence increases. Repetition over several cycles shows that these changes are reversible.

The analogous experiment for creep for a nylon polyamide sample in which the length is observed to change reversibly has been performed by Leaderman [50] and discussed by Alfrey [6].

In view of the present interpretation, these changes are due to variations of E_A with temperature. At lower temperatures, the chains form crystallites ori-

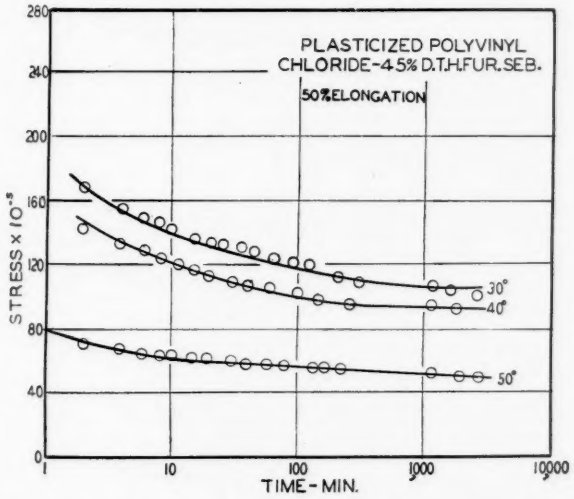

FIG. 41. *Relaxation of stress of a sample of plasticized polyvinyl chloride containing 45% DTHFS stretched and held at 50% elongation at several temperatures.*

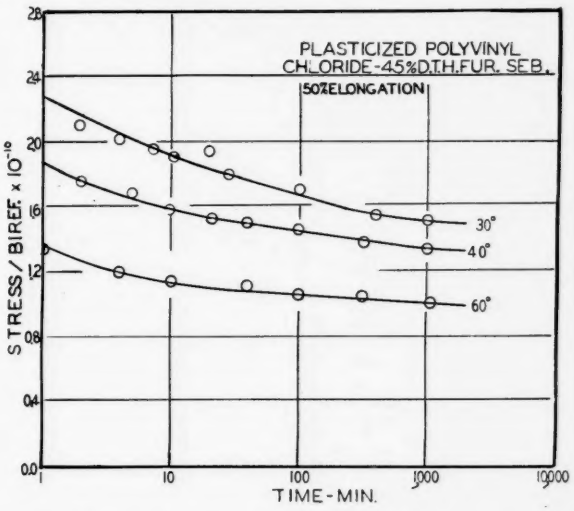

FIG. 42. *Variation of the ratio of stress to birefringence during the relaxation of a sample of plasticized polyvinyl chloride containing 45% DTHFS.*

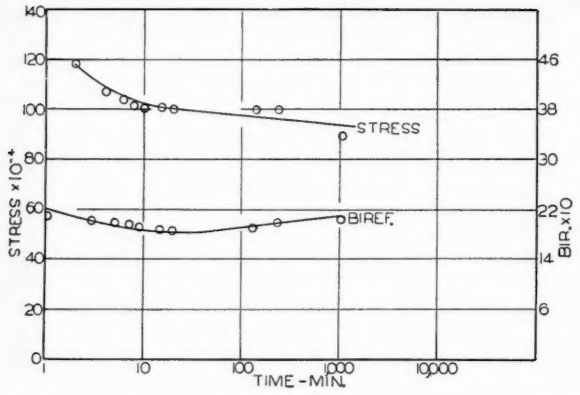

FIG. 43. *Relaxation of stress and birefringence of a sample of plasticized polyvinyl chloride containing 15% DTHFS stretched and held at 100% elongation at 100°.*

ented in the direction of stress. These remelt as the temperature is raised. The stress decreases as the temperature is lowered because of (*a*) the decrease in internal Brownian motion with decreasing temperature and (*b*) the "spontaneous elongation" associated with the squeezing of the chains into oriented crystallites, whereas the birefringence increases because of (*b*). It should be noted that the change in stress is greater than linear with temperature (as would be the case if the elasticity were due only to rubberlike entropy).

Thus, as in Figure 24, the stress may vary reversibly between 30° (or less) and 100°C, crystallization occurring in "equilibrium" with the structural constraints not relaxing out up to 100°C. However, if the temperature exceeds 100°C, more of these structural constraints will relax out. That is, areas of

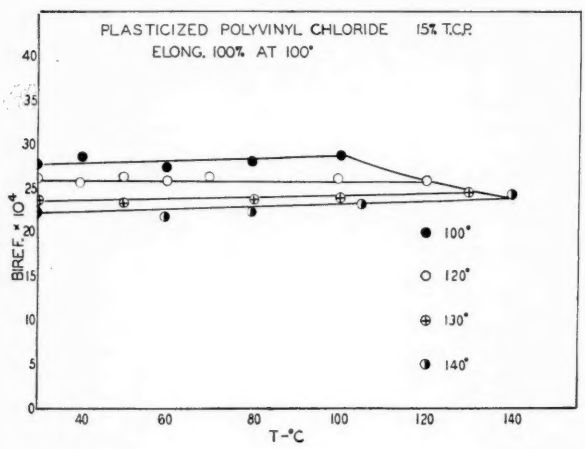

FIG. 45. *Birefringence-temperature cycle measured simultaneously with the stress curves of Figure 43.*

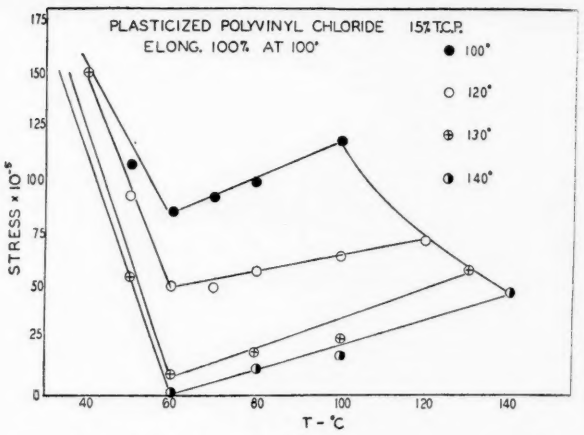

FIG. 44. *Stress-temperature cycle for a sample of plasticized polyvinyl chloride containing 15% TCP initially stretched, held, and relaxed at 100% elongation and 100°C.*

energy interaction which have been acting as cross links at the lower temperatures melt out and some entanglements are released. An irreversible structural relaxation occurs and the stress and birefringence both decrease so that after waiting at the higher temperature (130°C) a new quasi-equilibrium structure having fewer constraints results. Subsequent lowering of the temperature produces reversible changes in stress and birefringence in equilibrium with the new structure (see Figure 25).

In Figures 26 and 27 the behavior of the observed changes in stress and birefringence for this material are presented for temperatures between 30° and 130°C. (The reversible curves are indicated by a double arrow and the irreversible curves by a single one.)

For example, in Figure 26, the sample, after having relaxed to a pseudo-equilibrium state at 60°C, is cooled to 30°C. It is found that the stress decreases reversibly along *BA*. On increasing the temperature to 60°C again, point *B* is again reached. If heating is continued past 60°C, the stress decreases irreversibly along *BC*. If on reaching 80°C at point *C*, the sample is cooled to 30°C, the stress now varies reversibly along *CD*. Similarly, heating past 80°C produces more irreversible relaxation along *CE*, etc. The birefringence curves of Figure 27 are analogous.

The question which now arises is, "What sort of function is the state of the sample of previous thermal and mechanical history?" That is, how do the properties of a sample which has been initially stretched and relaxed at a temperature T_2 compare with those of a sample which has been initially stretched at a

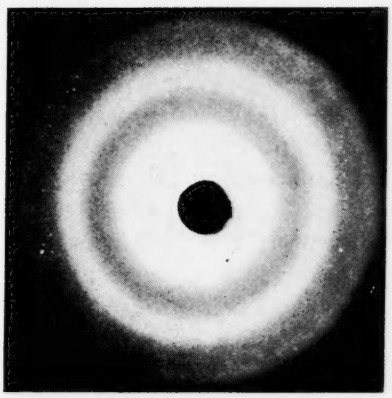

FIG. 46. *X-ray diffraction pattern (CuKα) for unstretched plasticized polyvinyl chloride containing 15% DTHFS at 30°C.*

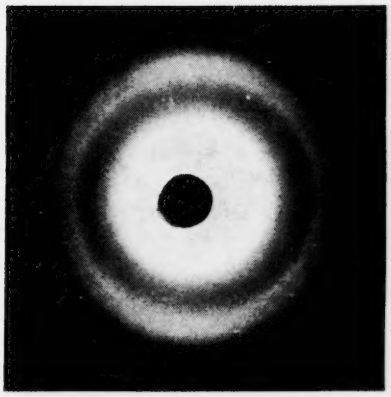

FIG. 47. *X-ray diffraction pattern for a sample of plasticized polyvinyl chloride containing 15% DTHFS stretched 100% at 40°C, relaxed at 60°C, and cooled to 30°C. The fiber axis is vertical.*

temperature T_1, relaxed, and then heated to T_2 (while held at constant length) and allowed to reach pseudo-equilibrium? In an attempt to answer the question, a set of runs was made on an undrawn elastic polyamide * (sample B) at an elongation of 600 percent. Samples were initially stretched at 30°, 60°, and 80°C and the stress-birefringence-temperature behavior was mapped by cyclic variations in temperature as before. The results are presented in Figures 28 to 33.

It is seen that for this type of experiment, the curves are practically superposable and that the same state is reached regardless of the sequence of the operations performed in attaining it. There are several interesting conclusions that may be drawn from this experiment. The fact that a single state is reached regardless of the direction of approach illustrates nicely the utility of the concept of the "pseudo-equilibrium state." This sequence of experiments demonstrates that the state is uniquely defined for temperatures below the temperature at which the initial relaxation occurs.

Also, it is seen that the number of structural constraints under such conditions is a unique single-valued function of the temperature. The stress, decaying at a given temperature, does not decay slowly to zero in a single process but decays toward the stress characteristic of a structure governed by these constraints.

The results also indicate that the pseudo-equilibrium structure is probably free of the short-range distortional energy which is introduced in the initial deformation. This may be concluded from the fact that the same state may be reached by two experiments involving an initial stretching at two different temperatures. The amount of distortion initially introduced is obviously dependent upon the number of structural constraints (which depends upon the temperature) present at the time of stretching. Since different amounts of distortional energy are introduced by stretching at two different temperatures, and subsequent processes all involve removal of this distortional energy and since the same final state is reached, one may conclude that the remaining amount of distortional energy is independent of the amount initially introduced.

The presence of the postulated crystalline order in these samples is readily demonstrable by x-ray diffraction, as has been shown by the work of Baker and Fuller [10]. For example, Figure 34 shows the x-ray diffraction pattern for an oriented (B) and an unoriented sample (A).

Plasticized Polyvinyl Chlorides

Figure 35 illustrates the stress-decay curve for plasticized polyvinyl chloride * and Figure 36 illustrates the corresponding birefringence relaxations. The curves show a slower-than-logarithmic decay usually associated with a broad distribution of relaxation times [3]. The temperature sensitivity of stress is greater at lower temperatures and the effect of increasing temperature appears to be to produce a horizontal shift to the left (correspond-

* Copolymer of 40 mol percent *N*, *N'*-diisobutyl hexamethylene diamine, 20 percent mono-*N*-isobutyl hexamethylene diamine, and 40 percent hexamethylene diamine with azelaic acid.

* Geon 202 containing 30 percent tricresyl phosphate.

ing to a very high activation energy according to the distribution of relaxation-time interpretation).

On the other hand, the birefringence curves show little temperature sensitivity in the low-temperature range and are flatter than the stress curves. Therefore the ratio curves (Figure 37) are not horizontal but flatten with time and appear to approach a limiting high temperature value.

The decay curves for polyvinyl chloride containing 35 percent ditetrahydrofurfural sebacate (DTHFS) (Figures 38 to 40); 45 percent (Figures 41 and 42); and 15 percent (Figure 43) show a somewhat similar general behavior.

In the low-temperature region, it appears that the distortional energy contribution to stress is dominant and that the entropy contribution is suppressed by energy interaction. Thus, there is a large stress which is sensitive to temperature, but the birefringence changes with time are small. As this distortion relaxes out, the stress approaches a value determined by steric cross links, entanglements, etc.

At higher temperatures the structure is not distorted on stretching, so that the stress-birefringence ratio does not vary with time. However, the stress does not vary directly with temperature in this case because the number of effective steric cross links as well as the kinetic energy of the segments varies with temperature.*

The variation in properties with temperature is somewhat interesting. In Figure 44 the stress-temperature cycle curve for the 15 percent TCP sample is plotted. The reversible and irreversible portions of the curve for this material are similar to those for the elastic polyamide with the exception that at low temperatures there is a reversal of slope of the reversible portion of the curve. This effect has been noted before by Meyer and Ferri and has been ascribed to thermal expansion. As the sample is cooled at constant length, there is a tendency for elongation due to entropy elasticity and attractive energy- (or crystallization-) type forces and a tendency for contraction due to ordinary thermal expansion. At the minimum, the two effects equalize, whereas at lower temperatures the contraction effect is greater. The sample becomes progressively stiffer as it is cooled, so that as a result of the constant length restraints there is a large force increase at the lower temperatures. The effect is described by equation (1*b*); a quantitative analysis of the data in terms of this equation will appear in a later paper.

The corresponding birefringence-temperature cycle is presented in Figure 45. The birefringence behavior also shows the reversible region but differs from the polyamide curves in that the slope of the reversible curve is positive rather than negative. The thermal expansion, being principally an energy contribution, does not influence the birefringence curve.

The similarity of these curves to the polyamide curves has indicated the possibility of crystallization playing a role here. X-ray diffraction has substantiated this. Figure 46 is an x-ray diffraction pattern for the unstretched 15-percent DTHFS whereas Figure 47 is the x-ray diffraction pattern for the same sample which has been elongated 100 percent and allowed to relax. These patterns show definite indications of crystalline order and orientation. This would provide the necessary structural rigidity for distortion to be the preferential mechanism of primary yield.

The crystalline nature of these substances has been shown to be a function of conditions of plasticization, method of preparation, and mechanical and thermal history. A study of these processes is being carried out by Professor Alfrey and Mr. Wiederhorn, together with the authors.

In this experimental survey, we have demonstrated and, in part, resolved, the stress-birefringence behavior of several materials and have demonstrated the effects of the several contributing "unit processes" which were discussed in the section on theory. Through their application several new aspects of the structural-mechanical behavior of these structures have been revealed.

Acknowledgment

The authors are indebted to the E. I. du Pont de Nemours & Co. for furnishing the films of elastic polyamides, and to Prof. Turner Alfrey and Mr. Norman Wiederhorn, of the Polytechnic Institute of Brooklyn, for supplying the plasticized polyvinyl chloride films.

Thanks are also expressed to the Engineering Department of Princeton University for permission to use and to modify their photoelasticity apparatus for birefringence measurements.

* The behavior may also be somewhat complicated by the fact that we are dealing with a two-phase system containing both plasticizer and polymer so that the behavior is also governed by the thermodynamics of the polymer-plasticizer interaction. The nature of this is being investigated at present and will be reported in a later communication.

Book Reviews

Organic Chemistry. Third English Edition. Paul Karrer. Translated by A. J. Mee. New York, Elsevier Publishing Company, Inc., 1947. 957 pages. Price, $8.50.

(Reviewed by L. W. Rainard, Alexander Smith & Sons Carpet Company)

One of the classics of organic chemical textbooks, Karrer's *Organic Chemistry,* is reissued as the Third English Edition with only a few minor revisions. The binding is sturdy—certainly of better quality than that of previous editions. The paper seems of good quality, suitable for a reference text that may find frequent and hard usage. The typography, which is of the same character as that in the previous editions, is clear and easy to read. In general, this volume is well constructed and worthy of its contents.

The subject matter is classified and arranged in much the same way as in previous editions. The general emphasis is on naturally occurring compounds. The sequence of titles indicates again that Karrer's presentation is logical and easily followed. There have been new sections added, notably a section on penicillin and one on the compounds of heavy hydrogen. However, the author's claim that the modern literature up to the end of 1945 has been reviewed and taken into consideration is hardly founded. It is not expected that a treatise of this type would cover modern physical organic chemistry in a detailed fashion, although one might expect a passing nod towards the physical aspects of organic chemistry with some discussion of the application of free radical chemistry, catalysis, mechanism, etc. to the typical classical synthetic problems. Modern organic theory has reached the status where any comprehensive text must take into consideration more of the physical aspects of reactions than this book does. The material presented here and the methods of attack described are, essentially, part of our scientific heritage. The method and reasoning involved must be made familiar, of course, to a practicing chemist. However, its day-to-day use would be limited in the laboratories of the modern industrial concern. More simplified and direct synthetic methods are in demand. Karrer's book will probably find its main use, as usual, in the university laboratory, although it seems doubtful that enough new material is presented to warrant the scrapping of earlier editions.

Despite these criticisms of the scope and the text, Karrer's *Organic Chemistry* will be of continued interest and value to the researcher. There is a large amount of information accumulated here, enough to touch on the interests of a very broad group.

Spinning Rayon Staple on the Cotton System. Published by the American Viscose Corporation, Textile Research Department, Marcus Hook, Pennsylvania.

(Reviewed by E. B. Grover, North Carolina State College School of Textiles)

Nearly a decade has passed since Courtaulds Limited of England published a small pamphlet "Fibro in the Cotton Industry." This was the first complete compilation of information for the spinner's use in processing cut staple rayon on cotton machinery.

Recently the American Viscose Corporation, which owes its beginnings to Courtaulds, published this handbook, *Spinning Rayon Staple on the Cotton System.* This book, notably free of advertising, amplifies, supplements, and brings up to date the technical, scientific, and manufacturing information initiated by Courtaulds pertaining to processing cut rayon staple on the cotton system. Its success in presenting the subject is based on the outstanding success of the Textile Research Department of the American Viscose Corporation.

Specifically, this book traces the manufacture of cut staple, followed with an analysis of the properties and physical characteristics of "Avisco" rayon staple. Chapters are devoted to the effect of denier, staple length, and humidity on the selection and processing of this material. The next section gives concise information to guide the practical textile

manufacturer, covering all mill processes from opening through the final finishing of the spun rayon fabric. Included also is a tabulation of several fabrics made of spun rayon and blends.

Of particular value are the series of graphs showing the effects on various final spun yarn properties due to variations in twist, denier, staple length, type of staple used, and the like.

As a whole, the book is attractively printed, well indexed, well illustrated, and should be of value to students of the subject, as well as to mill men.

Industrial Experimentation. K. A. Brownlee. Brooklyn, N. Y., Chemical Publishing Company, Inc., 1947. 151 pages. Price, $3.75.

(Reviewed by E. R. Schwarz, Textile Division, Massachusetts Institute of Technology)

This is a straightforward, simple presentation of the use of certain statistical techniques in industrial experimentation. It is pointed out in the foreword that the practice is sometimes followed of consulting the statistician only after the experiment is completed and then asking him what can be done with the results. It is essential to have the experiment in form suitable for statistical analysis and this, in general, can be done only when the experiment has been designed by someone with knowledge of the statistical methods which are to be applied.

Outstanding features are the chapters dealing with sampling methods and with the practical use of the analysis of variance. Only ordinary arithmetic and very simple algebra are used throughout and the inclusion of many numerical examples makes the book an easy-to-use working reference. The increasing use of the quality control chart in the textile industry makes knowledge of how to use proper sampling, correlation analysis, significance testing, and variance analysis necessary for the technologist. While *Industrial Experimentation* does not contain illustrative textile material, the application of the methods described to the textile field should be easy and direct.

A unique presentation, and perhaps the most valuable in practice, is that of the two-way, three-way, four-way, and five-way analyses of variance, together with an unusually lucid treatment of the incomplete variance analysis with replication.

In the past, variance analysis has not been used as frequently as it should have been. With this volume at hand, there can be no excuse for not employing this extremely powerful statistical tool. That other considerations have been subordinated by the author is an advantage rather than a disadvantage. Most effective use of the book will be made by those already reasonably well grounded in the fundamentals of statistics, but even the relatively uninitiated will find it of very real interest and value.

The only improvement which might be made is in the format of the volume rather than in its contents. The printing is sometimes not of the clearest, and the small type size and crowding of material is to be regretted. This, however, cannot be charged against the author, who has done a thoroughly good job, for which only the highest commendation can be given.

ABSTRACTS

SERVICES AVAILABLE

Reprints of the original articles abstracted in TEXTILE RESEARCH JOURNAL *are often available from the publishers. Otherwise, it may be possible to secure copies of the periodicals. Orders should be sent direct to the publishers.*

Photostat negatives of articles abstracted will be furnished to members of the Institute at a cost of 25 cents per page for pages not exceeding 7 inches in width and 50 cents per page for larger sizes up to 11½ x 14 inches. Photostats of patents are 50 cents per page. The library's service charge will be added.

Microfilm copies and paper enlargements of microfilm may be obtained from: Microfilms Inc., 313 N. First St., Ann Arbor, Mich.; New York Public Library, New York, N. Y.; Yale University Library, New Haven, Conn.; Harvard University Library, Cambridge, Mass.; and Library of Congress, Washington, D. C. Translations may also be obtained from the above sources.

The JOURNAL *is again offering to its subscribers reprints of the Abstracts and Book Reviews sections, printed on one side of the sheet so that the items may be clipped, pasted on cards, and filed for permanent reference. Subscriptions to this service for 1948 are $3.00 each. Orders for this special service should be mailed at once to Textile Research Institute, Inc., 10 East 40th Street, New York 16, N. Y.*

A list of periodicals abstracted, the abbreviations used in references to articles, and the addresses of publishers of English language publications is given in the January, 1948, issue, page 48.

ANALYSIS: TESTING: LABORATORY METHODS

★

Hydrolysis of Cellulose

Analysis of mixtures of monosaccharides obtained by the hydrolysis of cellulose and related products. A. Roudier. *Chim. anal.* **29**, 245–51 (1947); cf. *C.A.* **42**, 489*b* (through *Chem. Abstr.* **42**, 1152*g* (Feb. 20, 1948)).

Procedures are outlined for the analysis of a mixture of xylose, galactose, and glucose, a mixture of galactose, glucose, and arabinose, and a mixture of xylose, arabinose, glucose, mannose, and galactose. A bibliography of 83 titles of published papers and 4 textbooks is given.

Text. Research J. May 1948

Color Measurement on Fabrics

Color measurements on colored fabrics. P. M. Heertjes, E. van den Heuvel, and J. Lotichius. *Chem. Weekblad* **43**, 619–28 (1947) (through *Chem. Abstr.* **42**, 1430*b* (Feb. 20, 1948)).

The International Commission on Illumination system of color specification is discussed. A Keuffel & Esser Color Analyzer was modified by the removal of the spectroscope and the addition of a photoelectric cell and sources capable of furnishing 5 monochromatic bands; this makes possible the determination of the percentage of reflection at 5 wave lengths. The apparatus showed that in dyeing and printing the reflection usually decreases with increasing concentration of dye; with low dye concentrations and high wave lengths this is sometimes reversed. Variations in samples which appeared uniform on inspection were detected. The results obtained from mixtures of dyes were similar to those obtained from single dyes, if the ratio of the constituents was kept constant. After-treatment with Turkey-red oil, steam, and soap resulted in an increase in reflection for Alizarin Red, but not for Alizarin Orange. Samples dyed to the same shade with different dyes gave different reflections at each wave length. The difference in shade between mercerized and unmercerized cotton dyed with indigo and the shade of black materials could not be studied with the apparatus.

Text. Research J. May 1948

Color Measurement in Wool Dyeing

New applications of color measurement in the dyeing of wool. H. J. Selling. *J. Soc. Dyers and Colourists* **63**, 419–24 (Dec. 1947).

By analogy with the analysis of dyes in solution, the possibility of analyzing the amount of acid dyes on a woolen fabric was investigated. A study of the prediction of dyeing formulas of known dyes was also made in order that mixtures of these dyes might be chosen to match a sample containing unknown dyes.

Text. Research J. May 1948 Authors

Testing of Dyes

Instrumental methods applied to dyestuff testing. Anon. *Chem. and Eng. News* **26**, 866 (Mar. 1948).

A summary of the program of the winter meeting of the Optical Society of America in New York. Among the topics discussed are: use of the spectrophotometer for continuous measurements of dyeing baths during the dyeing process; a study of the colorimetric behavior of 171 pairs of typical dyes; use of the spectrophotometer for selection of colorants and for color-matching

in the plastics industry; and testing of dyestuff shipments by applying the spectrophotometer to dye solutions. R. W. Eyler

Text. Research J. May 1948

Fastness Test

A proposed system for testing and evaluating the fastness of dyestuffs or dyeings. E. W. Thommen. *Textil-Rundschau* **2**, 323–30 (Sept. 1947).

A method suggested as an international standard has been developed to satisfy the research dye-chemist, the colorist, and the finisher, as well as the dye salesman, which is based on dyeings of uniformly established depths of color so that dependence on prescribed dyes is eliminated. To exclude the uncertainty of manual testing and to determine resistance to washing and fulling a machine is used which washes and fulls, operates at a bath ratio from 1:2 to 1:100, and can carry out any number of simultaneous tests. It consists of a support carrying a shaft with an eccentric disc driven by a small A.C. motor. The stainless-steel containers holding the liquids required for the test have ribbed bottoms and are immersed movably at an inclination of 45° in a water bath heated by electricity, gas, or steam, controlled by a thermostat, and stirred with an agitator. A friction shoe, likewise ribbed, is attached to the shaft by an arm and moves in these containers. The fabric sample to be tested is attached to a simple carrier system and introduced into the container with the wash liquor. The machine furnishes results which correspond to manual operation when the friction shoe is pushed back and forth 30 times per min. for $\frac{1}{2}$ hr. The fulling is carried out in the customary bath ratio of 1:1 or 1:2 and can be adapted to any requirements by application of a weight. The samples being tested and the test liquor can be observed during the entire test period and any sample can be removed without stopping the machine. Photographs show the essential parts of the apparatus dismantled from two different angles of view. A description is given of the method proposed for interpreting the test results. Ilse Zeise

Text. Research J. May 1948

Flammability

Flammability varies with type test and fabric. Marjorie W. Sandholzer. *Textile World* **98**, 109, 110, 186–97 (Mar. 1948).

The horizontal, vertical, and inclined test methods are described and the results obtained with a wide variety of fabric samples using the 3 methods on each sample are listed. Accident reports summarize the type of fabrics worn when injuries have been the result of burning apparel. J. A. Woodruff

Text. Research J. May 1948

Laboratory Control

Improve twisting operations by laboratory control. H. C. Pratt. *Textile Inds.* **12**, 82–86 (Dec. 1947).

Control testing of each process in the mill will improve the efficiency of the twisting operation. The testing instruments and the methods of testing are described.

A. L. Landau

Text. Research J. May 1948

New pH Standard

Saturated potassium hydrogen tartrate solution as a pH standard. James J. Lingane. *Anal. Chem.* **19**, 810–11 (Oct. 1947).

A saturated aqueous solution of potassium hydrogen tartrate is a more convenient secondary standard for the calibration of pH measuring instruments than any of the buffer solutions generally used for this purpose. The saturated solution at 25°C is 0.034 *M* and has a pH of 3.57 ± 0.02. The recrystallized salt does not differ from the commercial C.P. material by more than ± 0.005 units. Solutions are more stable than potassium hydrogen phthalate, and CO_2 from the air does not affect the results.

A. R. Macormac

Text. Research J. May 1948

Structure of Polymers

Physical methods of investigation of the structure of polymer molecules in solution. V. N. Tsvetkov. *Vestnik Leningrad. Univ.* **1947**, No. 1, 51–102 (in Russian) (through *Chem. Abstr.* **42**, 1081*d* (Feb. 10, 1948)).

Critical review (111 references) and summarizing exposition, particularly of the author's recent work in the field.

Text. Research J. May 1948

Starch Viscosity

The V.I.-Viscosigraph, an apparatus for continuous measurement of the viscosity of starch suspensions. H. J. Selling and F. L. J. van Lamoen. *Chem. Weekblad* **43**, 602–6 (1947) (through *Chem. Abstr.* **42**, 1086*d* (Feb. 20, 1948)).

The V.I.-Viscosigraph comprises a vessel surrounded by incandescent coils, in which the starch paste can be heated to regulable temperatures, which can be read off on a thermometer. A stirrer rotating at 72 r.p.m. in the starch is coupled to the rotor of a synchronous motor mounted in the top of the apparatus The number of revolutions has a great effect on the measurements. A coil spring is attached to the motor housing, which is so mounted that it rotates freely on ball bearings. Depending upon the degree of resistance encountered by the stirrer in the starch solution and upon the rigidity of the coil spring used, the housing rotates over a certain angle during the stirring of the suspension. This angle can be read on a scale provided at the housing. By calibrating the coil spring the magnitude of the moment of the couple can be determined in g.cm. by the rotation of the housing. A recording mechanism is built on the apparatus by which the resistance encountered by the stirrer is read off directly in g.cm. from mm.-paper. The Viscosigraph is calibrated against thick oils of known viscosities. Determinations are accurate to within 2%. Addition of increasing quantities of borax (0.25–3.75 g.) to concentrated potato starch suspensions at first decreases

the viscosity, then increases it to higher values than without borax. Upon still larger additions the curves become irregular. Borax (1.5 g. and more) changes the nature of the pastes; e.g., prevents boiling over. Addition of an electrolyte, such as 0.1*N* KCl, gives a gradual curve of viscosity vs. time.

Text. Research J. May 1948

Wrinkle Recovery Meter

Monsanto's wrinkle recovery meter. Donald H. Powers. *Text. Col. and Converter* **69**, No. 11, 33 (1947) (through *Chem. Abstr.* **42**, 1060*d* (Feb. 10, 1948)).

The development of an apparatus for measuring the recovery of fabrics after creasing is reported.

Text. Research J. May 1948

CHEMICAL AND PHYSICAL RESEARCH

★

Cationic Exchange

Cationic exchange reactions of cellulose and their effect on insulation resistance. H. F. Church. *J. Soc. Chem. Ind.* (*London*) **66**, 221–6 (July 1947).

It is shown that a wide range of cations can enter into exchange reactions with cellulose and that, when the reaction with given cations is complete, equal numbers of atoms are attached to the cellulose irrespective of valency. Probable mechanisms are discussed. The electrical resistivity of cellulose in the form of insulating paper has also been studied when the material is modified in various ways by cationic exchange. It is shown that the best values of resistivity are obtained when the cations attached to the cellulose are bivalent and the worst when the exchange is by univalent ions. Of the univalent ions investigated, hydrogen causes the lowest resistivity. The implications of this are discussed and means of improving insulation resistance are proposed. The effects of cationic exchange on resistivity may readily be masked in commercial insulating papers by electrolytes deposited in the fibers. These must be removed by adequate washing if the full advantage of beneficial cationic exchange is to be achieved.

Text. Research J. May 1948 Author

Solvent Media for Cellulose

The solubility of cellulose in mixtures of nitrogen tetroxide with organic compounds. W. F. Fowler, Jr., C. C. Unruh, P. A. McGee, and W. O. Kenyon. *J. Am. Chem. Soc.* **69**, 1636–40 (July 1947).

Cotton linters with a cuprammonium viscosity of 7 sec. dissolves to give a clear, smooth, and viscous solution in mixtures of N_2O_4 with a large number (45 are listed) of organic compounds including nitrocompounds, sulfones, nitriles, and esters. The cellulose may be recovered by flowing the dope on a surface and allowing the solvent to evaporate, or by pouring the solution into a nonsolvent such as CCl_4. Analysis indicates that very little oxidation or nitration has taken place but the cuprammonium viscosity is considerably decreased. The solubilizing effect of the various components of the different solvent combinations on the hydrogen-bonding which holds the cellulose molecules together is discussed. Properties which are necessary for producing new solvents for cellulose by the present method are a substance (*I*) having a 3-electron bond plus a substance (*II*) having the following properties: (*a*) at least 1 electronegative group stabilized by resonance, (*b*) no reactivity or very slow reactivity with (*I*), and (*c*) miscible with or soluble in (*I*), and the combination of (*I*) and (*II*) does not react with cellulose.

A. R. Macormac

Text. Research J. May 1948

Orientation in Cellulose Gels

Deformation mechanism of cellulose gels. III. Changes in orientation on drying. P. H. Hermans, J. J. Hermans, D. Vermaas, and A. Weidinger. *J. Polymer Sci.* **2**, 632–6 (Dec. 1947).

The change in orientation upon drying regenerated viscose filaments, as determined by x-ray studies, was either very small or zero. The author concluded that, in so far as the crystallites are concerned, the theory of affined deformation applies neither to the process of stretching nor to that of drying. (*Cf.* TEXTILE RESEARCH JOURNAL **17**, 230 (Apr. 1947).) E. D. Klug

Text. Research J. May 1948

Color Standards

Lovibond color standards—Crisis or challenge? J. T. R. Andrews. *J. Am. Oil Chemists' Soc.* **25**, 20–3 (1948).

This report, prepared at the request of the A.O.C.S. Color Committee by a member of the Uniform Methods Committee of the American Oil Chemists' Society, brings up to date the present controversy of the American oil industry regarding prospects for future delivery and quality of Lovibond glasses. While Tintometer, Ltd., of England can supply Lovibond glasses, their recently announced policy is to do so only within certain limitations and under special circumstances. Loose slides will no longer be available except for replacement and to supply ASTM and TAG petroleum standards; slides will be sold no longer in $2 \times \frac{3}{4}$-in. size, but in $\frac{3}{8} \times \frac{3}{4}$-in. size. In future, except as noted, only complete color-measuring instruments will be sold by Tintometer, Ltd. Excerpts are included from correspondence of the Uniform Methods Committee with Tintometer, Ltd. D. Nickerson

Text. Research J. May 1948

Electro-Chemistry of Dyeing

Some aspects of the electro-chemistry of dyeing. S. M. Neale. *J. Soc. Dyers and Colourists* **63**, 368–71 (Dec. 1947).

An attempt is made to provide a simple physical picture of the effect of electrical forces upon the dyeing process. Since both fibers and color ions are electrically charged relative to the water by which they are sur-

rounded, they either attract or repel one another, according to whether they are oppositely or similarly charged. This electrostatic effect is not the principal factor in the affinity of a dye for the fiber, but the variations in the strength and character of the electrostatic force are responsible for the effects of salt in dyeing, and for the effect of acid on the dyeing of silk and wool. The progress of research on this problem is indicated. Authors

Text. Research J. May 1948

Fibrous Molecules in Solution

The form of fiber molecules in solution. Werner Kuhn. *Experientia* **3**, 315–18 (1947) (in German) (through *Chem. Abstr.* **42**, 1106*f* (Feb. 20, 1948)).

Bier's (cf. *C.A.* **40**, 6311[5]) assumption that long-chain molecules in solution behave like rigid rods is in contradiction to Kuhn's experience (cf. *C.A.* **40**, 5620[4,7], 6913[8], 6937[8]). Evidence is given of coiled molecules and partially free rotation. The change of shape of nitrocellulose molecules is of the order of 10^{-5} to 10^{-3} sec.

Text. Research J. May 1948

Viscosity of Polymer Solutions

Mechanical degradation of large molecules. W. J. Morris and Robert Schnurmann. *Nature* **160**, 674 (Nov. 1947).

Data are presented on the permanent viscosity loss as a function of the number of cycles of forcing a polymer solution in individual drops through a jet. R. W. Eyler

Text. Research J. May 1948

Effect of Reagents on Wool

Coiling of wool induced by certain reagents. Martin R. Freney. *Nature* **160**, 799 (Dec. 1947).

Observations on the coiling and uncoiling of wool fibers when immersed in certain solutions are reported. The effect of time of immersion and the effects in caustic soda, water, acid, potassium cyanide, sodium thioglycollate, sodium sulfide, ammonium hydroxide, and potassium hydroxide were noted. Prolonged action of caustic soda is reported to make the wool resistant to the disintegrating action of sodium sulfide.

Text. Research J. May 1948 R. W. Eyler

BLEACHING: DYEING: FINISHING

★

Acetate Dyeing

The fast coloration of cellulose acetate rayon, with particular reference to shades of good fastness to scouring. A. Mellor and H. C. Olpin. *J. Soc. Dyers and Colourists* **63**, 396–400 (Dec. 1947).

Azoic dyes may be applied to cellulose acetate rayon to give shades which are very fast to wet processing and are satisfactory either for effect threads or for multi-colored fabrics. Base and "napthol" are applied together, and diazotization and coupling proceed simultaneously in a nitrous acid bath. The process is completed by a soaping treatment. Indigoid vat dyes, and one or two anthraquinonoid vat dyes, provide useful supplementary colors. Dispersed-type dyes are not suitable for this purpose, but selected members are very useful for dyeing fast-to-light shades on soft furnishings. The blue dispersed dyes need protection from acid fumes. This phenomenon of "acid fading" is discussed from the point of view of dye selection and the use of protective agents, and practical recommendations are made which experience has shown to be sufficient to reduce it to negligible proportions. The application, by solvent dyeing, of various classes of dyes not normally having affinity for cellulose acetate rayon, is discussed briefly. This technique is still in its infancy. Aniline Black may also be applied.

Text. Research J. May 1948 Authors

Combination of Acid Dyes with Nylon

The combination of acid dyes with amine and amide groups in nylon fibre. P. W. Carlene, A. S. Fern, and T. Vickerstaff. *J. Soc. Dyers and Colourists* **63**, 388–93 (Dec. 1947).

Evidence for the existence of amine and amide groups in nylon is provided by a titration curve of nylon fiber with hydrochloric acid. The amine groups are more important in practical dyeing since these provide the ionic dye sites between pH 3.0 and 6.0, attachment of dye to positively charged amide groups occurring only at a lower pH value. The tendering action of certain acid dyes at very high concentrations on wool has also been observed on nylon. Selected acid, dispersed cellulose acetate rayon, and Solacet dyes have been applied to undrawn nylon monofil in a range of concentrations, and the tensile characteristics of the dyed monofil measured. With the majority of acid and Solacet dyes (applied from acid baths) a sharp drop in breaking load and extension occurs when the amine groups become saturated and attachment of dye to the amide groups begins. Dispersed cellulose acetate rayon and Solacet dyes applied from a neutral bath at comparable concentrations cause no such degradation. It is suggested that the development of an electrical charge on the amide groups by the absorption of a hydrogen ion restricts the free movement and slippage of the polymer chains and prevents their orientation when drawing is attempted. Dispersed cellulose acetate rayon dyes are presumed to be attached by hydrogen bonds to the carbonyl oxygen atoms of the amide groups by forces comparable with those between polyamide chains. They are thus capable of being more easily displaced so that drawing can occur.

Text. Research J. May 1948 Authors

Temperature Control in Dyeing

Industrial dye vat control. F. Blezzard. *J. Soc. Dyers and Colourists* **63**, 439–45 (Dec. 1947).

The incentive for the use of temperature control in dyeing lies in the demand for continued duplica-

tion of processing. Early attempts at regulation failed through incomplete knowledge of the required performance and the use of inadequate regulators. Very stringent control is necessary for success, and this paper outlines the development of up-to-date dye vat regulators and gives details of their performance.

Text. Research J. May 1948 Author

Dyeing Technology in Germany and America

Dyeing: A comparison between the changes in German and American practice. R. G. Fargher. *J. Soc. Dyers and Colourists* **63**, 425–9 (Dec. 1947).

Changes in German and American dyeing practice reflect the angles of approach and labor problems of the two countries. Refinements to existing machines have formed the major contribution from German technology; they are often associated with a general plan to reduce and control processing tensions. The American contribution is concerned largely with continuity of processing, often without reference to the control of tension. In both countries, the impact of chemical engineering on the design of finishing machinery is only now beginning to be felt. Author

Text. Research J. May 1948

Shrinkproofing

Friction between keratin surfaces as affected by some shrinkproofing treatments. M. Lipson and P. Howard. *Am. Dyestuff Reptr.* **36**, 470–2, 475–6 (Aug. 25, 1947); *cf.* TEXTILE RESEARCH JOURNAL **17**, 237 (Apr. 1947).

Text. Research J. May 1948

Slashers and Slashing

Slashers and slashing. R. A. Silcox. *Textile Age* **2**, 48, 50, 52–4, 56 (Feb. 1948).

An outline of the various types of creels which are used to supply the warp for slashing. The creels which are discussed are the over and under, the upright, inclined, magazine, and the cylinder creel. A. L. Landau

Text. Research J. May 1948

Glycerin Substitute

Lactolin as substitute for glycerol in the textile industry. E. Belani. *Monatschr. Textil-Ind.* **56**, No. 1, *Kolorist. Tl.* 17–19 (1941); cf. *C.A.* **35**, 2322[9] (through *Chem. Abstr.* **42**, 1060*b* (Feb. 10, 1948)).

Lactolin, aqueous 60% Na lactate, may replace glycerol in formulas for sizing of cotton and rayon yarns and finishing of fabrics; it aids in dispersing starch but is otherwise chemically indifferent to most materials used in these applications. Several formulas are given.

Text. Research J. May 1948

FIBERS: YARNS: FABRICS: MECHANICAL PROCESSES

★

Boll-Weevil Control

Boll-weevil control with chlordan, benzene hexachloride, and calcium arsenate dusts. Charles H. Brett and W. C. Rhoades. *J. Econ. Entomol.* **40**, 572–4 (1947) (through *Chem. Abstr.* **42**, 1011*h* (Feb. 10, 1948)).

In field tests, a talc dust containing 10% by weight of chlordan and applied at 10 lb. per acre proved as effective as Ca arsenate alone at 6 lb. per acre against *Anthonomus grandis* on cotton. Benzene hexachloride (10% γ-isomer) (*I*) in a 5% dust was somewhat more effective than chlordan or Ca arsenate dusts. In laboratory tests, the susceptibility of the weevils to *I* increased with rise in temperature; this was true of chlordan to a lesser extent. Dusts containing 4% γ-*I* were more toxic than dusts containing 4% chlordan concentrate.

Text. Research J. May 1948

Control of Cotton Thrips

Insecticides for control of thrips on cotton. R. K. Fletcher, J. C. Gaines, and W. L. Owen. *J. Econ. Entomol.* **40**, 594–6 (1947) (through *Chem. Abstr.* **42**, 1010*i* (Feb. 10, 1948)).

Field studies were made with various formulations of DDT in dusts and sprays and with benzene hexachloride (2.3% γ-isomer), Lethane B-71, and Lethane B-72 against *Frankliniella tritici* on cotton. Although thrips populations were reduced, the percentage of thrips-injured plants and the yield of cotton were not increased by the treatments. Applications at weekly intervals were necessary to prevent reinfestation. None of the treatments was profitable.

Text. Research J. May 1948

Properties of Cotton Fabrics

Discovering cotton. Leonard Smith and Geo. S. Buck, Jr. *Text. Col. and Converter* **69**, No. 11, 41, 62–4 (1947) (through *Chem. Abstr.* **42**, 1059*c* (Feb. 10, 1948)).

The properties of cotton fabrics are reviewed.

Text. Research J. May 1948

Filter Fabrics

Filtration through fabrics made of cellulose and synthetic continuous fibers. Jean Alibert. *Chimie and industrie* **58**, 341–5 (1947) (through *Chem. Abstr.* **42**, 797*c* (Feb. 10, 1948)).

Results are given of 3 filtration tests (removal of dust from air, clarification of a liquid, separation of a hydrated Al_2O_3 precipitate) using a variety of filter cloths made from different materials (cotton, nylon, "Rhofil," shrunk "Rhofil"), showing the advantages of the continuous-fiber fabrics, and their adaptability to various conditions by proper selection of weight, weave, etc.

Text. Research J. May 1948

Insect Repellent for Fabrics

Benzyl benzoate-dibutyl phthalate mixture for impregnating clothing. F. M. Snyder and F. A. Morton. *J. Econ. Entomol.* **40**, 586–7 (1947); cf. *C.A.* **40**, 6206[1]

(through *Chem. Abstr.* **42**, 1374*g* (Feb. 20, 1948)).

Experiments to determine the effectiveness against chiggers (*Entrombicula* sp.) of clothing impregnated with mixtures of benzyl benzoate (*I*) and dibutyl phthalate (*II*) are described. Methods of impregnating the clothing and of determining the effectiveness of the treated garments are detailed. Since *II* was found to be only slightly less effective against chiggers than *I* (Snyder and Morton, *C.A. 41*, 3580*b*) mixtures of *I* and *II* were impregnated into bleached cotton twill in ratios of 75 *I*-25 *II*, 50–50, and 25–75. The 50–50 mixture withstood the same number of washings as *I* and one more wash than *II* and paralyzed chiggers about as efficiently as *I*. Cotton uniforms retained the 50–50 mixture and *I* after washing a little better than wool uniforms. The 50–50 mixture in cotton clothing withstood ageing outdoors 12 or more days longer than *I*; in wool, the 50–50 mixture and *I* gave equal protection (58 days) outdoors.

Text. Research J. May 1948

Felting

The felting of animal fibers. J. Menkart and J. B. Speakman. *J. Soc. Dyers and Colourists* **64**, 14–19 (Jan. 1948); *cf.* TEXTILE RESEARCH JOURNAL **18**, 59 (Jan. 1948).

Text. Research J. May 1948

Adsorption by Fibers

Sorption of nitrogen and water vapor on textile fibers. John W. Rowen and R. L. Blaine. *Ind. Eng. Chem.* **39**, 1659–63 (Dec. 1947).

Measurements were made of the adsorption of nitrogen and water vapor on 6 purified textile fibers and titanium dioxide. All the fibers had a relatively low capacity for adsorption of nitrogen as compared with the capacity for adsorption of water vapor. The surface area values ranged from 0.31 sq.m. per g. for nylon to 0.93 sq.m. per g. for viscose rayon. The value of the free surface energies of adsorption as calculated by the Gibbs adsorption equation were the same for wool, cotton, silk, and rayon fibers but differed for the 2 synthetic polymers, nylon and acetate rayon. Authors

Text. Research J. May 1948

Hemp Fiber

The effect of fertilizers on the chemical compositon and quality of dew-retted hemp fiber. Lyle E. Hessler. *J. Am. Soc. Agron.* **39**, 812–16 (1947) (through *Chem. Abstr.* **42**, 1007*b* (Feb. 10, 1948)).

N fertilizers increased the growth of hemp and gave greater yields of dew-retted hemp fibers, but at the same time the fiber was coarser and weaker. The cellulose content of the fiber was significantly increased where the complete fertilizer was used. During retting the more labile secondary constituents tend to level off in concentration regardless of fertilizer treatment. Fineness of fiber gave a significant positive correlation coefficient with breaking strength. All encrustants showed a negative correlation with the primary fiber constituent, cellulose; and lignin, protein, and ash gave highly significant correlation coefficients, whereas pentosans gave a significant *r*.

Text. Research J. May 1948

Wool-Rayon Blends

Raising the count limit of wool. R. S. Audley. *Fibres* **8**, 372–3 (Nov. 1947).

After reviewing broadly the relationships of wool fiber length and fineness to count limits, the author states that principally uniformity of fiber length in tops is the factor that affects the spin at a later stage. Furthermore, when considering count limit from a particular quality, fiber length influences the maximum count that can be spun. Quality for quality, white tops spin to higher counts than colored ones. A formula to find the fiber fineness (in inches) required to spin a given count is given. When viscose staple fiber is blended with wool, the spin is considerably improved and it becomes desirable, as well as possible, to use lower twists. As the rayon content increases, the twist decreases and vice versa with an increase in wool content. On the finer-quality wools, count limit approximates quality number, but falls off sharply on the crossbred range of wools. By the judicious blending of rayon staple fiber with these crossbred wools, new uses can be found for wool qualities which now have only limited application. With blends of crossbred and rayon, required strength for weaving can be obtained without the sizing process. How count limits are successfully raised by such mixtures is indicated by a blend of 46s quality Colonial crossbred that normally would not be expected to spin to a count finer than, say, 32s, but when mixed with a 1.5-denier rayon staple fiber it will spin to 48s. In another instance, 50% 56s quality crossbred blended with 50% 4-in. staple rayon of 1.5 denier has been spun to a count as fine as 1/80s and could be spun commerically to 56s.

Text. Research J. May 1948 L. A. Fiori

Vinyon Type N Fibers

Some properties and uses of "Vinyon" type N fibers. E. Stowell. *Papers of AATT* **3**, 30–4 (Dec. 1947).

A review is given of the pertinent characteristics of Vinyon type N fibers and uses are suggested. Five types of yarns are said to be at present produced by combinations of stretching and heating treatments of a single continuous, dry-spun yarn source. J. A. Woodruff

Text. Research J. May 1948

Vinyon Developments

A review of Vinyon developments. Anon. *Am. Wool and Cotton Reptr.* **6**, 13–14 (Feb. 5, 1948).

A review of the development of Vinyon and the methods of producing this fiber.

Text. Research J. May 1948

Cardroom "Snowballs"

Cardroom "snowballs"—a potential source of end breaks. Anon. *Text. Mercury and Argus* **117**, 801,

803 (Dec. 5, 1947); *Saco-Lowell Bull.* **19**, 11–12 (June 1947).

A campaign to eliminate card room "snowballs" is presented. Particular attention should be paid to the clothing selvedges of the cylinder and doffer to detect soft spots in the foundation. Improperly set selvedge guides, loose settings, closely set cylinder screens, and dead air spaces caused by faulty plate settings are sources of these defects.

Text. Research J. May 1948 L. A. Fiori

New Twister

Modern combined doubling and twisting machine. Anon. *Textile Recorder* **65**, 50–1 (Feb. 1948).

A discussion of a new combined doubling and twisting machine for rayon, silk, and other yarns. Features reviewed are a new type of broken-end stop motion, a positively driven feed roller, and spindle mounting assembly. Several close-up views are shown. L. A. Fiori

Text. Research J. May 1948

Tension Control

Tension controlled by variety of drives. A. P. Mansfield. *Textile World* **98**, 126, 127, 129, 131, 222, 223 (Feb. 1948).

Higher production is possible for all processes, from spinning through finishing, by the application of proper tension controls.

A. L. Landau

Text. Research J. May 1948

Warping Rayon

Cotton system excellent for warping Bemberg. J. Gassman. *Textile World* **98**, 116–17 (Feb. 1948).

The cotton warper may be used very successfully for warping rayon. A slow-speed drum-driven warper head is required to wind the yarn from spools onto the section beam, as the speed should not be over 60 yds. per min. Rebeaming may be done on a machine which is similar to the cotton slasher, without the size box and drying cylinders, and with the addition of a lease stand.

A. L. Landau

Text. Research J. May 1948

Loom Fixing

Manual guides: Draper loom fixing. Anon. *Textile World* **98**, 120–1 (Feb. 1948).

A reprint of a manual for fixing model XD Draper looms in which the causes of defects in weaving are listed. A. L. Landau

Text. Research J. May 1948

Card Lap Weight

What weight lap. Anon. *Saco-Lowell Bull.* **19**, 9–10 (June 1947).

A 15-oz. lap, or one as near 15 oz. as possible, is proposed as a universal choice for the standard weight per yd. The very nature of a "heavy" lap reduces variation per yd., increases picker production, accentuates cleaning and combing by the lickerin during carding because the lap passes under the feed foll more slowly, and causes the variation across the face of the feed plate, from inch to inch, to be in a lower ratio to the whole mass of fiber than the same variation would represent in a lighter lap. L. A. Fiori

Text. Research J. May 1948

Picker-Lap Weights

Regularity of laps. Anon. *Text. Weekly* **40**, 1076, 1078 (Dec. 12, 1947).

In addition to mechanical considerations responsible for lap weight irregularities is the problem of relative humidity. Where there is automatic humidity control, lap weight fluctuations are held at a minimum, but when there is no control altered moisture content causes excessive lap variation. To insure that the "dry" weight of cotton fed to the cards is maintained at as constant a level as possible to avoid too many alterations at the drawing frame, a table of conversion factors determines what the weight of the lap should be at any relative humidity. Hence unnecessary changes are not made at the drawing frame merely for humidity changes. Variations in laps are accentuated a hundred-fold in the yarn; therefore a coefficient of variation should be used for establishing weight limits. L. A. Fiori

Text. Research J. May 1948

MISCELLANEOUS

★

Action of Light on Cotton

The action of light on dyed and undyed cotton. G. S. Egerton. *Am. Dyestuff Reptr.* **36**, 561–70, 573 (Oct. 6, 1947); *cf.* TEXTILE RESEARCH JOURNAL **17**, 517 (Sept. 1947).

Text. Research J. May 1948

Cotton Production

Production per man hour in cotton manufacture. R. M. Marks. *J. Text. Inst.* **39**, P35–6 (Jan. 1948).

The supply of automatic looms in England is likely to be inadequate since it is estimated that it would take 24 yrs. to provide all the automatic looms needed by industry. Emphasis must therefore be placed on labor-saving methods rather than on labor-saving machines. The importance of time and motion study to textiles is pointed out. Obvious methods of approach are (1) use of larger yarn packages, (2) increase in shuttle size, in cross section and length, (3) winding more compactly, and (4) basing wages on the work done by the operator and not that done by the machine. L. A. Fiori

Text. Research J. May 1948

Winding for Knitting

Knit goods technology. Anon. *Am. Wool and Cotton Reptr.* **8**, 11, 12, 33, 34 (Feb. 19, 1948).

Winding machines and types of winds which can be used for knitting are discussed. The pineapple cone package, the most modern packaging for rayon, is fully described.

A. L. Landau

Text. Research J. May 1948

Automatic Loom

"Sainte-Colombe" loom. W. H. Barker. *Textile Weekly* **41**, 338, 340, 342 (Feb. 20, 1948); **41**, 396, 398 (Feb. 27, 1948).

Features of the automatic and non-automatic looms are described

briefly and methods adopted in the workshop, from the erection of the loom to its installation in the factory, are outlined. The stop-on-the-pick motion which eliminates starting places, saves pick finding, and increases output demonstrates a big step forward in loom efficiency. This device operates in conjunction with the center filling fork; when the filling breaks the loom stops before the reed reaches the fell of the cloth. The loss in sequence in shuttle movements, especially when using 2, 3, or 4 shuttles, seldom occurs. It is pointed out that the term "looms per weaver" should be "ends per weaver" since the number of looms a weaver can manage is determined by the number of warp ends together with the quality of yarns and type of fabrics being woven. L. A. Fiori

Text. Research J. May 1948

Loom-Beam Barrel

A new aluminum loom-beam barrel. H. H. Nuernberger. *Rayon Text. Mo.* **29**, 54 (Mar. 1948).

The advantages of using an aluminum loom-beam barrel in place of the conventional wood barrel are considered. Three methods outlining how cast-iron heads, steel tie rods, and shafts of the old beams can be reused with an aluminum replacement barrel are described.

Text. Research J. May 1948 L. A. Fiori

Timing by Oscillograph

Machine timing at full speed done by oscillograph. M. Scheraga. *Textile World* **98**, 118, 119, 188, 190, 191 (Jan. 1948).

The cathode-ray oscillograph may be employed to determine the speeds, adjustments, and cycle positions of any machine motion to which it may be connected. The article describes the methods with which this instrument has been used to test looms. A. L. Landau

Text. Research J. May 1948

Fabric-Reinforced Plastics

Fabric-reinforced plastics. W. J. Brown. London, Cleaver-Hune Press, 1947, 147 pp., 7s. 6d. (through *Chem. Abstr.* **42**, 1081*g* (Feb. 10, 1948)).

Reviewed in *Engineering* **164**, 317 (1947).

Text. Research J. May 1948

Polyamide Resins

Polyamide resins. A. G. Hovey. *Chemurgic Digest*, **7**, 18–20 (Jan. 1948).

A discussion of polyamide resin made from linoleic and linolenic acids from soybean oil and ethylene diamine. Properties and uses are described with special emphasis on applications in packaging.

Text. Research J. May 1948 R. W. Eyler

Polyvinylidene Chloride Plastics

Polyvinylidene chloride. J. J. P. Staudinger. *Brit. Plastics.* **19**, 381–9 (Sept. 1947).

Monomer manufacture, polymerization, and copolymerization are discussed in the first of two parts of a comprehensive review.

Text. Research J. May 1948 R. W. Eyler

Polyvinylidene chloride. J. J. P. Staudinger. *Brit. Plastics* **19**, 453–61 (Oct. 1947).

A discussion of the structure, crystallization, orientation, heat stability, dehydrochlorination, possible plasticizers, fabrication methods, properties, and applications in the second part of a review. 119 references. R. W. Eyler

Text. Research J. May 1948

Process Control by Tracer Techniques

Chemical process control with radioactivity. Alan P. Schreiber. *Chem. Eng.* **55**, 103–5 (Jan. 1948).

Suggestions for uses of radioactivity and tracer techniques in chemical process control are given. Possible methods in the rayon industry for studying sulfur removal in the coagulating and desulfurizing baths, detecting the presence of toxic gases, regulating the preparation of viscose solution, tracing reactions, and for measuring specific gravity and liquid level are described.

Text. Research J. May 1948 R. W. Eyler

Process Water Supply

Water supply. Anon. *Chem. Eng.* **55**, 137–44 (Jan. 1948).

A comprehensive report of the factors influencing quantity and quality of water supply which might be of importance to process industries. Sources of water, site selection, ground water supply, the water table, the weather cycles, ground permeability, safe pumping rates, restoring ground water, surface water supply, competition for water, the fish problem, water analyses and quality, and reference material are among topics discussed. Charts for the United States showing weighted average hardness, water temperature, normal annual runoff, and stream flow are given. Tables showing typical industrial water needs, typical analyses of surface and ground waters, and source and treatment of public water supplies are presented.

Text. Research J. May 1948 R. W. Eyler

Wool-Wax Derivatives

Heavy metal soaps of wool-wax acids. Lubricating greases and other uses. E. S. Lower. *Ind. Chemist* **23**, 645–51 (1947) (through *Chem. Abstr.* **42**, 1074*g* (Feb. 10, 1948)).

A review with 13 references. Cf. *C.A. 41*, 5326*h*.

Text. Research J. May 1948

Gill Box Leathers

Life of gill box leathers. Anon. *Fibres* **9**, 60 (Feb. 1948).

Before use, gill leathers should be stored in order to become thoroughly set. A heavier gage of leathers is demanded with coarser wools so that they can better withstand the cutting action of the fibers. Many other aids and precautions for lengthening the life of gill leathers are described. L. A. Fiori

Text. Research J. May 1948